NOTE TO USERS

uOttawa

L'Université canadienne
Canada's university

FACULTÉ DES ÉTUDES SUPÉRIEURES ET POSTOCTORALES

uOttawa

L'Université canadienne
Canada's university

FACULTY OF GRADUATE AND POSDOCTORAL STUDIES

Stéphane Roberge
AUTEUR DE LA THÈSE / AUTHOR OF THESIS

M.A.Sc. (Chemical Engineering)
GRADE / DEGREE

Department of Chemical Engineering
FACULTÉ, ÉCOLE, DÉPARTEMENT / FACULTY, SCHOOL, DEPARTMENT

Styrene/Butyl Acrylate Mini-Emulsion-Based Pressure Sensitive Adhesives

TITRE DE LA THÈSE / TITLE OF THESIS

Marc A. Dubé
DIRECTEUR (DIRECTRICE) DE LA THÈSE / THESIS SUPERVISOR

CO-DIRECTEUR (CO-DIRECTRICE) DE LA THÈSE / THESIS CO-SUPERVISOR

EXAMINATEURS (EXAMINATRICES) DE LA THÈSE / THESIS EXAMINERS

Kevin Kennedy

Jason Zhang

Gary W. Slater
LE DOYEN DE LA FACULTÉ DES ÉTUDES SUPÉRIEURES ET POSTDOCTORALES /
DEAN OF THE FACULTY OF GRADUATE AND POSTDOCORAL STUDIES

UNIVERSITY OF OTTAWA

Department of Chemical Engineering

STYRENE/BUTYL ACRYLATE MINI-EMULSION-BASED PRESSURE SENSITIVE ADHESIVES

by

Stéphane Roberge

A thesis submitted to the Faculty of Graduate and Postdoctoral Studies in partial fulfillment of the requirements for the degree of

Master of Applied Science

in Chemical Engineering

Your file Votre référence
ISBN: 0-494-11394-4
Our file Notre référence
ISBN: 0-494-11394-4

Abstract

Adhesives are defined as substances capable of holding at least two surfaces together. A class of adhesives called pressure-sensitive adhesives (or PSAs) is characterized by instantaneous adhesion upon application of light pressure.

In order to develop new application-specific products and improve existing processes, there is a need to identify the factors that influence the performance of PSAs. Operating conditions like feed composition, temperature, and solid content will affect latex properties such as copolymer composition, molecular weight distribution (MWD) and particle size distribution (PSD). Those latex properties can in turn affect the performance of the adhesive.

Because of environmental concerns and government regulations to substitute solvent-based systems by water-borne products, there is a growing interest in producing such PSAs by emulsion (or mini-emulsion) polymerization. Mini-emulsions allow for improved control over the PSD compared to conventional emulsion polymerizations. Coupled with control over the MWD and copolymer composition, mini-emulsions could offer the possibility of tailoring the desired properties of PSAs. It was of interest in this thesis, to measure the effect of varying particle size and copolymer composition on adhesive properties.

Based on this primary objective, a series of styrene/butyl acrylate mini-emulsion copolymerizations were carried out in a 1.2L stainless steel reactor. Conversions were monitored off-line using gravimetry and in-line using ATR-FTIR spectroscopy. By using a constrained mixture design, the influences of particle size and polymer composition were investigated. As a result of a 3^2 factorial design, 11 runs (9 runs and 2 replicates) were performed. Important industrial adhesive tests, loop tack, peel strength and shear strength, were measured and modeled empirically using a full second order polynomial. For every model, there were no trends in the residuals and no lack of fit was found. The models described a statistically significant percentage of the variability in the data. While particle size was found to be the most influential component for both the tack and peel strength models, the relationship was described by a negative parabola for tack and by a negative slope for peel strength. In the case of shear strength, the relationship with

respect to particle size was described by a negative slope and both the particle size and copolymer composition were found to be significantly influential. The final forms of the models also allowed 3-D response surfaces to be built and the optimal adhesive performance region was located near the smallest particle diameter investigated with the highest styrene composition. A possible explanation for the positive effect of smaller particles on every adhesive property could involve a concept where smaller particles could pack more tightly together during the drying process thus increasing the area of contact between the adhesive and the substrate. Ultimately, this study has shown that the control over particle size afforded by mini-emulsions could enable us to affect the properties of PSA in a controlled manner.

Traditional polymerization monitoring is often carried out using off-line characterization of samples from a process flow line. A disadvantage of off-line techniques for conversion and composition monitoring, such as gravimetry and ^{1}H-NMR spectroscopy is the time lag between sampling and results. IR spectroscopy techniques are especially suited for real-time reaction monitoring as they allow spectral measurements to be obtained directly in the process stream without the need for sampling devices for on-line analysis. Because in-line monitoring using ATR-FTIR spectroscopy was successful on different emulsion systems, it was of interest in this thesis to validate this technique for mini-emulsions.

Based on this secondary objective, the in-line monitoring of mini-emulsions using ATR-FTIR spectroscopy was investigated. A series of styrene/butyl acrylate mini-emulsion copolymerizations were carried out in a 1.2L stainless steel reactor. ATR-FTIR spectroscopy was used to track the concentration of monomers, thereby providing conversion and polymer composition data. Off-line gravimetry and ^{1}H-NMR spectroscopy were used to provide a comparison with the ATR-FTIR data. After inconsistent results were obtained with univariate methods, a multivariate or PLS method using the full spectra of the reactions gave much more promising results for the in-line mini-emulsion polymerization monitoring of monomer concentrations and conversions. No significant differences were found between the off-line and ATR-FTIR spectroscopy data coupled with multivariate statistics confirming that ATR-FTIR spectroscopy is a

reliable tool for monitoring conversion and polymer composition in mini-emulsion polymerizations.

Résumé

Les adhésifs sont définis comme étant des substances capables de tenir au moins deux surfaces ensemble. Une classe d'adhésifs appelés adhésifs sensibles à la pression (ou ASP) est caractérisée par une adhérence instantanée après l'application d'une légère pression.

Afin de développer de nouveaux produits spécifiques à ces applications et d'améliorer les procédés déjà existants, il devient nécessaire d'identifier les facteurs qui influencent les performances de ces ASP. Les conditions de réaction comme la composition à l'alimentation, la température et la consistance affecteront les propriétés du latex comme la composition du copolymère, la distribution de poids moléculaire (DPM) et la distribution des grosseurs de particule (DGP). Ces propriétés du latex peuvent à leurs tours affecter les performances de l'adhésif.

En raison des soucis environnementaux et des règlements gouvernementaux pour substituer les systèmes à base de solvant par des systèmes à base d'eau, l'intérêt pour la production de ces ASP par polymérisation en émulsion (ou en mini-émulsion) devient de plus en plus grandissante. Les mini-émulsions procure un meilleur contrôle de la DGP comparé aux polymérisations conventionnelles par émulsion. En offrant également un contrôle sur la composition du copolymère et de sa DPM, les mini-émulsions offrent la possibilité de choisir les propriétés désirées de l'ASP. Dans cette thèse, il devenait intéressant d'évaluer les effets du changement de la grosseur des particules et de la composition du copolymère sur les propriétés de ces adhésifs.

Basé sur ce premier objectif, une série de copolymérisations en mini-émulsion utilisant l'acrylate butylique et le styrène ont été effectués dans un réacteur en acier inoxydable de 1.2 L. Les conversions des réactions étaient surveillées à l'aide d'une méthode de gravimétrie et d'une méthode spectroscopique employant un système ATR-FTIR. En employant une conception avec contrainte sur les recettes de réactions, les influences de la grosseur des particules et de la composition du copolymère ont été étudiées. Étant donné qu'un modèle factoriel de 3^2 était utilisé, 11 réactions (9 réactions standard et 2 répétitions) ont été exécutées. Des indicateurs de performance couramment utilisés par l'industrie comme la force d'adhésion, la force de déchirement et la résistance

au cisaillement ont été mesurés et incorporés dans des modèles empiriques utilisant des polynômes de second degré. Pour chaque modèle, il n'y avait aucune tendance des résiduels et aucun manque d'ajustement n'a été observé. Les modèles ont décrit un pourcentage statistiquement significatif de la variabilité dans les données. Tandis que la grosseur des particules s'avérait la composante la plus influente pour les modèles de force d'adhésion et de déchirement, le rapport a été décrit par une parabole négative pour la force d'adhésion et par une pente négative pour la force de déchirement. Dans le cas de la résistance au cisaillement, le modèle a été décrit par une pente négative en ce qui concerne la grosseur des particules. Cependant, les deux facteurs, la grosseur des particules et la composition du copolymère, se sont avérées sensiblement influents. Les formes finales des modèles ont également permis à des surfaces en 3-D d'être établies. La région optimale pour les performances d'adhésifs a été située près des plus petits diamètres de particules étudiés avec la composition en styrène la plus élevée dans le copolymère. Une explication possible pour l'effet positif des plus petites particules sur chaque propriété adhésive pourrait impliquer un concept où de plus petites particules pourraient s'entasser plus étroitement ensemble pendant le processus de séchage augmentant de ce fait la superficie de contact entre l'adhésif et le substrat. Finalement, cette étude a prouvé que le contrôle de la grosseur des particules accordée par les mini-émulsions pourrait nous permettre d'influencer les propriétés des ASPs de façon plus précise qu'auparavant.

La surveillance traditionnelle des polymérisations a longtemps été effectuée en utilisant la caractérisation des échantillons provenant d'une ligne d'échantillonnage du processus. Un inconvénient de ces techniques comme la gravimétrie et la spectroscopie ^{1}H-NMR pour la surveillance des conversions et compositions est le délai entre le prélèvement et les résultats. La technique spectroscopique par infrarouge (IR) est particulièrement appropriée pour la surveillance en temps réel de réactions en permettant à des mesures spectrales d'être obtenues directement du processus sans le besoin de prélever des échantillons pour analyse. Puisqu'en ligne la surveillance utilisant la spectroscopie par infrarouge avec le système ATR-FTIR a été appliqués avec succès sur différents systèmes d'émulsion. Il devenait donc intéressant pour cette thèse de valider cette technique pour des mini-émulsions.

Basé sur ce second objectif, la surveillance intégrée des mini-émulsions employant la spectroscopie par infrarouge avec le système ATR-FTIR a été étudiée. Une série de copolymérisations en mini-émulsion utilisant l'acrylate butylique et le styrène ont été effectués dans un réacteur en acier inoxydable 1.2 L. La spectroscopie par infrarouge avec le système ATR-FTIR a été employée pour surveiller la concentration des monomères, fournissant de ce fait la conversion et la composition du copolymère. La gravimétrie et la spectroscopie ^{1}H-NMR ont été employées comme méthodes conventionnelles pour fournir une base de comparaison avec la technique utilisant le système ATR-FTIR. Après que des résultats insatisfaisant aient été obtenus avec des méthodes à simple variable, une méthode à multiple variables ou PLS employant toutes les informations spectrales des réactions a donné des résultats beaucoup plus prometteurs pour la surveillance intégrée des polymérisations en mini-émulsion. Aucune différence significative n'a été trouvée entre les données du système de spectroscopie ATR-FTIR combiné aux statistiques à variables multiples et les méthodes conventionnelles de surveillance confirmant que la spectroscopie par infrarouge intégrant le système ATR-FTIR est un outil fiable pour surveiller la conversion et la composition des polymères dans des polymérisations en mini-émulsion.

Statement of Contribution of Collaborators

I hereby declare that I am the sole author of this thesis. I performed the polymerization experiments, polymer characterizations, pressure-sensitive adhesives testing, and data analysis except for the acquisition of ^{1}H-NMR data, which were contracted out to the Department of Chemistry at the University of Ottawa.

My thesis supervisor Dr. Marc A. Dubé provided the scientific guidance throughout the project and editorial comments for the written work.

Stéphane Roberge Date: April 17, 2005

Acknowledgements

I would like to express my gratitude to my supervisor Dr. Marc A. Dubé for all the support and guidance he provided me with throughout this thesis. I am grateful to all the members of the Polymer Reaction Engineering group, especially, Renata Jovanovic, Hong Hua, Nick Brooks and Gabriela Fonseca with whom I had the chance to work with. I would like to thank the technicians of the Department of Chemical Engineering at the University of Ottawa, Louis Tremblay, Gérard Nina and Franco Ziroldo for their help in repairing and maintaining all the lab equipment.

For the financial support during this project, I am grateful to the Ontario Ministry of Training, Colleges and Universities for three Ontario Graduate Scholarships, to the Natural Sciences and Engineering Research Council of Canada for three Canadian Graduate Scholarships and to the University of Ottawa for one Admission and six Excellence Scholarships.

Table of Contents

Chapter 1 – Introduction 1

1.1 Thesis Objectives 2

1.2 Thesis Outline 3

References 4

Chapter 2 - Background 6

2.1 Free-radical Polymerization Kinetics 6

Initiation 6

Propagation 7

Termination 8

Chain Transfer 9

Rates of Reaction 10

Autoacceleration 11

Composition and Reactivity Ratios 12

2.2 Emulsion Polymerization Kinetics 13

Three Stages of Emulsion Polymerization 14

2.3 Mini-emulsion Kinetics 15

Degradation Mechanisms 16

2.4 IR Spectroscopy 17

Fundamentals of IR Spectroscopy 17

Functional Groups 17

Quantitative Analysis 18

Fourier Transform Infrared (FTIR) 18

Attenuated Total Reflectance (ATR) 19

Applications of ATR-FTIR 20

2.5 PSAs with St/BA Systems in Mini-emulsions 20

Tack 21

Peel Strength 21

Shear Strength 22

Modeling Adhesive Performances 22

References 24
Chapter 3 - Experimental Procedures 29
3.1 Reagent 29
3.2 Experimental Design 29
3.3 Apparatus 31
3.4 Monomer Mixture Preparation 32
3.5 Polymerization 33
3.6 Characterization 34
Gravimetry 34
^{1}H-NMR Spectroscopy 35
ATR-FTIR Spectroscopy 35
GPC 36
BI-DCP 37
Gel Content 38
Glass Transition Temperature (T_g) 39
Adhesive Testing 39
References 40
Chapter 4 – Paper on IR Monitoring 42
Abstract 43
Introduction 44
Background 44
ATR-FTIR Spectroscopy 44
Conventional Emulsions 45
Mini-emulsions 46
Experimental Section 48
Reagents 48
Experimental Procedure 48
Characterization 49
Results and Discussion 50
Inappropriate background 51
Inappropriate signal to noise ratio 51

Probe fouling 52
Temperature variations 52
Deviation from Beer's law 53
New peak assignment (Univariate method) 54
Multivariate method 61
Conclusions 67
Acknowledgements 68
References 68
Chapter 5 – Paper on PSA Performance 71
Abstract 72
Introduction 73
Background 74
PSAs 74
Conventional Emulsions 75
Mini-emulsions 76
Modeling Adhesive Performances 78
Experimental Section 79
Reagents 80
Experimental Procedure 80
Characterization 81
Experimental Design 83
Gravimetry 85
Monitoring of pH 85
Copolymer Compositions 86
Glass Transition Temperatures (T_g) 86
Molecular Weight 87
Gel Content 88
Modeling Adhesive Performance 88
Conclusions 96
Acknowledgements 98
References 98

Chapter 6 – Conclusions and Recommendations 101
References 103
Appendix A – Sample Calculations 105
Polymerization recipe 106
Experimental calculations for gravimetric data 107
Experimental calculations for ATR-FTIR data (univariate method) 108
Appendix B – Extra Figures and Tables 109

List of Tables

Chapter 3 – Experimental Procedure 29
Table 1: Batch recipes – main objective 30
Table 2: Batch recipes – secondary objective 30
Table 3: Mark-Houwink parameters determined in THF 37
Chapter 4 – Paper on IR Monitoring 42
Table 1: Batch recipes 51
Chapter 5 – Paper on PSA Performance 71
Table 1: Batch recipes 83
Table 2: Experimental Results 89
Table 3: Analysis of Variance (ANOVA) for Tack 89
Appendix A – Sample Calculations 105
Table A.1: Polymerization Recipe 106
Table A.2: Experimental values for gravimetric data 107
Table A.3 Experimental values for ATR-FTIR data 108

List of Figures

Chapter 2 – Background 6
Figure 1: Different Intervals of an Emulsion Polymerization 15
Figure 2: Total internal reflection at the interface of an internal reflection element. Depth of penetration of the evanescent wave is approximately 1 μm 19
Chapter 3 – Experimental Procedure 29
Figure 1: 1.2L stainless steel batch reactor 31
Figure 2: ReactIR™ 1000 32
Figure 3: Sonicator 33
Chapter 4 – Paper on IR Monitoring 42
Figure 1: Reaction spectrum from the homopolymerization of styrene in mini-emulsion 52
Figure 2: Temperature profile from the homopolymerization of styrene in mini-emulsion 53
Figure 3: Linear regression for Beer's law validation 54
Figure 4: Typical homopolymerization spectra of styrene in mini-emulsion 55
Figure 5: Monomer region for the homopolymerization of styrene in mini-emulsion 56
Figure 6: Polymer region for the homopolymerization of styrene in mini-emulsion 57
Figure 7: Homopolymerization of styrene in mini-emulsion monitored with Equation 1 58
Figure 8: Homopolymerization of styrene in mini-emulsion monitored with Equation 3 59
Figure 9: Copolymerization of styrene/butyl acrylate (50/50) in mini-emulsion 60
Figure 10: Copolymerization of styrene/butyl acrylate (20/80) in mini-emulsion 60
Figure 11: Typical copolymerization spectra of styrene/butyl acrylate in mini-emulsion 62
Figure 12: Common monomer peaks in the copolymerization of styrene/butyl acrylate. 62
Figure 13: PRESS analysis for the PLS model 63
Figure 14: Styrene concentration calibration 64
Figure 15: Butyl acrylate concentration calibration 64
Figure 16: Styrene concentration validation 65
Figure 17: Butyl acrylate concentration validation 65
Figure 18: PLS individual conversion predictions for Run 51 66
Figure 19: PLS overall conversion predictions for Run 51 67

Chapter 5 – Paper on PSA Performance 71
Figure 1: Conversion versus time for Runs 1, 4, 7 85
Figure 2: Cumulative copolymer compositions for different feed compositions 86
Figure 3: PSA properties as a function of molecular weight 87
Figure 4: Tack vs. particle size and polymer composition. 91
Figure 5: Peel strength vs. particle size and polymer composition 92
Figure 6: Shear strength vs. particle size and polymer composition 94
Figure 7: 3-D response surface for the tack model 95
Figure 8: 3-D response surface for the peel strength model 95
Figure 9: 3-D response surface for the shear strength model 96
Appendix B – Extra Figures and Tables 109
Figure B.1: Styrene peak assignment (Rivard, T. M.A.Sc. thesis, Department of Chemical Engineering, University of Ottawa, 2002). 110
Figure B.2: Butyl acrylate peak assignment (Rivard, T. M.A.Sc. thesis, Department of Chemical Engineering, University of Ottawa, 2002) 111
Figure B.3: ^{1}H-NMR spectrum for styrene/butyl acrylate/acrylic acid 112
Figure B.4: Example of particle size determination with BI-DCP 113
Figure B.5: PLS individual conversion predictions for Run 7 114
Figure B.6: PLS overall conversion predictions for Run 7 114
Figure B.7: PLS individual conversion predictions for Run 71 115
Figure B.8: PLS overall conversion predictions for Run 71 115
Figure B.9: PLS individual conversion predictions for Run 34 116
Figure B.10: PLS overall conversion predictions for Run 34 116
Figure B.11: Temperature profiles for all the runs 117
Figure B.12: pH profiles for all the runs 117
Figure B.13: Conversion versus time for Runs 1, 2, 3, 4, 5, 6 118
Figure B.14: Conversion versus time for Runs 7, 8, 9, 5-2, 5-3 118
Figure B.15: Conversion versus time for Runs 3-1, 3-2, 3-4, 5-1, 7-1 119
Figure B.16: Cumulative copolymer composition for Run 1 119
Figure B.17: Cumulative copolymer composition for Run 2 120
Figure B.18: Cumulative copolymer composition for Run 3 120

Figure B.19: Cumulative copolymer composition for Run 4 121
Figure B.20: Cumulative copolymer composition for Run 5 121
Figure B.21: Cumulative copolymer composition for Run 6 122
Figure B.22: Cumulative copolymer composition for Run 7 122
Figure B.23: Cumulative copolymer composition for Run 8 123
Figure B.24: Cumulative copolymer composition for Run 9 123
Figure B.25: Cumulative copolymer composition for Run 5-2 124
Figure B.26: Cumulative copolymer composition for Run 5-3 124
Figure B.27: Cumulative copolymer composition for Run 3-1 125
Figure B.28: Cumulative copolymer composition for Run 3-2 125
Figure B.29: Cumulative copolymer composition for Run 3-4 126
Figure B.30: Cumulative copolymer composition for Run 5-1 126
Figure B.31: Cumulative copolymer composition for Run 7-1 127

Nomenclature

Symbols

f	Initiator efficiency (dimensionless)
f_i	Instantaneous fraction of monomer i (dimensionless)
F_i	Instantaneous mole fraction of monomer i (dimensionless)
k_{fCTA}	Chain transfer to CTA rate constant (L/mol min)
k_d	Decomposition of initiator rate constant (L/mol min)
$k_{fm,ij}$	Chain transfer to monomer rate constant, terminal monomer i and receiving monomer j (L/mol min)
k_{fp}	Chain transfer to polymer rate constant (L/mol min)
$k_{i,j}$	Initiation of monomer j rate constant (L/mol min)
k_p	Polymerization rate constant (L/mol min)
$k_{p,ij}$	Propagation rate constant of monomer j to terminal monomer i, (L/mol min)
$k_{tc,ij}$	Termination by combination rate constant, terminal monomers for the radical chains are i and j, respectively (L/mol min)
$k_{td,ij}$	Termination by disproportionation rate constant, terminal monomers for the radical chains are i and j, respectively (L/mol min)
M_1	Styrene (dimensionless)
M_2	Butyl acrylate (dimensionless)
P_{n+m}	Dead polymer of length n+m (dimensionless)
r_i	Reactivity ratio of monomer i (dimensionless)
R_d	Rate of decomposition of initiator (mol/L min)
R_i	Rate of initiation (mol/L min)
R_p	Rate of polymerization (mol/L min)
$R_{r+1,i}$	Radical chain of length r+1, ending in monomer i and j, respectively (dimensionless)
R_t	Rate of termination (mol/L min)
$R\cdot$	Free radical (dimensionless)

$R\cdot_{1,i}$	Radical chain with 1 monomer, ending in monomer i (dimensionless)
$R\cdot_{m,i}$	Radical chain of length m, ending in monomer i (dimensionless)
$R\cdot_{n,i}$	Radical chain of length n, ending in monomer i (dimensionless)
$R\cdot_{r,i}$	Radical chain of length r, ending in monomer i (dimensionless)
X	Overall conversion (wt. % or mol fraction)
x_i	Conversion of monomer I (wt. % or mol fraction)

Abbreviations

AA	Acrylic Acid
ASTM	American Society for Testing and Materials
ATR-FTIR	Attenuated Total Reflectance Fourier Transform Infrared
BA	Butyl Acrylate
BI-DCP	Brookhaven Disc Centrifuge Photosedimentometer
$CaCl_2$	Calcium Chloride
CMC	Critical Micelle Concentration
CTA	Chain Transfer Agent
GPC	Gel Permeation Chromatography
^{1}H-NMR	Proton Nuclear Magnetic Resonance Spectroscopy
KPS	Potassium Persulfate
NaOH	Sodium Hydroxide
NIR	Near Infrared
ODA	Octadecyl Acrylate
PSA	Pressure Sensitive Adhesive
PSD	Particle size distribution
PSTC	Pressure Sensitive Tape Council
SDS	Sodium Dodecyl Sulfate
St	Styrene
T_g	Glass Transition Temperature
THF	Tetrahydrofuran

Chapter 1 – Introduction

Polymers are macromolecules made of large numbers of much smaller molecules (i.e. monomers) linked together. The reactions by which they combine are termed polymerizations. In chain-growth polymerization, high-molecular-weight polymer is formed and the polymerization involves the reaction of monomers with active centres that may be free radicals, anions, or cations. In this study, we are concerned strictly with free-radical chain polymerization.

Free-radical polymerization can be carried out in different media such as bulk, solution or emulsion. The main components for an emulsion polymerization are water, surfactant, monomer and a water-soluble initiator. Monomer droplets normally have diameters in the range of 1 to 10 microns (Odian, 1991). An emulsion is formed by agitating the first three components, which are then heated. The initiator is subsequently added, and free radicals are produced by thermal decomposition of the initiator so that a free radical polymerization can begin. The final product is a stable colloidal suspension of polymer particles having diameters of 0.1 to 1 microns, although much larger particles can be made by special techniques (Rudin, 1999).

For the past several years, mini-emulsion polymerization had been proposed essentially as an alternative to "classic" emulsion polymerization because of the way in which the particles are formed. The main difference as compared to emulsion polymerization is the size of the monomer droplets. The basis for the mini-emulsion polymerization process is an energetic homogenization to reduce the size of the monomer droplets and the use of both a co-emulsifier and an emulsifier to protect these droplets against degradation. The droplet size can range from 0.1 to 0.5 microns in diameter (Capek and Chern, 2001) and the latexes produced by mini-emulsion are characterized by a broader particle size distribution (PSD) (Asua, 2002). The particle sizes can range from 0.1 to 1 micron in diameter (Lovell and El-Aasser, 1997).

An efficient mini-emulsion polymerization (efficient in terms of particle formation) is very useful as it allows us to control the number and size of particles being

formed in a manner very different from particles formed by micellar or homogeneous nucleation. In principle, it also offers many of the advantages of emulsion polymerization, including relatively rapid kinetics (with respect to bulk or suspension), and high molecular weights.

Many industrial applications require materials with specific properties that can only be achieved through the use of two monomers, i.e. by copolymerization. One example is the styrene (St) and butyl acrylate (BA) system. Depending on their composition and molecular weight, among other properties, the resulting polymers from this system can be used to produce different types of adhesives, coatings and paints. Because of environmental concerns and government regulations to substitute solvent-based systems by water-borne products, there is a growing interest in producing such copolymers by emulsion (or mini-emulsion) polymerization (Asua, 2002).

Adhesives are defined as substances capable of holding at least two surfaces together. A class of adhesives called pressure-sensitive adhesives (or PSAs) is characterized by instantaneous adhesion upon application of light pressure (Benedek and Heymans, 1997). The most common applications for PSAs are tapes, labels and protective films. In order to develop new application-specific products and improve existing processes, there is a need to identify the factors that influence the performance of PSAs. Reaction components and process conditions will affect latex properties such as copolymer composition, molecular weight distribution (MWD) and PSD. Those latex properties can affect rheological properties and film formation processes. Furthermore, latex rheology and film formation process can affect the performance of the adhesive.

1.1 Thesis Objectives

Mini-emulsion polymerizations are very useful as they allow one to control the number and size of the particles being formed. This improved control of the PSD coupled with a control over the MWD and composition of the copolymer could offer the possibility of tailoring the desired properties of PSAs. It is of interest in this thesis, to measure the effect of particle size and copolymer composition on adhesive properties.

Adhesive properties are sometimes fine-tuned by compounding the base polymer latex with various additives like tackifiers, plasticizers and fillers. Some un-compounded polymers are starting to replace compounded adhesives, especially in the area of PSAs, where un-compounded polyacrylates and their copolymers (like BA and St) are replacing the complex compounded materials (Satas, 1972).

In this study, the main objective was to understand the relationships between particle size and copolymer composition on the adhesive performance of the PSA. Thus, a study of the St/BA system in mini-emulsion and the investigation of the performance of mini-emulsion-based adhesives were undertaken. Other components in the PSA formulation (e.g. concentration of acrylic acid) were kept constant.

Traditional polymerization monitoring is often carried out using off-line characterization of samples from a process flow line. A disadvantage of off-line techniques for conversion and composition monitoring, such as gravimetry and ^{1}H-NMR spectroscopy is the time lag between sampling and results. Characterization techniques such as mid- and near-infrared, and Raman spectroscopy are especially suitable for real-time reaction monitoring (Kammona et al., 1999). IR spectroscopy is particularly important because of the high information content in the infrared spectrum and the various options available for sample measurement. Recently, the successful use of the ReactIR™ 1000 reaction analysis system to monitor emulsion homo-, co- and terpolymerizations in-line was reported (Hua and Dubé, 2001, 2002). Spectral measurements were obtained directly in the process stream without the need for sampling devices for on-line analysis. The next logical step would be to implement this technology for mini-emulsions. Because in-line monitoring using ATR-FTIR spectroscopy was successful on different emulsion systems, a second objective of this thesis was to validate the method for mini-emulsions.

1.2 Thesis Outline

This thesis consists of five chapters. Chapter 2 provides background information on IR spectroscopy and polymerization kinetics. As well, a literature review of papers dealing with the St/BA system and PSAs is included. The experimental design, apparatus,

and procedures followed during the experiment and the different methods used for the characterization of the latex are presented in Chapter 3. Chapter 4 contains a manuscript to be submitted for publication, which deals with IR monitoring of mini-emulsions and Chapter 5 contains a manuscript dealing with the understanding of the relationship between latex properties and the performance of the PSA. The final chapter provides a general discussion of the thesis as well as conclusions and recommendations based on the results obtained. Sample calculations are found in Appendix A. Because of the intention that some chapters could be read separately, the repetition of some common ideas and elements (e.g. experimental procedures) was inevitable.

References

1. Asua, J.M. Miniemulsion Polymerization. Prog. Polym. Sci. 2002, 27(7), 1283-1337.
2. Benedek, I.; Heymans, L.J. *Pressure-Sensitive Adhesives Technology*, Marcel Dekker Inc.: New York, 1997.
3. Capek, I.; C.S., Chern. Radical Polymerization in Direct Mini-Emulsion Systems. Adv. Polym. Sci. 2001, 155, 105-127.
4. Hua, H.; Dubé, M.A. Terpolymerization Monitoring with ATR-FTIR Spectroscopy. J. Polym. Sci.: Part A: Polym. Chem. 2001, 39, 1860-1876.
5. Hua, H.; Dubé, M.A. In-Line Monitoring of Emulsion Homo- and Copolymerizations Using ATR-FTIR Spectrometry. Polymer Reaction Engineering. 2002, 10(1-2), 21-40.
6. Kammona, O.; Chatzi; E.G.; Kiparissides, C. Recent developments in hardware sensors for the on-line monitoring of polymerization reactions. J. Macromol. Sci. – Rev. Macromol. Chem. Phys. 1999, C39(1), 57-134.
7. Lovell, P.A.; M.S., El-Aasser. *Emulsion Polymerization and Emulsion Polymers*, John Wiley and Sons, Inc.: England, 1997; 1-515.
8. Odian, G.G. *Principles of Polymerization*, 3rd Ed.; John Wiley and Sons, Inc.: New York, 1991; 1-374.

9. Rudin, A. *The Elements of Polymer Science and Engineering*, 2nd Ed.; Academic Press: San Diego, 1999; 1-522.
10. Satas, D. Tailoring pressure sensitive adhesive polymers. Adhes. Age. 1972, 15(10), 19-23.

Chapter 2 - Background

2.1 Free-radical Polymerization Kinetics

Free-radical chain growth polymerization is a chain reaction consisting of a sequence of three steps: initiation, propagation, termination, and at times, chain transfer. Note that throughout this thesis, monomer 1 refers to styrene and monomer 2 to butyl acrylate.

Initiation

The first step in free-radical polymerization is the initiation of the reaction. It involves the decomposition of an initiator (I) to free radicals (R•) that will allow the polymerization to take place by addition of a monomer to these radicals. Radicals can be produced by a variety of thermal, photochemical, and redox methods. The decomposition of the initiator in our study is realized by thermal, homolytic dissociation of a bond in the initiator upon absorption of energy generated by heat:

$$I \xrightarrow{k_d} 2R^{\bullet} \tag{1}$$

where k_d is the rate constant for initiator decomposition. Recombination of a certain quantity of free radicals takes place and the efficiency factor (f) is used to take this effect into account. The next step involves the reaction between the free radicals produced in equation (1) and the monomers, M_1 and M_2, present in the solution. Because the system used in this study contains two monomers, only two reactions are possible:

$$R^{\bullet} + M_1 \xrightarrow{k_{i,1}} R^{\bullet}_{1,1} \tag{2}$$

$$R^{\bullet} + M_2 \xrightarrow{k_{i,2}} R^{\bullet}_{1,2} \tag{3}$$

where $k_{i,j}$ is the initiation constant for a reaction in which a monomer j is added (1 for M_1 and 2 for M_2) and $R_{1,i}\bullet$ is a radical chain with 1 monomer of which the terminal monomer is i.

Propagation

The second step in free-radical polymerization involves the rapid addition of monomers to the growing radical chains formed in equations (2) and (3) to produce a radical chain larger by one monomer for each reaction. Large numbers of monomers can also be added to the radical chain (i.e. > 1000). The terminal model is one popular theory that attempts to describe free-radical chain polymerization kinetics. In this theory, it is assumed that the nature of the monomer to be added to the growing polymer chain is only influenced by the last unit of that chain and for the case of copolymerization with two different monomers; four different reactions can take place:

$$R^{\bullet}_{r,1} + M_1 \xrightarrow{k_{p,11}} R^{\bullet}_{r+1,1} \tag{4}$$

$$R^{\bullet}_{r,1} + M_2 \xrightarrow{k_{p,12}} R^{\bullet}_{r+1,2} \tag{5}$$

$$R^{\bullet}_{r,2} + M_1 \xrightarrow{k_{p,21}} R^{\bullet}_{r+1,1} \tag{6}$$

$$R^{\bullet}_{r,2} + M_2 \xrightarrow{k_{p,22}} R^{\bullet}_{r+1,2} \tag{7}$$

where r is the number of monomers in the chain and $k_{p,ij}$ is the propagation rate parameter for a radical chain in which terminal monomer i adds a monomer j. It must be understood that any of the two monomers present can be added to the radical chain. However, the probability of each monomer being added to the chain is usually not the same, as will be explained later.

Termination

The third step in free-radical polymerization is termination by mutual annihilation of two radicals. Two different methods for termination are possible. The first involves the combination of two radical chains of lengths n and m, respectively, to form one dead polymer molecule of length n+m. This process is called termination by combination and three reactions can occur:

$$R^{\bullet}_{n,1} + R^{\bullet}_{m,1} \xrightarrow{k_{tc,11}} R_n M_1 M_1 R_m \longrightarrow P_{n+m} \tag{8}$$

$$R^{\bullet}_{n,1} + R^{\bullet}_{m,2} \xrightarrow{k_{tc,12}} R_n M_1 M_2 R_m \longrightarrow P_{n+m} \tag{9}$$

$$R^{\bullet}_{n,2} + R^{\bullet}_{m,2} \xrightarrow{k_{tc,22}} R_n M_2 M_2 R_m \longrightarrow P_{n+m} \tag{10}$$

where $k_{tc,ij}$ is the termination by combination rate parameter in which the terminal monomers for the radical chains are i and j, respectively.

The second method involves the transfer of a hydrogen radical from the radical centre of one chain to the other resulting in the formation of two dead polymers. Both polymers will have a length corresponding to the length of their radical chain before termination. However, the end of one polymer chain will be saturated and the end of the other polymer chain will be unsaturated. This process is called termination by disproportionation. The polymer containing a terminal double bond may react with another radical chain to form a branched polymer. For a copolymerization system consisting of two different monomers, three reactions are possible:

$$R^{\bullet}_{n,1} + R^{\bullet}_{m,1} \xrightarrow{k_{td,11}} P_n + P_m \tag{11}$$

$$R^{\bullet}_{n,1} + R^{\bullet}_{m,2} \xrightarrow{k_{td,12}} P_n + P_m \tag{12}$$

$$R^{\bullet}_{n,2} + R^{\bullet}_{m,2} \xrightarrow{k_{td,22}} P_n + P_m \tag{13}$$

where $k_{td,ij}$ is the termination by disproportionation rate parameter in which the terminal monomers for the radical chains are i and j, respectively.

Both methods of termination can occur simultaneously although often one finds that one of the methods will be dominant depending on the polymer system. When this is the case, the overall termination constant (k_t) is equal to the sum of k_{tc} and k_{td}.

Chain Transfer

A fourth type of reaction can occur during polymerization. This reaction, known as chain transfer, involves the transfer of the active radical from a radical chain to another molecule such as monomer, initiator, solvent or another additive. Typically, a dead polymer chain and a small radical are formed. The following reactions are possible for a system of two monomers:

$$R^{\bullet}_{n,1} + M_1 \xrightarrow{k_{fm,11}} P_n + R^{\bullet}_{1,1} \tag{14}$$

$$R^{\bullet}_{n,1} + M_2 \xrightarrow{k_{fm,12}} P_n + R^{\bullet}_{1,2} \tag{15}$$

$$R^{\bullet}_{n,2} + M_1 \xrightarrow{k_{fm,21}} P_n + R^{\bullet}_{1,1} \tag{16}$$

$$R^{\bullet}_{n,2} + M_2 \xrightarrow{k_{fm,22}} P_n + R^{\bullet}_{1,2} \tag{17}$$

where $k_{fm,ij}$ is the rate constant for chain transfer to monomer in which the terminal monomer is i and the receiving monomer is j. In these reactions, the active radical centre is transferred to a monomer molecule, which may then propagate and create a radical chain. The net effect is that smaller polymer chains are being produced and this is reflected by a lower overall polymer molecular weight. Transfer to monomer reactions may also produce terminal double bonds, which can lead to branching.

In a way similar to that for small molecules, polymer chains can react with radicals in transfer reactions:

$$R^{\bullet}_n + P_m \xrightarrow{k_{fp}} P_n + R^{\bullet}_m \tag{18}$$

where k_{fp} is the rate constant for chain transfer a polymer. The radical is transferred from a polymer of length n to a polymer of length m. This reaction involves the removal of an atom from the polymer backbone and results in a trifunctional branch point.

If a lower molecular weight is desired, specific molecules such as chain transfer agents (CTA) can be added to the reaction mixture in order to increase the number of transfer reactions. Mercaptans are typically used as chain transfer agents and react according to the following scheme:

$$R_n^{\bullet} + RSH \xrightarrow{k_{fCTA}} P_n + RS^{\bullet} \tag{19}$$

where k_{fCTA} is the rate constant for chain transfer to CTA. Transfer reactions play an important role in the development of the molecular weight distribution. If one particular reaction is dominant over the others, the final copolymer may have a significantly lower molecular weight or more branching than expected.

Rates of Reaction

As previously mentioned, equation (1) is governed by the initiation rate constant and initiator efficiency. As long as these two values are known, k_{i1} and k_{i2} are not required to calculate the overall rate of initiation. The rate of decomposition of the initiator (R_d) depends on the efficiency factor (f) and the concentration of initiator [I]. Hence, the rate of decomposition of the initiator can be expressed as:

$$R_d = f k_d [I] \tag{20}$$

It is understood that the addition of the first monomer to the newly created free radical is very fast. Therefore, the limiting reaction in the initiation step is the decomposition of the initiator and the rate of initiation (R_i) corresponds to twice the rate of decomposition of the initiator (R_d).

The rate of polymerization (R_p) is determined by the concentrations of monomer and radical chains in solution. Then, the rate of propagation can be expressed as:

$$R_p = k_p[M][R\bullet] \tag{21}$$

In practice, it is very difficult to monitor the concentration of radical chains over time. Hence, this equation becomes difficult to solve. However, a quasi steady-state assumption can be made. This implies that the concentration of radical chains will initially rise but will reach a steady-state value very quickly. Thus, it can be assumed that the termination rate (R_t) is equal to the rate of initiation. The rate of termination also depends on the concentration of radical chains:

$$R_i = R_t = 2k_t[R\bullet]^2 \tag{22}$$

When combining equations (21) and (22), the concentration of radical chains disappears and the equation becomes much simpler to solve:

$$R_p = k_p[M]\sqrt{\left(\frac{2fk_d[I]}{k_t}\right)} \tag{23}$$

Autoacceleration

Many free-radical polymerizations are characterized by the presence of an autoacceleration in the rate of polymerization. As stated in equation 23, monomer concentration is directly proportional to the rate of polymerization but the following effect has been observed: the reaction rate increases as the conversion decreases. Such behaviour is referred to as the gel effect. Because the termination rate constant in equation 23 is diffusion-controlled, the gel effect can be explained by a decrease in k_t with increasing viscosity during the termination process.

Bimolecular termination occurs by way of a 3-step mechanism which includes translational diffusion, segmental diffusion, and chemical reaction. Translational diffusion is governed by the ability of two macroradicals to approach each other. Segmental diffusion involves the diffusion of the active radical centres toward each other.

Finally, the chemical reaction between the active radical centres occurs. For example, at the beginning of a bulk polymerization, very little polymer has been formed and the viscosity of the system is relatively low. At this point, the rate-limiting termination step is segmental diffusion. As the reaction proceeds, there is a noticeable increase in viscosity due to the entanglement of the polymer chains. This in turn leads to a decrease in the rate of translational diffusion, which now becomes rate-limiting and thus, a reduction in termination rate. During the later stages of the polymerization, the viscosity becomes so great that translational movement of the macroradicals is no longer possible. The only means for two active radical centres to meet and terminate is by the addition of monomer. Eventually, even the monomer cannot diffuse and the reaction mixture behaves like a solid. Note that in emulsion polymerizations, due to the high polymer concentration in the reaction loci (as will be explained later), diffusion-controlled termination will be active at a very early stage in the reaction. The rate of polymerization, R_p, is a function of the termination rate constant. The substantial decrease in k_t due to diffusion-controlled termination often results in a rapid rise in R_p, which is referred to as autoacceleration.

Composition and Reactivity Ratios

For this study, the system is a free-radical mini-emulsion copolymerization of styrene and butyl acrylate. The following equation, known as the Mayo-Lewis equation, is used to predict copolymer composition:

$$\frac{d[M_1]}{d[M_2]} = \frac{[M_1](r_1[M_1]+[M_2])}{[M_2](r_2[M_2]+[M_1])} \tag{24}$$

where r_1 and r_2 are the reactivity ratios of M_1 and M_2 respectively. The reactivity ratios for the copolymerization propagation step are related to the propagation rate constant as follows:

$$r_1 = \frac{k_{p,11}}{k_{p,12}} \tag{25}$$

$$r_2 = \frac{k_{p,22}}{k_{p,21}} \tag{26}$$

Equation 24 can also be expressed in terms of mole fractions instead of concentrations:

$$F_1 = 1 - F_2 = \frac{r_1 f_1^2 + f_1 f_2}{r_1 f_1^2 + 2 f_1 f_2 + r_2 f_2^2} \tag{27}$$

where F_1 is the instantaneous mole fraction of M_1 in the copolymer, and f_1 and f_2 are the instantaneous fractions of M_1 and M_2 in the reaction mixture.

Note that a composition drift could occur in the copolymer chain if the two reactivity ratios differ from one another. A composition drift is a change in the chemical composition of the copolymer chain formed throughout the polymerization. The composition of the copolymer will have a great influence on its glass transition temperature (T_g), which in turn will determine some of the adhesive properties like tackiness (Aubrey, 1977). Thus, great care must be taken to allow for minimal composition drift. If needed, a semi-batch control policy could be implemented to deal with such a composition drift.

2.2 Emulsion Polymerization Kinetics

The main ingredients in an emulsion polymerization are the monomer(s), the water, the surfactant(s) and the initiator(s). Chain transfer agents and buffers can be added to control the molecular weight and pH, respectively. When the concentration of surfactant exceeds its critical micelle concentration (CMC), the excess surfactant molecules aggregate to form small colloidal clusters referred to as micelles. In principle, polymer particles can be formed by the entry of radicals into the micelles (heterogeneous nucleation), precipitation of growing oligomers in the aqueous phase (homogeneous nucleation), and radical entry in monomer droplets. In conventional emulsion polymerization, monomer droplets are relatively large (1-10 μm) compared to the size of monomer-swollen micelles (10-20 nm), and hence the surface area of the micelles is

much greater than that of the monomer droplets (Asua, 2002). Consequently, the probability for a radical to enter into the monomer droplets is very low, and most particles are formed by homogeneous and heterogeneous nucleation.

Three Stages of Emulsion Polymerization

According to Harkins model (Harkins, 1947), a batch emulsion polymerization is divided into three intervals and a simplified representation is given in Figure 1.

- Interval I: This is the particle formation, or nucleation stage. The reaction rate and the number of particles increase as a function of time in a closed reactor. The end of this interval corresponds to the disappearance of micelles (Harkins considered that micelles are the only loci of particle nucleation).
- Interval II: The number of particles remains constant, and the monomer droplets, which play the role of monomer reservoir for the growing particles, maintain the concentration of monomer in the particles at the saturation point. The reaction rate is considered to be constant during this stage.
- Interval III: The beginning of the final stage corresponds to the disappearance of the monomer droplets. The concentration of monomer in the particles decreases, but the number of particles remains theoretically constant. During this period, the rate can either decrease, or increase depending on the reaction conditions. A drop in monomer concentration in the particles causes the decrease. The increase can often be attributed to an accumulation of radicals inside the particles due to the well-known gel, or Tromsdorff effect, brought on by an increase in the local viscosity.

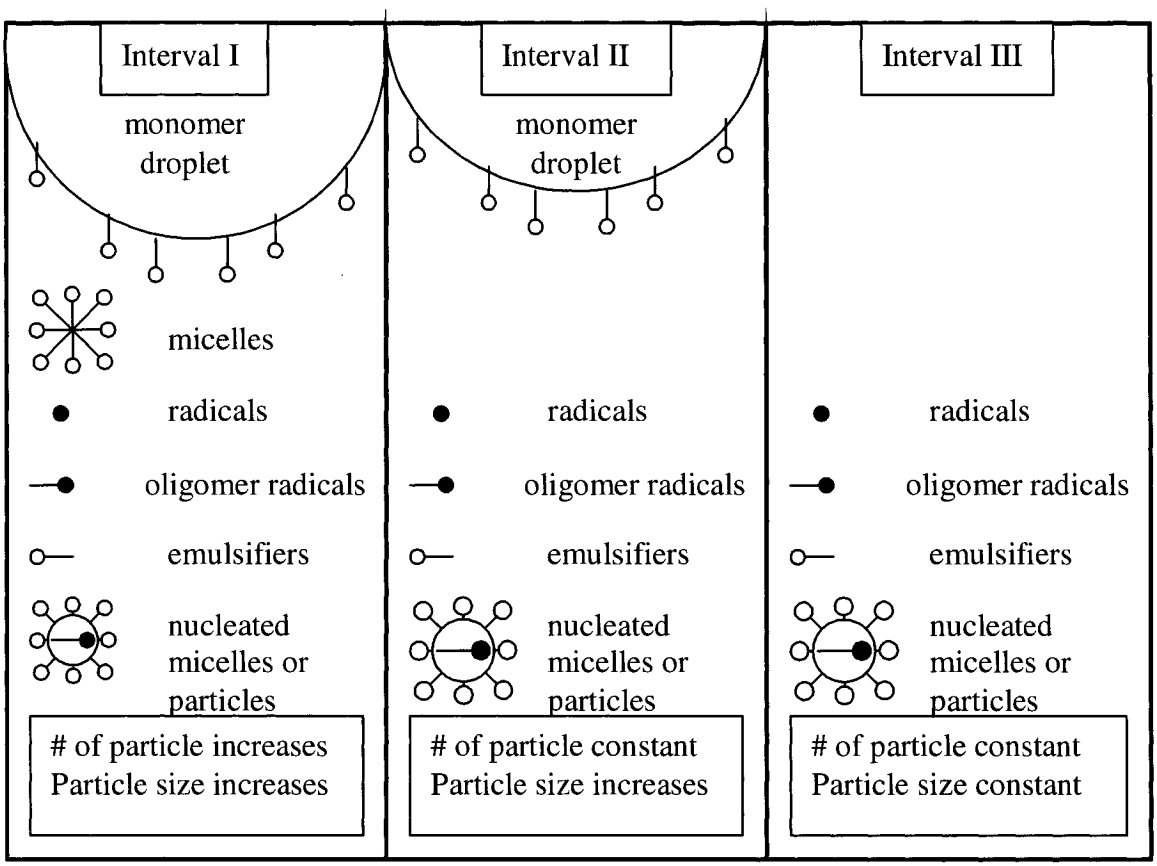

Figure 1: Different Intervals of an Emulsion Polymerization

2.3 Mini-emulsion Kinetics

The basis for mini-emulsion polymerization is an energetic homogenization process to reduce the size of the monomer droplets and the ingredients are basically the same ones found in a conventional emulsion with the exception of the co-surfactant. The droplet size can range from 50 to 500 nm in diameter (Capek and Chern, 2001) and the latex produced by mini-emulsion is characterized by a broader particle size distribution (PSD) (Asua, 2002) ranging from 50 to 1000 nm in diameter (Lovell and El-Aasser, 1997). If we manage to reduce the size of the droplets sufficiently, the resulting large surface area of the droplets allows them to compete effectively against the micelles to

capture the oligomeric radicals and to become the main loci of polymerization. The presence of micelles in mini-emulsion is dependent on the amount of surfactant used in the formulation and on the homogenization procedure. The ideal situation, where no micelles are formed, is obtained when the surfactant concentration does not exceed the CMC and the homogenization procedure gives sufficiently small monomer droplets.

Degradation Mechanisms

An important concept in mini-emulsion polymerization is the degradation of the monomer droplets by two mechanisms. The first is the coalescence of the interactive monomer droplets due to attractive van der Waals forces. The result is the fusion of two colliding droplets. This coalescence process can be minimized by adequate surfactant coverage on the droplet surface to counteract the van der Waals forces. The second mechanism is the Ostwald ripening process (Asua, 2002). This destabilization process refers to the diffusional degradation of droplets caused by the transport of monomer from the smaller droplets exhibiting a higher chemical potential, across the aqueous phase, and then to the large droplets. Ostwald ripening results in an increase in the average droplet size and a reduction in the total surface area of the monomer droplets. The Ostwald ripening effect can be minimized with an oil soluble co-surfactant. If they are properly stabilized, the number of particles at the end of the reaction will be the same as the number of droplets at the beginning. Ideally, droplet nucleation is the unique mechanism of particle formation in mini-emulsions if the formation of micelles can be avoided. Consequently, the stage of particle nucleation with monomer transport through the aqueous phase is avoided (Interval I and II in conventional emulsion). These critical differences mean that mini-emulsions will behave differently from a kinetic point of view than a conventional emulsion. It has been proposed that there is no period of constant rate during a mini-emulsion comparable to that proposed for conventional emulsion according to Harkins theory. This is due to the fact that the droplets are the site of polymerization and do not act as reservoirs. The rate of polymerization is not dependent on monomer diffusion from the droplets to the polymer particles (Ouzineb, 2003). Bechthold et al.

(2000) reported similar results in their investigation of the kinetics of mini-emulsion polymerization of styrene by calorimetry.

2.4 IR Spectroscopy

Fundamentals of IR Spectroscopy

Infrared or IR spectroscopy is a type of absorption spectroscopy, which is used to measure the ability of a sample to absorb different wavelengths of infrared radiation (Hyper Dictionary, 2003). The energy of infrared radiation is comparable in magnitude to the vibrational energy of chemical bonds. Then, if a vibrating molecule is hit with some infrared light, it will only absorb the frequencies in the light that matches exactly the frequencies of the different vibrational movements that make up that molecule. When this light is absorbed, the vibrational movements in the molecule will continue at the same frequencies but with larger amplitudes. The remaining light not absorbed by any of the vibrational movements in the molecule (or the reflection spectra) will be detected and analyzed to determine what frequencies were absorbed.

Functional Groups

From these analyses, an IR spectrum consisting of peaks whose frequencies are characteristic of the chemical bond present in the molecule can be constructed. By matching the peak positions with known compounds, IR spectra can be used to determine the presence or absence of certain functional groups. These characteristic frequencies can also be associated with functional groups in polymer chains because they are relatively unaffected by the chemical nature of the rest of the molecule and have nearly the same vibrational energy (or spectral region) regardless of the attached molecular skeleton (Colthup et al., 1990). Sometimes, specific couplings can occur with regularly ordered functional groups in polymers, and this condition shifts the group frequencies. Correlations between the presence of certain functional groups in the polymer chain and

the appearance of specific IR absorbance frequencies can lead to specific group frequencies for polymers.

Quantitative Analysis

Infrared spectroscopy includes wavelengths ranging from 0.7 to 1000 μm or wavenumbers ranging from 10 to 12800 cm^{-1} (the wavenumbers are simply the inverse of the wavelengths). This interval can be divided into three distinct spectral regions; namely near-infrared (NIR) ranging from 4000 to 12800 cm^{-1}, mid-infrared (MIR) ranging from 400 to 4000 cm^{-1} and far-infrared (FIR) ranging from 10 to 400 cm^{-1}. The NIR spectral region involves overtones and combination bands with lower frequencies of vibrations than in the MIR spectral region. Thus, the absorbencies in the NIR region are typically weaker than in the MIR region. The MIR spectral region encompasses the frequencies corresponding to the fundamental vibrations of virtually all functional groups of organic molecules. These spectral lines are typically narrow and distinct, and are easy to identify. As a result, quantitative analyses performed in the MIR region are usually straightforward and robust. A quantitative analysis is made possible by applying Beer's law, which stipulates that the absorbance intensity at a certain frequency is proportional to the concentration of the component that absorbs at that frequency.

Fourier Transform Infrared (FTIR)

For the measurement of the reflection spectra, either a dispersive spectrometer or an interferometer is used. Interferometers have a signal-to-noise ratio and spectral resolution superior to dispersive spectrometers in the conventional measurement of bulk samples (Suetaka, 1995). When an instrument is based on an interferometric measurement, it is classified as a Fourier transform infrared (FTIR) instrument (Gunzler and Gremlich, 2002). In general, Fourier transform is the method of choice for enhancing the spectral resolution or for analyzing a wide spectral region. Dispersive spectrometers are better suited for the observation of small spectral regions (Suetaka, 1995).

Attenuated Total Reflectance (ATR)

In conventional infrared spectroscopy, the intense absorption of water overlaps the majority of the mid-infrared spectral region. This makes it very difficult to collect any kind of information in this region. Applying the principle of internal reflection spectroscopy, the attenuated total reflectance (ATR) is a versatile, non-destructive technique for obtaining the infrared spectrum of materials either too thick or too strongly absorbing. In this technique, the sample is placed in contact with an internal reflection element (IRE) with high refractive index and low IR absorption in the region of interest. Diamonds are the most commonly used IREs (Gunzler and Gremlich, 2002). When the IR beam enters the internal reflection element below an angle that exceeds the critical angle for total internal reflection, an evanescent wave (see Figure 2) is set up which penetrates a small distance beyond the IRE surface into space.

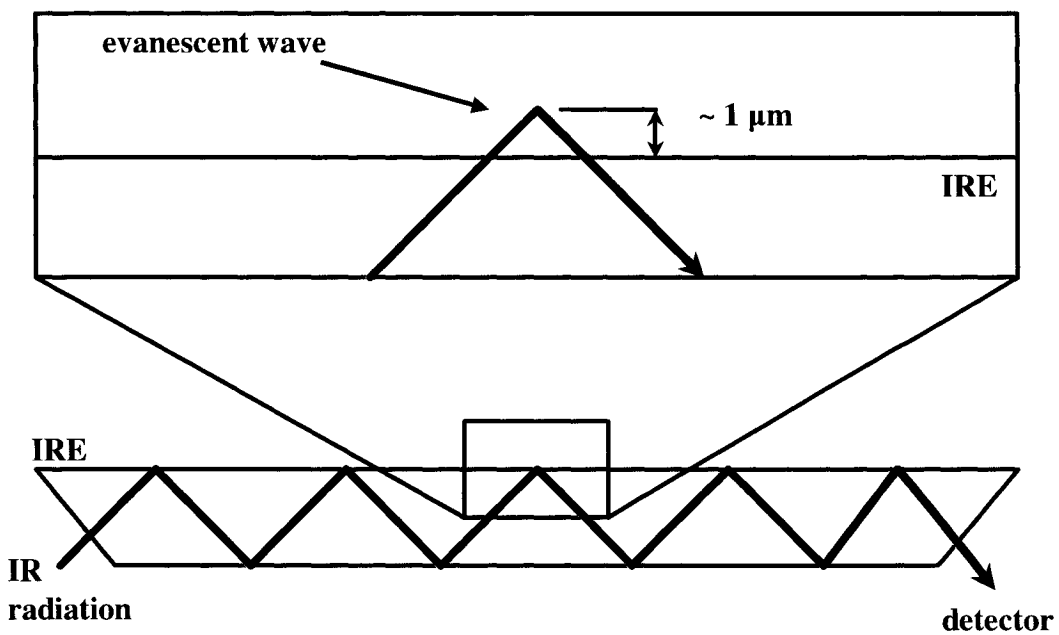

Figure 2: Total internal reflection at the interface of an internal reflection element. Depth of penetration of the evanescent wave is approximately 1 µm

A sample brought into intimate contact with the IRE can interact with the evanescent wave by absorbing specific infrared frequencies. The penetration depth of this evanescent wave can be designed to be well suited for quantitative analysis. What makes ATR a powerful technique is the fact that the intensity of the evanescent wave decays exponentially with the distance from the surface of the IRE. As the effective penetration depth is usually a fraction of the wavelength, total internal reflectance is generally insensitive to sample thickness and it allows thick or strongly absorbing samples (like water) to be analyzed.

Applications of ATR-FTIR

In the past, Attenuated Total Reflectance – Fourier Transform InfraRed (ATR-FTIR) spectroscopy was mainly used for the investigation of solids, liquids and thin films (Smith, 1996). Recent technological advancements have enabled the use of ATR-FTIR spectroscopy for the monitoring of polymerizations. The technology was successfully implemented in the monitoring of conversion and composition in a variety of polymerization media. For example, Full et al. (1992) followed the kinetics of a micro-emulsion with internal reflectance infrared spectroscopy. Storey et al. (1999, 2000) monitored the kinetics of a living cationic polymerization. Hua and Dubé (2001) and Jovanovic and Dubé (2001) successfully monitored several solution polymerizations. Hua and Dubé (2001, 2002) successfully applied the technology for the first time to an emulsion polymerization. There appear to be no studies evaluating the performance of ATR-FTIR spectroscopy for the monitoring of mini-emulsion polymerizations.

2.5 PSAs with St/BA Systems in Mini-emulsions

A PSA must be soft and tacky hence, its glass transition temperature (T_g) should be low, ranging from -20°C to -60°C. Polymers with low T_g, typically from a class of alkyl acrylates such as poly(butyl acrylate) and poly(2-ethylhexyl acrylate) are inherently soft and tacky but do not possess adequate shear strength. A balanced combination of tack, peel strength and shear strength is a primary concern for a PSA. As a consequence,

the copolymerization of an alkyl acrylate having a low T_g with a thermoplastic such as styrene or methyl methacrylate having a high T_g is useful to regulate this combination of tack, peel strength and shear strength. In addition, monomers with functional groups such as acrylic or methacrylic acids could be added to improve peel and shear strength although their addition often reduces tack (Jovanovic et al., 2004). Since tack, peel strength and shear strength are the three general adhesive properties that determine PSA performance, a brief description of each property will follow.

Tack

Tack is defined as the property that enables an adhesive to form a bond of measurable strength with a surface of another material upon brief contact under light pressure (ASTM 2979-88, 1995) or no pressure (PSTC-5, 2000). Tackiness should increase when the glass transition temperature (T_g) of the copolymer decreases (Aubrey, 1977) and T_g should in turn decrease when the copolymer composition is enriched with a soft polymer like poly(butyl acrylate). Because T_g depends on chain flexibility, all factors affecting chain flexibility such as sequence length distribution, molecular weight distribution, and cross-linking density will affect T_g. This concept was supported by Satas (1972, 1989) who concluded that tackiness should increase with low molecular weights. He demonstrated that an initially high value of tack associated with a low molecular weight would decrease and eventually level off when the molecular weight was increased. An increase in surfactant concentration could result in a decrease of tackiness if the water resistance is reduced or the surfactant molecules migrate to interfaces (Taylor, 2002). On the other hand, Brooks et al. (1984) reported that the influence of a proprietary stabilizer on the tack of a BA/VAc/MAA emulsion-based PSA was low.

Peel Strength

Peel strength represents the force required to remove a standard PSA strip from a specified test surface under a standard test angle (90^o or 180^o) under standard conditions. The incorporation of a high T_g component like poly(styrene) should improve peel strength up to the point where the adhesive becomes too stiff and does not wet the

surface, thus decreasing peel strength (Benedek et al., 1997). Low molecular weight polymers will show a mediocre resistance to peel and as the molecular weight continues to increase, the resistance to peel will eventually reach a maximum before starting to deteriorate at higher molecular weights (Satas, 1972, 1989). When surfactant molecules migrate to the film-substrate interface, peel strength could be affected. Charmeau et al. (1999) suggested that the increase of peel strength when the concentration of surfactant was also increased corresponded to the formation of a monolayer of surfactant at the PSA surface while a decrease in peel strength corresponded to the formation of a similar but much thicker layer that would behave as a weak boundary layer. Adhesive thickness is also a factor influencing peel strength. Peel strength is said to behave (increase or decrease) exponentially with respect to adhesive thickness (Benedek et al., 1997).

Shear Strength

Shear strength is the internal or cohesive strength of the adhesive mass. Usually, it represents the length of time it takes for a standard strip of PSA to fall from a test panel after application of a load. Shear resistance increases as the concentration of the high T_g component increases (Benedek et al., 1997). The resistance to shear will also be dependent on the molecular weight distribution of the polymer (Satas, 1972, 1989). High molecular weight polymers present a good resistance to shear but this property will degrade rapidly at lower molecular weights. As well, a broad molecular weight distribution will result in a lower shear resistance compared to a narrow one (Benedek et al., 1997). The presence of highly mobile small molecules like surfactant molecules is expected to decrease shear resistance.

Modeling Adhesive Performances

As mentioned previously, the performance of an adhesive depends heavily on its latex properties. Latex properties such as copolymer composition, MWD, PSD and gel content can be controlled by adjusting the operating conditions. Therefore, a good knowledge of the effect of operating conditions on the latex properties is required. In addition, the relationship between the latex properties and the performance of the

adhesive is of equivalent importance. The relationship between the operating conditions and the latex properties can be obtained by mathematical modeling of the polymerization reactor and extensive experimentation. Considerable efforts have already been devoted to the modeling and control of at least some of the latex properties mentioned above (Dubé et al., 1997, Gao and Penlidis, 2003) and hence, this study will focus on discovering the impact of latex properties on adhesive performance. The development of these relationships in the context of mini-emulsions has been limited (Jovanovic et al., 2004). In that exploratory investigation, the performance of BA/methyl methacrylate PSAs produced in a conventional emulsion and a mini-emulsion was compared. Structure-property relationships between the adhesive properties and the weight-average molecular weight and average particle size were also examined. They found that adhesives made from both polymerization processes (conventional and mini-emulsion) showed similar characteristics that could be tailored to obtain the desired properties. They also concluded that mini-emulsions could provide a greater control over the latex properties because of the compartmentalized nature of the particles and finer control of the particle size.

Mini-emulsion polymerization has exploded onto the research scene in terms of the numbers of publications and the development of a wide range of useful polymeric materials (Asua, 2002). However, this type of polymerization is characterized by complex kinetics and no adhesive property studies for free radical copolymerizations of styrene/butyl acrylate in mini-emulsion were found. Adhesive studies on similar systems using conventional emulsion could provide a basis for comparison.

Elizalde et al. (2002) presented a model relating the adhesive properties and the complete MWD of n-butyl acrylate/styrene latexes of fixed copolymer molar composition (85/15) using partial least squares regression (PLS-R). The model was validated and combined with a control strategy to tailor the copolymer composition and MWD.

Plessis et al. (2001 a, b) investigated a seeded semibatch emulsion polymerization of n-BA, with varying amounts of styrene as comonomer using potassium persulfate as the initiator at 75°C. They increased the amount of styrene from 0 to 10% and found that they could control the amount of gel and the level of branching by using the styrene as a control variable. They also found that the adhesive properties could be modified by adding small amounts of styrene. Furthermore, they investigated the effect of CTA

(dodecane-1-thiol) on the kinetics, gel fraction, level of branching, and MWD of the sol. By increasing the CTA concentration, they noticed that the gel fraction and the sol weight-average molecular weight showed a strong dependence. On the other hand, no effects were observed on the kinetics or the level of branching.

Tobing and Klein (2001), compared the performance of PSAs made from a semi-continuous emulsion and a solution polymerization. The PSAs were made from two different polymers: poly(2-ethyl-hexyl acrylate-stat-acrylic acid) and poly(n-butyl acrylate-stat-acrylic acid) at 97.5/2.5 wt%. They found that the difference in film network morphology caused significantly lower shear holding power for the emulsion-based PSA compared with that of the solvent-borne film. Unlike shear holding power, the loop tack and peel of the acrylic PSAs were mainly controlled by the same sol/gel molecular parameters, regardless of originating from an emulsion or solution polymerization. The important molecular parameters were sol-to-gel ratio, entanglement molecular weight, weight average molecular weight, and to a lesser extent, glass transition temperature.

References

1. Araujo, O.; Giudici, R.; Saldivar, E.; Ray, W.H. Modeling and experimental studies of emulsion copolymerization systems. I. Experimental results. Journal of Applied Polymer Science. 2001, 79(13), 2360-2379
2. ASTM D2979-88. Standard Test Method for Pressure-Sensitive Tack of Adhesives Using an Inverted Probe Machine, Annual Book of ASTM Standards, American Society for Testing and Materials: Philadelphia, 1995; Vol. 15.06.
3. Asua, J.M. Miniemulsion Polymerization. Prog. Polym. Sci. 2002, 27(7), 1283-1337.
4. Aubrey, D.W. *Pressure Sensitive Adhesives - Principles of Formulation. Developments in Adhesives*, Wake, W.C., Ed.; Applied Sci., Publishers: Barking, England, 1977.

5. Barclay, B.R.; Penlidis, A.; Gao, J. Modelling and simulation of complex aspects of multicomponent emulsion polymerization. Polymer Reaction Engineering. 2003, 11(4), 737-814
6. Bechthold, N.; Landfester, K. Kinetics of miniemulsion polymerization as revealed by calorimetry. Macromolecules. 2000, 33(13), 4682-4689.
7. Benedek, I.; Heymans, L.J. *Pressure-Sensitive Adhesives Technology*, Marcel Dekker Inc.: New York, 1997.
8. Brooks, T.W.; Kell, R.M.; Boss, L.G.; Nordhaus, D.E. Analysis of Factors Important in Emulsion Acrylic Pressure Sensitive, Adhesive Design. TAPPI Proceedings. TAPPI Polymers, Laminations and Coating Conference, Boston, September, 1984, 469-476.
9. Capek, I.; Chern, C.S. Radical Polymerization in Direct Mini-Emulsion Systems. Adv. Polym. Sci. 2001, 155, 105-127.
10. Charmeau, J.Y.; Gerin, P.A.; Vovelle, L.; Schirer, R.; Holl, Y. Adhesion of Latex Films. III. Surfactant Effects at Various Peel Rates. J. Adhes. Sci. Technol. 1999, 13(2), 203-215.
11. Colthup, N.B.; Daly, L.H.; Wiberley, S.E. *Introduction to Infrared and Raman Spectroscopy*, 3rd edition, Academic Press, Inc., San Diego, 1990, 1-547.
12. Dubé, M.A.; Soares, J.B.P.; Penlidis, A. Mathematical Modeling of Multicomponent Chain-Growth Polymerizations in Batch, Semibatch, and Continuous Reactors: A Review. Ind. Eng. Chem. Res. 1997, 36(4), 966-1015.
13. Elizalde, O.; Vicente, M.; Leiza, J.R.; Asua, J.M. Control of the adhesive properties of n-butyl acrylate/styrene latexes. Polym. React. Eng. 2002, 10(4), 265-283.
14. Forcada, J.; Asua, J.M. Emulsion copolymerization of styrene and methyl methacrylate. II. Molecular weights J. Polym. Sci.: Part A: Polym. Chem. 1991, 29(9), 1231-1242.
15. Full, A.P.; Puing, J.E.; Gron, L.U.; Kaler, E.W.; Minter, J.R.; Mourey, T.H.; Texter, J. Polymerization of Tetrahydrofurfuryl Methacrylate in Three-Component Anionic Microemulsions. Macromolecules. 1992, 25(20), 5157-5164.

16. Gao, J.; Penlidis, A. Comprehensive simulator/database package for reviewing free-radical homopolymerizations. Journal of Macromolecular Science - Reviews in Macromolecular Chemistry and Physics. 1996, 36(2), 199
17. Gao, J.; Penlidis, A. Comprehensive simulator/database package for reviewing free-radical copolymerizations. Journal of Macromolecular Science - Reviews in Macromolecular Chemistry and Physics. 1998, 38(4), 651-780
18. Gao, J.; Penlidis, A. Mathematical modeling and computer simulator/database for emulsion polymerizations. Progress in Polymer Science. 2002, 27(3), 403-535
19. Ghielmi, A.; Fiorentino, S.; Storti, G.; Mazotti, M.; Morbidelli, M. Long chain branching in emulsion polymerization. J. Polym. Sci.: Part A: Polym. Chem. 1997, 35(5), 827-858.
20. Gunzler, H.; Gremlich, H.U. *IR Spectroscopy, An introduction*, Wiley-VCH; Germany, 2002, 1-361.
21. Harkins, W.D. A General Theory of the Mechanism of Emulsion Polymerization. J. Am. Chem. Soc. 1947, 69(6), 1428-1444.
22. Hua, H.; Dubé, M.A. Off-line monitoring of butyl acrylate, methyl methacrylate and vinyl acetate homo- and copolymerizations in toluene using ATR-FTIR spectroscopy. Polymer. 2001, 42, 6009-6018.
23. Hua, H.; Dubé, M.A. Terpolymerization Monitoring with ATR-FTIR Spectroscopy. J. Polym. Sci.: Part A: Polym. Chem. 2001, 39, 1860-1876.
24. Hua, H.; Dubé, M.A. In-Line Monitoring of Emulsion Homo- and Copolymerizations Using ATR-FTIR Spectrometry. Polymer Reaction Engineering. 2002, 10(1-2), 21-40.
25. Jovanovic, R.; Dubé, M.A. Off-line monitoring of butyl acrylate and vinyl acetate homopolymerization and copolymerization in toluene. Journal of Applied Polymer Science. 2001, 82(12), 2958-2977.
26. Jovanovic, R.; Ouzineb, K.; McKenna, T.F.; Dubé, M.A. Butyl acrylate/methyl methacrylate latexes: Adhesive properties. Macromolecular Symposia. 2004, 206, 43-56.

27. Kammona, O.; Chatzi; E.G.; Kiparissides, C. Recent developments in hardware sensors for the on-line monitoring of polymerization reactions. J. Macromol. Sci. – Rev. Macromol. Chem. Phys. 1999, C39(1), 57-134.
28. Lovell, P.A.; El-Aasser, M.S. *Emulsion Polymerization and Emulsion Polymers*, John Wiley and Sons, Inc.: England, 1997; 1-515.
29. Odian, G.G. *Principles of Polymerization*, 3rd Ed.; John Wiley and Sons, Inc.: New York, 1991; 1-374.
30. Ouzineb, K. PhD thesis, Department of Chemistry, University of Claude Bernard Lyon I, Lyon, France, 2003.
31. Plessis, C.; Arzamendi, G.; Leiza, J.R.; Alberdi, J.M.; Schoonbrood, H.A.S.; Charmot, D.; Asua, J.M. Seeded semibatch emulsion polymerization of butyl acrylate: Effect of the chain-transfer agent on the kinetics and structural properties. J. Polym. Sci.: Part A: Polym. Chem. 2001, 39(7), 1106-1119.
32. Plessis, C.; Arzamendi, G.; Leiza, J.R.; Schoonbrood, H.A.S.; Charmot, D.; Asua, J.M. Kinetics and polymer microstructure of the seeded semibatch emulsion copolymerization of n-butyl acrylate and styrene. Macromolecules. 2001, 34(15), 5147-5157.
33. PSTC-5. Quick Stick of Pressure Sensitive Tapes, Test Methods for Pressure Sensitive Adhesive Tapes (13th ed), Pressure Sensitive Tape Council: Northbrook, 2000.
34. Rudin, A. *The Elements of Polymer Science and Engineering*, 2nd Ed.; Academic Press: San Diego, 1999; 1-522.
35. Saldivar, E.; Ray, W.H. Control of semicontinuous emulsion copolymerization reactors. Journal of Engineering and Applied Science. 1997, 43(8), 2021-2033
36. Saldivar, E.; Ray, W.H. Mathematical modeling of emulsion copolymerization reactors: Experimental validation and application to complex systems. Industrial & Engineering Chemistry Research. 1997, 36(4), 1322-1336
37. Saldivar, E.; Dafniotis, P.; Ray, W.H. Mathematical modeling of emulsion copolymerization reactors. I. Model formulation and application to reactors operating with micellar nucleation. Journal of Macromolecular Science - Reviews in Macromolecular Chemistry and Physics. 1998, 38(2), 207-325

38. Samer, C.J.; Schork, F.J. Dynamic modeling of continuous miniemulsion polymerization reactors. Polymer Reaction Engineering. 1997, 5(3), 85-124
39. Satas, D. Tailoring pressure sensitive adhesive polymers. Adhes. Age. 1972, 15(10), 19-23.
40. Satas, D. *Handbook of Pressure Sensitive Adhesive Technology*; Van Nostrand Reinhold: New York, 1989.
41. Smith, B.C. *Fundamentals of Fourier Transform Infrared Spectroscopy*, CRC Press, Boca Raton FL, 1996, 1-202.
42. Storey, R.F.; Donnaley, A.B. Initiation effects in the living cationic polymerization of isobutylene. Macromolecules. 1999, 32(21), 7003-7011.
43. Storey, R.F.; Maggio, T.L. Real-time monitoring of carbocationic polymerization of isobutylene via ATR-FTIR spectroscopy. Macromolecules. 2000, 33(3), 681-688.
44. Suetaka, W. *Surface Infrared and Raman Spectroscopy, Methods and Application*, Plenum Press, New York, 1995, 1-270.
45. Taylor, M.A. *Polymer Dispersions and Their Industrial Applications*, Wiley-VCH: Weinheim, 2002.
46. Tobing, S.D.; Klein, A. Molecular parameters and their relation to the adhesive performance of acrylic pressure-sensitive adhesives. Journal of Applied Polymer Science. 2001, 79(12), 2230-2244.

Chapter 3 - Experimental Procedures

3.1 Reagent

The reagents: Styrene (St), Butyl Acrylate (BA), Acrylic Acid (AA), octadecyl acrylate (ODA), the chain transfer agent (CTA) n-dodecyl mercaptan, sodium dodecyl sulfate (SDS), Triton X-405, sodium hydrogen carbonate ($NaHCO_3$), and potassium persulfate (KPS) were used without any further purification. All components used to perform the characterizations, i.e., toluene, ethanol, methanol, chloroform-d, tetrahydrofuran (THF), sodium hydroxide (NaOH), and calcium chloride ($CaCl_2$) were also used as received.

3.2 Experimental Design

Full conversion experiments were designed to understand the relationships between the latex properties and the performance of the PSA and these experiments are shown in Table 1. In addition, full conversion experiments were also used to validate the ATR-FTIR monitoring method for mini-emulsions and are shown in Table 2. All recipes were performed as mini-emulsions with a sonication time of 3 minutes, a reaction temperature of 80°C and a solids content of 50 wt.%. The following concentrations of ingredients were also kept constant: water = 90 phm, $NaHCO_3$ = 1 phm, KPS = 0.75 phm, AA = 4 phm, CTA = 0.25 phm where phm represents parts per hundred parts of monomer. The temperature and pH profile for all the runs can be found in Appendix B.

Table 1: Batch recipes – main objective

	St (phm)[1]	BA (phm)	Triton (phm)	SDS (phm)	ODA (phm)
Run 1	5	95	0.5	0.03	0.5
Run 2	5	95	1	0.06	1
Run 3	5	95	2.5	0.15	2.5
Run 4	10	90	0.5	0.03	0.5
Run 5	10	90	1	0.06	1
Run 6	10	90	2.5	0.15	2.5
Run 7	15	85	0.5	0.03	0.5
Run 8	15	85	1	0.06	1
Run 9	15	85	2.5	0.15	2.5
Run 5-2	10	90	1	0.06	1
Run 5-3	10	90	1	0.06	1

[1]phm = parts per hundred parts monomer

Table 2: Batch recipes – secondary objective

		St (phm)[1]	BA (phm)	Triton (phm)	SDS (phm)	ODA (phm)
Runs used for the model	Run 2	5	95	1	0.06	1
	Run 3	5	95	2.5	0.15	2.5
	Run 4	10	90	0.5	0.03	0.5
	Run 5	10	90	1	0.06	1
	Run 6	10	90	2.5	0.15	2.5
	Run 8	15	85	1	0.06	1
	Run 3-1	5	95	2.5	0.15	2.5
	Run 3-2	5	95	2.5	0.15	2.5
Runs used for the validation	Run 1	5	95	0.5	0.03	0.5
	Run 3-4	10	90	1	0.06	1
	Run 5-1	10	90	1	0.06	1
	Run 7	15	85	0.5	0.03	0.5
	Run 7-1	15	85	0.5	0.03	0.5

[1]phm = parts per hundred parts monomer

3.3 Apparatus

Mini-emulsion copolymerizations were performed in a Labmax™ setup (Mettler Toledo) which comprises a jacketed 1.2L stainless steel batch reactor. An anchor stirrer was used to mix the reactor contents at 200 rpm. The reactor was equipped with a nitrogen line to purge and/or pressurize the reactor, a sampling line, an initiator-loading cell, a reflux condenser with a vent line, and a port for the IR probe. The final position of the probe was about 2 mm above the blades of the agitator to ensure the monitoring of well-mixed latex. The reaction temperature and stirring speed were controlled by Camille® software (Mettler-Toledo). Figure 1 shows the Labmax™ reactor setup.

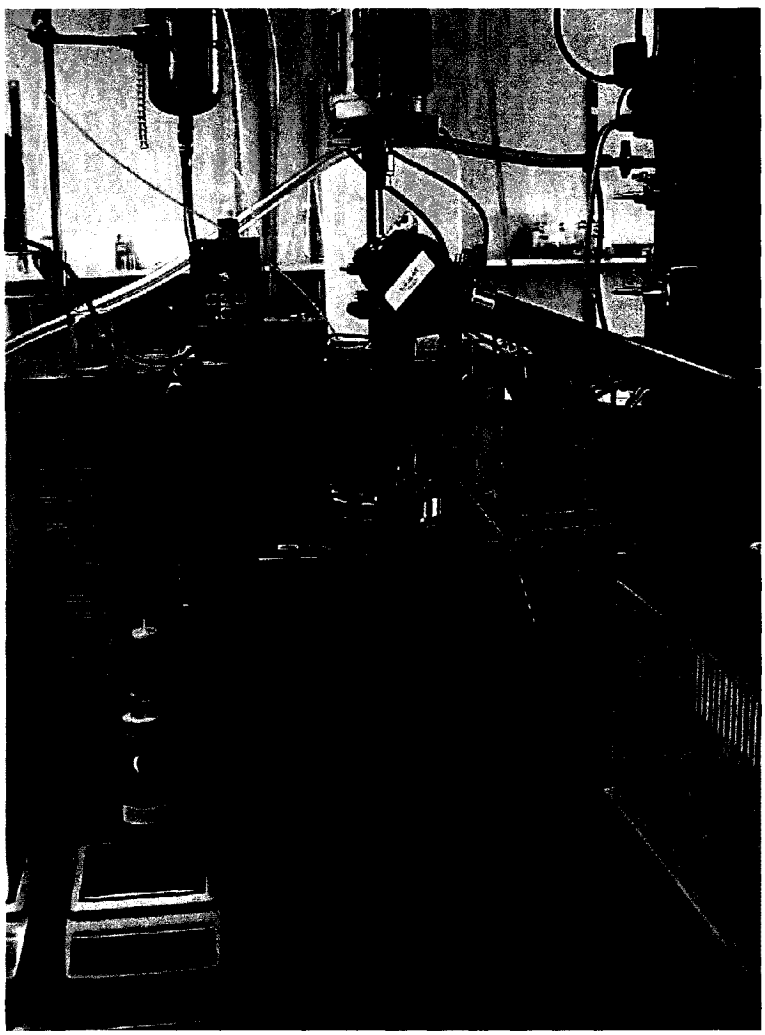

Figure 1: 1.2L stainless steel batch reactor

A ReactIR™ 1000 (ASI Applied Systems, Inc., Mettler Toledo) reaction analysis system was used in-line to collect mid-FTIR spectra (4000-650 cm^{-1}) of the mini-emulsion copolymerization reactions. The apparatus was equipped with a light conduit and a diamond composite probe inserted into the reactor. This setup allowed for non-destructive in-line monitoring of hostile reaction environment (Jovanovic, 2001). The IR apparatus is shown in Figure 2.

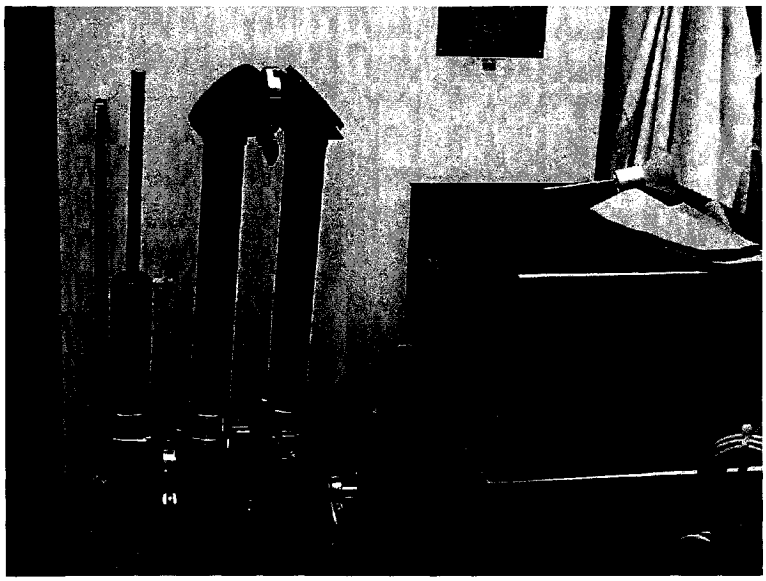

Figure 2: ReactIR™ 1000

3.4 Monomer Mixture Preparation

St, BA, and ODA were poured in a beaker and mixed with a magnetic agitator for 15 minutes. Water, Triton X-405, and SDS were also poured in a beaker and mixed with a magnetic agitator for 15 minutes. Both solutions were then poured in one beaker and mixed for one hour. After one hour, the mixture was sonicated using a Fisher Scientific 550 sonic dismenbrator. The sonicator shown in Figure 3 is a device that emits sound waves to break down the monomer droplets into smaller droplets. Samples of 200 mL were poured in a plastic container and sonicated for a fixed period of time (3 minutes) at a constant intensity (Level 6). The collision of the particles caused by the sound waves inside the container generated an appreciable amount of heat and the process had to be

performed in an ice bath. When necessary, AA and $NaHCO_3$ could be added to the already sonicated mixture.

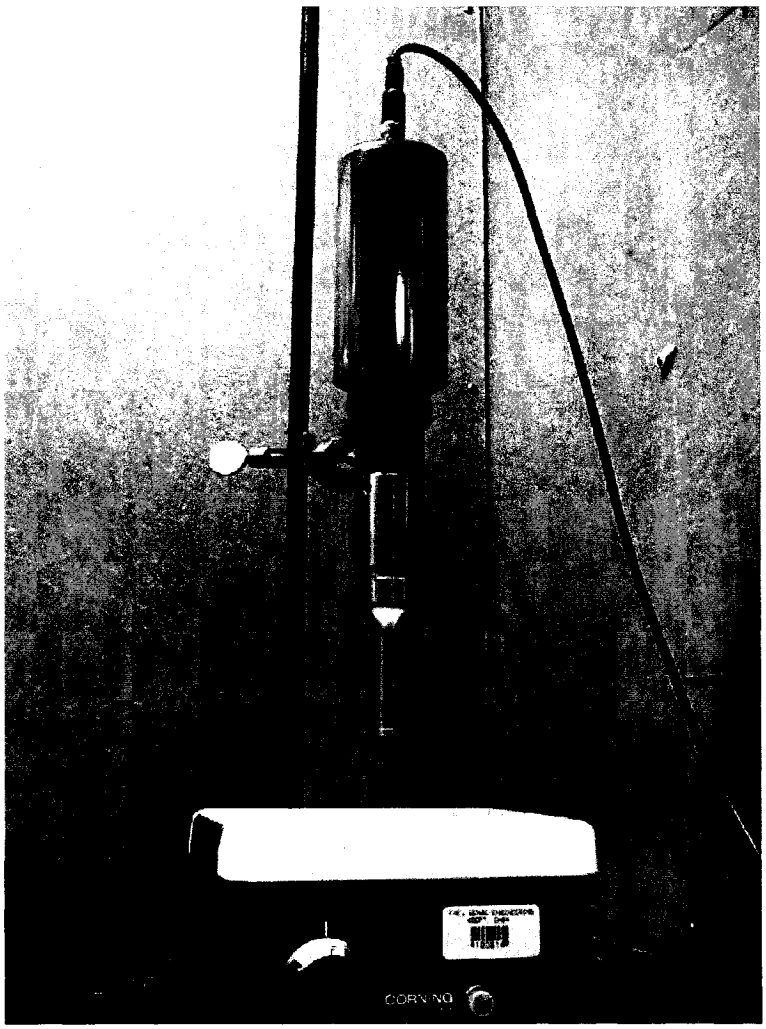

Figure 3: Sonicator

3.5 Polymerization

Full conversion mini-emulsion copolymerizations of St/BA were run at 80°C. First, the IR probe was inserted into the empty reactor to record the air background spectrum. Next the sonicated mixture was poured into the reactor and the reactor was closed. The temperature control program was then activated to heat the reaction mixture. Before the initiator was injected, the system was purged of oxygen by bubbling N_2

through the mixture for at least 40 minutes. When the set point temperature was reached, the initiator dissolved in de-ionized water was deoxygenated by bubbling N_2 through it and charged into the loading cell. The initiator solution was then charged into the reactor. Reaction monitoring and process temperature monitoring were started simultaneously after the initiator had been charged. This corresponded to polymerization time zero. During the reaction, at suitable time intervals, samples were taken through a sampling port, cooled down in a cold bath and approximately 3g of the sample was poured into a pre-weighed dish and allowed to dry.

3.6 Characterization

Gravimetry

The conversion, X (wt. fraction), was measured by gravimetry and was based on total monomer conversion. The overall conversions for all the runs can be found in Appendix B. As mention previously, samples were poured into pre-weighed dishes and weighed. They were dried in a fume hood at room temperature for at least one day and then in a vacuum oven at about 30°C for another day. The following equation was used to calculate the % solids (sample calculations can be found in Appendix A):

$$\%\ \text{solids} = \frac{(\text{wt. of dried sample and dish - wt.of empty dish})}{(\text{wt. of dish and sample - wt. of empty dish})} \text{X } 100 \qquad (1)$$

The conversion was calculated after correcting for all the other reagents present in the sample using the following equation:

$$\text{X(wt. fraction)} = \frac{\%\ \text{solids}/100 - \text{wt. fr. Triton - wt. fr. SDS - wt. fr. ODA - wt. fr KPS - wt. fr CTA}}{\text{initial wt. fr. monomers}} \qquad (2)$$

^{1}H-NMR Spectroscopy

Proton nuclear magnetic resonance spectroscopy (^{1}H-NMR) is used frequently to determine the average or cumulative composition of copolymers. The requirements for the applicability of NMR to any system are that all polymer chains be soluble in a suitable deuterated solvent and that the peaks do not overlap each other. For most polymer samples this is feasible, unless the polymers are too heavily crosslinked or chemically too heterogeneous.

Analyses were carried out at room temperature in deuterated chloroform (about 2% weight per volume solution), which was used as the solvent and the reference. The measurements were made with a Bruker AMX-500 Fourier transform ^{1}H-NMR spectrometer. The acquisition time was 4.6 seconds and 16 scans were performed per readout. The relative amounts of monomer bound in the copolymer were estimated from the areas under the appropriate absorption peaks of the spectra. Refer to Appendix B for an example of a ^{1}H-NMR spectrum. The spectral peaks for the $-OCH_2$ group in BA were located at ~3.4-4 ppm and the cyclic (5H) group in St was located at ~6.6-7.2 ppm. The copolymer composition for all the runs can be found in Appendix B.

ATR-FTIR Spectroscopy

ATR-FTIR spectroscopy is a method where a strongly absorbing medium is placed on one or both sides of a reflective crystal. In principle, it can be used to analyze emulsions and latexes (Lovell and El-Aasser, 1997). The number of scans and resolution must be selected to provide an adequate signal to noise ratio. For the monitoring of St/BA mini-emulsion copolymerizations in this study, 128 scans and a resolution of 4 cm^{-1} were assumed to give a satisfactory signal to noise ratio. To ensure continuous monitoring, the reaction spectra were acquired every 2 minutes.

The absorbance of different functional groups inside the monomers or polymers was monitored through the course of the reaction. Each functional group was associated with a characteristic peak and the concentration of a component was proportional to the absorbance, which could be measured as peak height, peak height ratio, peak area or peak area ratio. Real-time peak profiles of monomers (changes in absorption for a specific

component) were used to calculate the conversion and the copolymer composition. Sample calculations can be found in Appendix A and monomer peak assignments can be found in Appendix B. For the univariate method, the following expression was used to obtain the conversion of the individual monomers, x, in the reaction mixture:

$$x\,(\text{mol fraction}) = 1 - \frac{\text{peak height at time t}}{\text{peak height at time t} = 0} \tag{3}$$

where peak height at time t=0 represents the absorbance of the component in the reaction mixture prior to polymerization. Overall conversion, X, can be expressed in mol or mass fraction using the following expression:

$$X\,(\text{mol fraction}) = \frac{n_1}{n_1 + n_2} x_1\,(\text{mol fraction}) + \frac{n_2}{n_1 + n_2} x_2\,(\text{mol fraction}) \tag{4}$$

where $\frac{n_i}{n_i + n_j}$ represents the mole fraction of monomer i in the reaction mixture. The expression could also be written as a function of mass fraction:

$$X\,(\text{mass fraction}) = \frac{m_1}{m_1 + m_2} x_1\,(\text{mol fraction}) + \frac{m_2}{m_1 + m_2} x_2\,(\text{mol fraction}) \tag{5}$$

where $\frac{m_i}{m_i + m_j}$ represents the mass fraction of monomer i in the reaction mixture.

Gel Permeation Chromatography

Average molecular weights were measure using size exclusion chromatography (SEC). The technique, also known as gel permeation chromatography (GPC), consists of a column fractionation method in which solvated polymer molecules are separated according to their hydrodynamic volumes. The separation occurs as the solute molecules in a flowing liquid move through a stationary bed of porous particles. Solute molecules of

a given size are excluded from some of the pores of the column packing, which itself has a distribution of pore sizes. Larger solute molecules can permeate a smaller proportion of the pores and thus exit from the column earlier than smaller molecules (Lovell and El-Aasser, 1997).

Polymer molecular weight averages and distributions were determined with a Waters Associates GPC system equipped with three Waters Styragel-HR columns (10^3, 10^4, and 10^6 Å pore size) installed in series, thermostated to 30°C, and a Waters 410 differential refractometer thermostated to 38°C. THF was used as the mobile phase and was delivered at 0.3 mL/min. Polymer samples were dissolved in THF to produce solutions with a concentration of approximately 0.005 g/10mL and filtered through 0.45 μm filters to remove any high molecular weight gel. A quantity of 200 μL of each solution was injected into the GPC and the data were analyzed using the Millennium 32™ (version 3.05) chromatography manager software. Polymer molecular weights were calculated using the universal calibration principle, given the Mark-Houwink, K and α, parameters of polymer in THF shown in Table 3 (Hua, 2000). The values of K and α for the copolymers were obtained using weighted averages based on the cumulative copolymer composition data.

Table 3: Mark-Houwink parameters determined in THF

Polymer	K (x 10^3 mL/g)	α
Polystyrene	16	0.700
Polybutyl acrylate	11	0.708

BI-DCP

Latex particle size and PSD were determined using a Brookhaven disc centrifuge photosedimentometer (BI-DCP). For particles smaller than 3 microns, centrifugation is employed to accelerate sedimentation (Lovell and El-Aasser, 1997). The practical lower limit is about 0.1 microns and is dictated by the fact that, with decreasing particle size, the influence of diffusion (Brownian motion) becomes increasingly important until it can

no longer be neglected in comparison to the sedimentation displacement, even at high centrifugation speeds. The upper practical limit is dictated by the speed of sedimentation with particles having a diameter larger than about 3 microns traversing the sample cell in too short a time to measure the sedimentation velocity with sufficient accuracy. The principle of disc centrifuge is the following:

$$t = \frac{k\eta \ln(r_d / r_i)}{\Omega^2 \Delta\rho \, d^2} \tag{6}$$

where d is the diameter of a spherical particle, t is the appearance time of the particle at the detector, Ω is the rotational velocity (rpm), $\Delta\rho$ is the density difference (ρ - ρ_0) of particle and medium, η is the medium viscosity, k is a constant, and r_d and r_i are the path of the particle from the initial radius (r_i) at the surface of the spin fluid to the radius at the detector (r_d).

All final latexes were analyzed for particle size using a Brookhaven BI-DCP instrument. Refer to Appendix B for an example of a particle size determination. A gradient fluid containing 0.1 mL of dodecanol, 0.2 mL methanol, and 15 mL of water was first prepared and injected into a spinning disc. To ensure accurate instrument reading, 0.2 mL of a polystyrene (PS) standard solution with a narrow particle size distribution was injected. The standard PS solution consisted of 3 mL of distilled de-ionized water, 1 mL of methanol, and 3 drops of the PS standard. The same amount (0.2 mL) of the sample solution was then injected and this solution consisted of 3 mL of distilled de-ionized water, 1 mL of methanol, and 3 drops of the sample. By accounting for the size of the previously injected sample, the same gradient was used to determine the PSD of several samples. The number-averaged diameter for each PSD was used as the particle diameter for the latexes in this thesis.

Gel Content

Gel content was determined using the membrane partitioning method (Tobing and Klein, 2001). A known amount of sample was sealed between two

polytetrafluoroethylene membranes (pore size of 0.2 um and diameter of 47mm). Enclosed samples were shaken for 72 hours in THF. Sealed pouches were air-dried until a constant weight was achieved. The difference between the initial and final weight of the sample was used to calculate the gel content.

Glass Transition Temperature (T_g)

One of the most common models used for the prediction of T_g in polymers is the Fox model (Fox, 1956) where T_g is the overall T_g and T_{gi} is the T_g of homopolymer i, where i varies from 1 to n. Similarly, w_i represents the weight fraction of homopolymer i, where i varies from 1 to m.

$$\frac{1}{T_g} = \frac{w_1}{T_{g1}} + \frac{w_2}{T_{g2}} + \ldots \frac{w_n}{T_{gm}} \tag{7}$$

Using T_{g1} (pSt) = 375 K, T_{g2} (pBA) = 221 K, T_{g3} (pAA) = 379 K for the T_g's of the homopolymers, the overall T_g's using the Fox model were calculated.

Adhesive Testing

Before casting the film, particle agglomerates were removed from the latexes using a size #30 mesh. Each latex were then coated onto a polyethylene terephthalate carrier using a Meyer rod #30 to give a dry film thickness of 30 μm when dried at room temperature. The films were dried for 2 days before testing. All the tests were performed according to the Test Methods for Pressure Sensitive Tapes (Pressure Sensitive Tape Council or PSTC, 2000) with stainless steel substrates. Three adhesive tests were performed to evaluate the tack, peel strength and shear strength of the PSAs. Two films were cast per latex and three specimens from each film were used for each adhesive test. A hierarchical design was used to test run-to-run and film-to-film differences. The analyses of the results have shown no film-to-film differences; therefore the average of the six measurements was used in the analysis of the results.

Tack was measured using the PSTC-16 (loop tack) standard. A specimen of 25.4 x 177.8 mm was cut and one inch on both sides was masked with masking tape. A loop

with the adhesive facing outside was formed and placed in the upper grip of an Instron 1100 universal tester (Instron, Inc.). The loop was then brought into contact with the substrate mounted onto a loop tack fixture inserted into the bottom grip. When the loop covered and area of 25.4 x 25.4 mm, the upper grip was brought up at a crosshead speed of 300 mm/min. The maximum force required to remove the specimen was recorded as the loop tack.

Peel strength was measured using the PSTC-101 (180° peel) standard. A specimen of 25.4 x 304.8 mm was cut and laminated onto the substrate using a 2040 g rubber coated roller. The average force per 10 mm to peel the specimen from the substrate was recorded. The testing speed for the Instron 1100 universal tester (Instron, Inc.) was 300 mm/min.

Shear strength was measured using the PSTC-107 standard. A specimen of 25.4 x 152.4 mm was cut and an area of 25.4 x 25.4 mm was laminated onto the substrate using a 2040 g rubber coated roller. A 500 g weight was placed at the end of the specimen. Time to failure was recorded automatically using Labview™ software (National Instruments).

References

1. Fox, T.G. Bull. Am. Phys. Soc. 1956, 1, 123.
2. Hua, H.; Dubé, M.A. In-Line Monitoring of Emulsion Homo- and Copolymerizations Using ATR-FTIR Spectrometry. Polymer Reaction Engineering. 2002, 10(1-2), 21-40.
3. Jovanovic, R. MASc. thesis, Department of Chemical Engineering, University of Ottawa, Ottawa, 2001.
4. Jovanovic, R.; Dubé M.A. Off-Line Monitoring of Butyl Acrylate and Vinyl Acetate Homopolymerization and Copolymerization in Toluene. Journal of Applied Polymer Science. 2001, 82, 2958-2977.
5. Lovell, P.A.; M.S., El-Aasser. Emulsion Polymerization and Emulsion Polymers, John Wiley and Sons, Inc.: England, 1997; 1-515.

6. Pressure Sensitive Tape Council. Test Methods for Pressure Sensitive Adhesive Tapes. 13th ed. Pressure Sensitive Tape Council, Northbrook, IL, USA, 2000.
7. Rudin, A. *The Elements of Polymer Science and Engineering*, 2nd Ed.; Academic Press: San Diego, 1999; 1-522.
8. Satas, D. *Handbook of Pressure Sensitive Adhesive Technology*, 2nd Ed.; Van Nostrand Reinhold: New York, 1989; 1-830.
9. Tobing, S.D.; Klein, A. Molecular parameters and their relation to the adhesive performance of acrylic pressure-sensitive adhesives. Journal of Applied Polymer Science. 2001, 79(12), 2230-2244.

Chapter 4 – Paper on IR Monitoring

Introduction

Traditional polymerization monitoring is often carried out using off-line characterization of samples from a process flow line. A disadvantage of off-line techniques for conversion and composition monitoring, such as gravimetry and ^{1}H-NMR spectroscopy is the time lag between sampling and results. Despite their accuracy, these techniques can rarely be used for real-time process monitoring and control. Spectroscopic techniques such as mid- and near-infrared, and Raman spectroscopy are especially suitable for real-time reaction monitoring.[1] They can provide structural and kinetic information without costly modifications to existing process equipment. IR spectroscopy is particularly important because of the high information content in the infrared spectrum and the various options available for sample measurement. IR spectroscopy has become one of the most important analytical methods for preparative as well as analytical chemists.[2] Recently, we have reported the successful use of the ReactIR™ 1000 reaction analysis system to monitor emulsion homo-, co- and terpolymerizations in-line.[3, 4, 5] Spectral measurements were obtained directly in the process stream without the need for sampling devices for on-line analysis. Because this technology has never been applied to mini-emulsions to our knowledge, our goal was to evaluate the in-line monitoring of this process using ATR-FTIR spectroscopy.

Background

ATR-FTIR Spectroscopy

In conventional infrared spectroscopy, the intense absorption of water overlaps the majority of the mid-infrared spectral region. This makes it very difficult to collect any kind of information in this region. Applying the principle of internal reflection spectroscopy, attenuated total reflectance (ATR) is a versatile, non-destructive technique for obtaining the infrared spectrum of materials either too thick or too strongly absorbing. In this technique, the sample is placed in contact with an internal reflection element (IRE) with a high refractive index and low IR absorption in the region of interest. Diamonds are

the most commonly used IRE.[2] When the IR beam enters the internal reflection element below an angle that exceeds the critical angle for total internal reflection, an evanescent wave is set up which penetrates a small distance beyond the IRE surface into space. A sample brought into intimate contact with the IRE can interact with the evanescent wave by absorbing specific infrared frequencies. The penetration depth of this evanescent wave can be designed to be well suited for quantitative analysis and is generally in the range of 1 to 10 μm. What makes ATR a powerful technique is the fact that the intensity of the evanescent wave decays exponentially with the distance from the surface of the IRE. As the effective penetration depth is usually a fraction of the wavelength, total internal reflectance is generally insensitive to sample thickness and it allows thick or strongly absorbing samples (like water) to be analyzed.

Recent technological advancements have enabled the use of Attenuated Total Reflectance–Fourier Transform Infrared (ATR-FTIR) spectroscopy for the monitoring of polymerizations.[6] The technology was successfully implemented in the monitoring of conversion and composition for a variety of polymerizations. For example, Full et al.[7] followed the kinetics of a micro-emulsion with internal reflectance infrared spectroscopy. Storey et al.[8, 9] monitored the kinetics of a living cationic polymerization. Research in our laboratories has resulted in the successful monitoring of solution and emulsion polymerizations for a variety of polymer systems.[3, 4, 5, 10] There appear to be no published studies evaluating the performance of ATR-FTIR spectroscopy for the monitoring of mini-emulsion polymerizations.

Conventional Emulsions

The presence of water and the heterogeneity of emulsion polymerizations make them particularly challenging to monitor using IR spectroscopy. In conventional emulsion polymerizations, the main ingredients are the monomer(s), water, surfactant and initiator. Chain transfer agents and buffers are often added to control the molecular weight and pH, respectively. When the concentration of surfactant exceeds its critical micelle concentration (CMC), the excess surfactant molecules aggregate together to form small colloidal clusters referred to as micelles. In principle, polymer particles can be

formed by the entry of radicals into the micelle (heterogeneous nucleation), precipitation of growing oligomers in the aqueous phase (homogeneous nucleation), and radical entry in monomer droplets. In conventional emulsion polymerization, monomer droplets are relatively large (1-10 μm) compared to the size of monomer-swollen micelles (10-20 nm), and hence the surface area of the micelles is much greater than that of the monomer droplets.[11] Consequently, the probability for a radical to enter into the monomer droplets is very low, and most particles are formed by homogeneous and heterogeneous nucleation. According to Harkins' model [12], a batch emulsion polymerization is divided into three intervals:

- Interval I: This is the particle formation, or nucleation stage. The reaction rate and the number of particles increase as a function of time in a closed reactor. The end of this interval corresponds to the disappearance of micelles (Harkins considered that micelles are the only loci of particle nucleation).
- Interval II: The number of particles remains constant, and the monomer droplets, which play the role of reservoir for the growing particle, maintain the concentration of monomer in the particles at the saturation point. The reaction rate is considered to be constant during this stage.
- Interval III: The beginning of the final stage corresponds to the disappearance of the monomer droplets. The concentration of monomer in the particles decreases, but the number of particles remains theoretically constant. During this period, the rate can either decrease, or increase depending on the conditions. A drop in monomer concentration in the particles causes a decrease in the rate of polymerization whereas an increase in rate can often be attributed to an accumulation of radicals inside the particles due to the well-known gel, or Tromsdorff effect, brought on by an increase in the local viscosity.

Mini-emulsions

The basis for mini-emulsion polymerization is an energetic homogenization process to reduce the size of the monomer droplets with the ingredients being basically the same as that found in a conventional emulsion with the exception of the co-surfactant.

The droplet size can range from 50 to 500 nm in diameter [13] and the latex produced by mini-emulsion is characterized by a broader particle size distribution (PSD) [11] ranging from 50 to 1000 nm in diameter.[14] If we manage to reduce the size of the droplets sufficiently, the resulting large surface area of the droplets allows them to compete effectively against the micelles to capture the oligomeric radicals and to become the main loci of polymerization. The presence of micelles in mini-emulsions is dependent on the amount of surfactant used in the formulation and on the homogenization procedure. The ideal situation, where no micelles are formed, is obtained when the surfactant concentration does not exceed the CMC and the homogenization procedure gives sufficiently small monomer droplets. An important concept in mini-emulsion polymerization is the degradation of the monomer droplets by two mechanisms. The first is the coalescence of the interactive monomer droplets due to attractive van der Waals forces. The result is the fusion of two colliding droplets. This coalescence process can be minimized by adequate surfactant coverage on the droplet surface to counteract the van der Waals forces. The second mechanism is the Ostwald ripening process.[11] This destabilization process refers to the diffusional degradation of droplets caused by the transport of monomer from the smaller droplets exhibiting a higher chemical potential, across the aqueous phase, and then to the large droplets. Ostwald ripening results in an increase in the average droplet size and a reduction in the total surface area of the monomer droplets. The Ostwald ripening effect can be minimized with an oil soluble co-surfactant. If they are properly stabilized, the number of particles at the end of the reaction will be the same as the number of droplets at the beginning. Ideally, droplet nucleation is the unique mechanism of particle formation in mini-emulsions if the formation of micelles can be avoided. Consequently, the stage of particle nucleation with monomer transport through the aqueous phase is avoided (Interval I and II in conventional emulsion). These critical differences mean that mini-emulsions will behave differently, from a kinetic point of view, than a conventional emulsion. It was proposed that there is no period of constant rate during a mini-emulsion comparable to that proposed for conventional emulsion in Harkins' theory. This is due to the fact that the droplets are the site of polymerization and do not act as reservoirs. The rate of polymerization is not dependent on monomer diffusion from the droplets to the polymer

particles.[15] Bechthold et al.[16] reported similar results in their investigation of the kinetics of mini-emulsion polymerization of styrene by calorimetry.

Before we could start to follow the conversion of mini-emulsions with an in-line monitoring technique making use of ATR-FTIR spectroscopy, we had to identify and address potential factors that could prevent us from achieving our goal. These potential factors involved an inappropriate background overlapping meaningful peaks, a small signal to noise ratio creating too much noise in the spectrum and hiding meaningful peaks, fouling of the optical device inserted in the reactor preventing us from "seeing" the true monomer concentrations, temperature variations because absorptivity increases with temperature, a deviation from Beer's law because aggregation effects could prevent the absorptivity form changing linearly with concentration [2], and an inappropriate peak assignment.

Experimental Section

Reagents

The reagents: Styrene (St), Butyl Acrylate (BA), Acrylic Acid (AA), octadecyl acrylate (ODA), the chain transfer agent (CTA) n-dodecyl mercaptan, sodium dodecyl sulfate (SDS), Triton X-405, sodium hydrogen carbonate ($NaHCO_3$), and potassium persulfate (KPS) were used without any further purification. All components used to perform the characterizations, i.e., toluene, ethanol, methanol, chloroform-d, tetrahydrofuran (THF), sodium hydroxide (NaOH), and calcium chloride ($CaCl_2$) were used as received.

Experimental Procedure

The reactions were performed in a jacketed 1.2L stainless steel reactor with a Labmax™ setup (Mettler Toledo) and stirred at 200 rpm. The reactor was equipped with a nitrogen purging/pressurizing line, reflux condenser, sampling line and a port for the IR

insertion probe. Stirring speed and temperature were automatically controlled using Camille™ software (Mettler Toledo).

St, BA and ODA were mixed for 15 minutes in a beaker while water, Triton X-405, and SDS were mixed for 15 minutes in a separate vessel. Both solutions were then combined and mixed for one hour with a magnetic stirrer. The mixture was then sonicated using a Fisher Scientific 550 sonic dismenbrator for 3 min at Level 6. The mixture was simultaneously cooled in an ice bath and well mixed while undergoing sonication.

The polymerizations were run at 80°C. The air background spectrum was recorded before the mixture was poured into the reactor. The reaction mixture was then heated and purged of oxygen by bubbling N_2 through it for at least 40 minutes. When the set point temperature was reached, a deoxygenated initiator solution made with KPS and distilled deionized water was charged into the reactor. This corresponded to time zero for the polymerization. At suitable time intervals, samples were taken through the sampling port for off-line analysis by gravimetry and ^{1}H-NMR spectroscopy.

Characterization

Gravimetry

Mass conversion based on the total polymer in the reaction mixture and percent solids were measured using gravimetry.

^{1}H-NMR Spectroscopy

Proton nuclear magnetic resonance spectroscopy (^{1}H-NMR) was used to determine the average or cumulative composition of copolymers. Analyses were carried out at room temperature in deuterated chloroform (about 2% weight per volume solution) with a Bruker AMX-500 Fourier transform ^{1}H-NMR spectrometer. The acquisition time was 4.6 seconds and 16 scans were performed per sample. The relative amounts of monomer bound in the copolymer were estimated from the areas under the appropriate

absorption peaks of the spectra. The spectral peaks for the $-OCH_2$ group in BA were located at ~3.4-4 ppm and the cyclic (5H) group in St was located at ~6.6-7.2 ppm.

ATR-FTIR Spectroscopy

The polymerizations were monitored in-line with the ReactIR™ 1000 (ASI Applied Systems, Mettler Toledo) using ATR-FTIR spectroscopy. The data were collected over a spectral range of 4000-700 cm^{-1}, with 128 scans and a resolution of 4 cm^{-1}. The number of scans and resolution were selected to provide an adequate signal to noise ratio. To ensure continuous monitoring, the reaction spectra were acquired every 2 minutes. This monitoring system was previously described in detail.[5, 10]

Results and Discussion

Our initial approach was to investigate the potential factors previously described (inappropriate background, inappropriate signal to noise ratio, probe fouling, temperature variations, deviation from Beer's law and the new peak assignment). A series of reactions was selected to build and validate an ATR-FTIR monitoring model for mini-emulsions. Table 1 provides a list of reactions analyzed for this monitoring model. All recipes were performed as mini-emulsions with a sonication time of 3 minutes, a reaction temperature of 80°C and a solids content of 50 wt.%. The following concentrations of ingredients were also kept constant: water = 90 phm, $NaHCO_3$ = 1 phm, KPS = 0.75 phm, AA = 4 phm, CTA = 0.25 phm where phm represents parts per hundred parts of monomer. The only exception was for the homopolymerization of styrene in mini-emulsion where the reaction temperature was 60°C. No AA was added and the concentrations of Triton, SDS and ODA were 2.5 phm, 0.15 phm and 2.5 phm, respectively.

Table 1: Batch recipes

		St (phm)[1]	BA (phm)	Triton (phm)	SDS (phm)	ODA (phm)
Runs used for the model	Run 2	5	95	1	0.06	1
	Run 3	5	95	2.5	0.15	2.5
	Run 4	10	90	0.5	0.03	0.5
	Run 5	10	90	1	0.06	1
	Run 6	10	90	2.5	0.15	2.5
	Run 8	15	85	1	0.06	1
	Run 3-1	5	95	2.5	0.15	2.5
	Run 3-2	5	95	2.5	0.15	2.5
Runs used for the validation	Run 1	5	95	0.5	0.03	0.5
	Run 3-4	10	90	1	0.06	1
	Run 5-1	10	90	1	0.06	1
	Run 7	15	85	0.5	0.03	0.5
	Run 7-1	15	85	0.5	0.03	0.5

[1]phm = parts per hundred parts monomer

Inappropriate background

It was found that an air background was sufficient to follow the reaction because a background spectrum using either water or the first or last reaction spectrum did not provide more information (or meaningful peaks).

Inappropriate signal to noise ratio

Figure 1 shows an example of a single reaction spectrum (mixture spectrum of the homopolymerization of styrene in mini-emulsion) and clearly shows that the signal to noise ratio was sufficiently large to allow the identification of many single component peaks from the pure styrene spectrum.

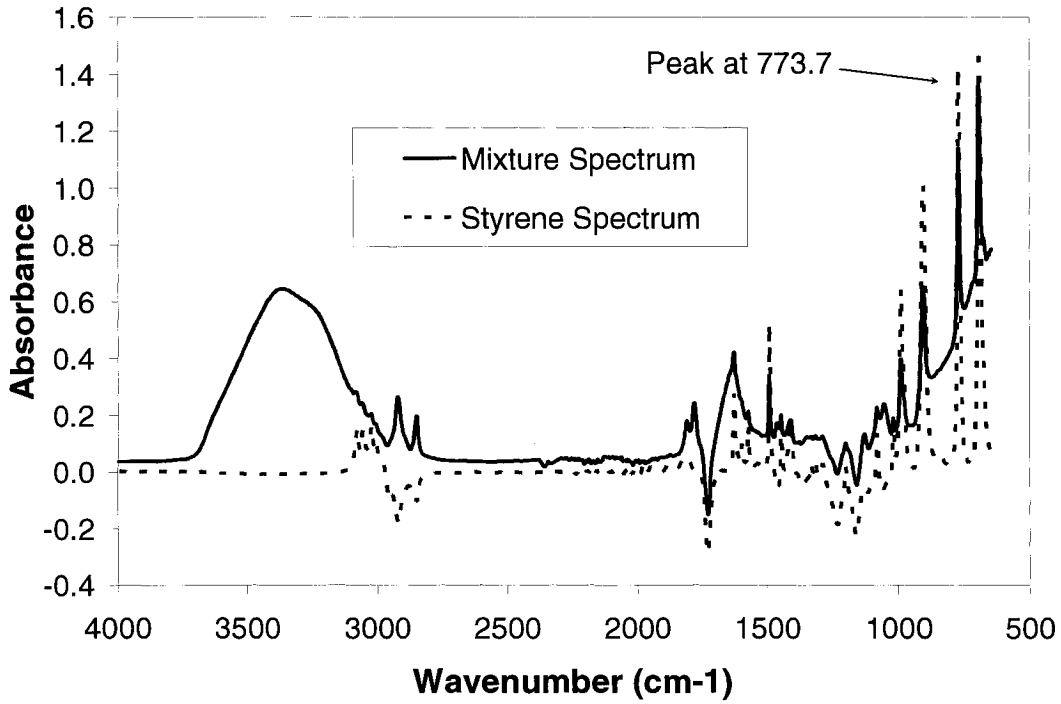

Figure 1: Reaction spectrum from the homopolymerization of styrene in mini-emulsion

Probe fouling

A visual inspection of the probe after the reaction led to the conclusion that there was no probe fouling. We then accepted the assumption that no significant probe fouling was occurring during the reaction.

Temperature variations

The effect of temperature on the absorbance was measured for pure toluene (associated peak at 2921 cm^{-1}) and for a mixture of styrene and toluene (associated peak at 3062 cm^{-1}) over temperatures ranging from 45 to 75°C. Those data were fitted to a linear model and the slopes were 0.0003 and 0.0009 absorbance/°C for the pure toluene and for the mixture of styrene and toluene, respectively. This meant that, if the temperature was to vary by 1°C during the experiment, it could propagate an error of approximately 1% in the calculations for the conversion. Since the temperature of the

reaction mixture never varied by much more than 1 degree Celsius during the experiment, the temperature effect was deemed to be insignificant. Figure 2 shows the temperature variations during the homopolymerization of styrene in mini-emulsion with the associated peak at 773.7 cm^{-1}. From this figure, we can see the subtle effect of temperature on the peak height.

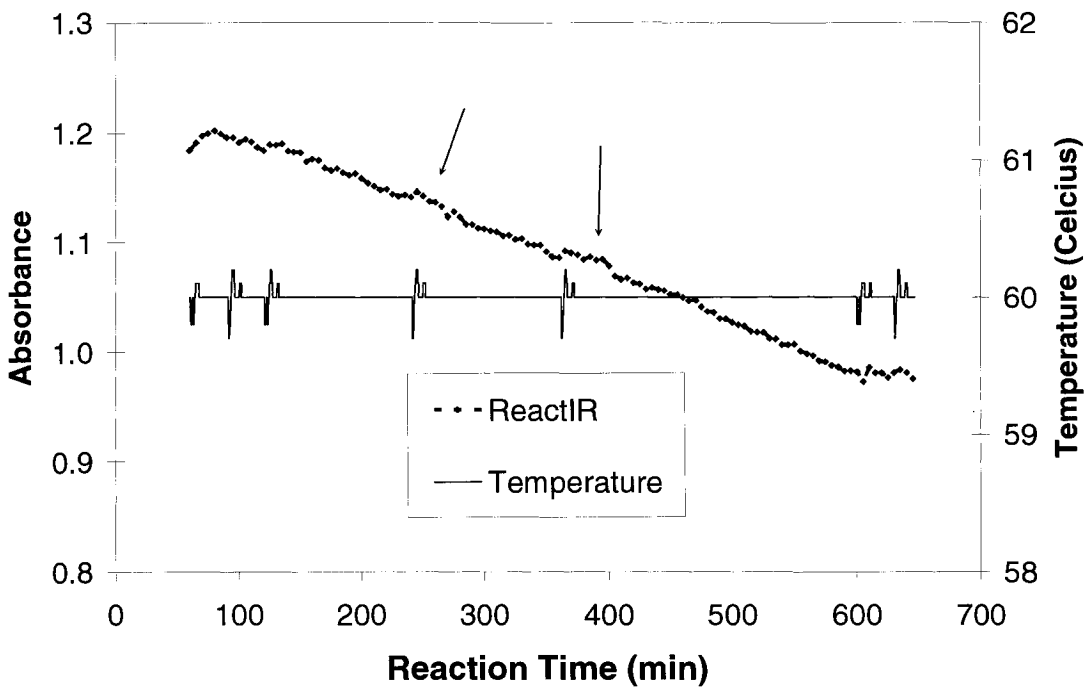

Figure 2: Temperature profile from the homopolymerization of styrene in mini-emulsion

Deviation from Beer's law

Two conditions are implied in the derivation of Beer's law. The first is that the resolution element being measured is monochromatic (the intensity of the region of the spectrum that is actually measured must have a small spread of wavelengths). The second condition is that the absorptivity should not change with concentration (by aggregation effect). If cell thickness and wavelength are held constant, a plot of concentration versus absorbance for a single component will be a straight line, if Beer's law holds. If Beer's law does not hold exactly, the plot will be slightly non-linear but can still be used for

analyses. Following our discussion in the probe fouling section, it was already accepted that no aggregation effect was present during the reaction since it would have fouled the probe. A few known concentrations of styrene were measured off-line to assess this condition. Figure 3 shows the concentration of styrene behaving linearly with absorbance. Thus, we concluded that Beer's law holds for these reaction conditions.

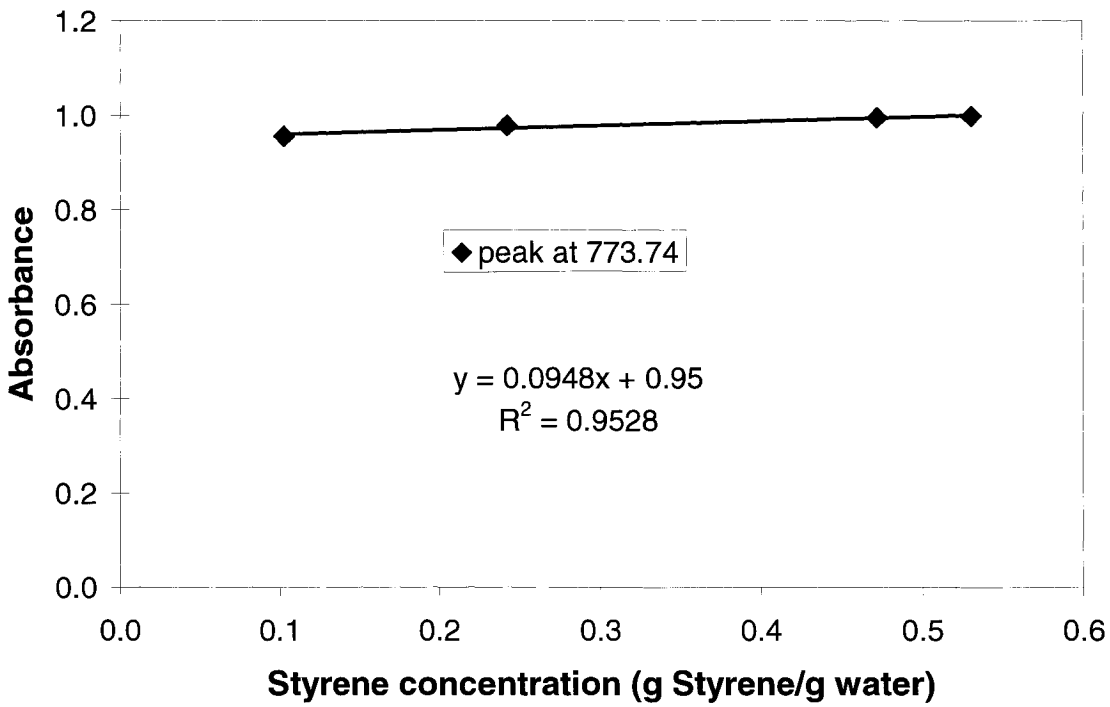

Figure 3: Linear regression for Beer's law validation

New peak assignment (Univariate method)

The absorbance of different functional groups inside the monomers or polymers was monitored throughout the course of the reaction. Typical homopolymerization spectra of styrene in mini-emulsion are shown in Figure 4. Each functional group was associated with a characteristic peak and the concentration of a component was proportional to the absorbance, which could be measured as a peak height. Real-time peak profiles of monomers (changes in absorption for a specific component) were usually

used to calculate the conversion and had already successfully been applied for conventional emulsion and solution polymerizations. [5, 10]

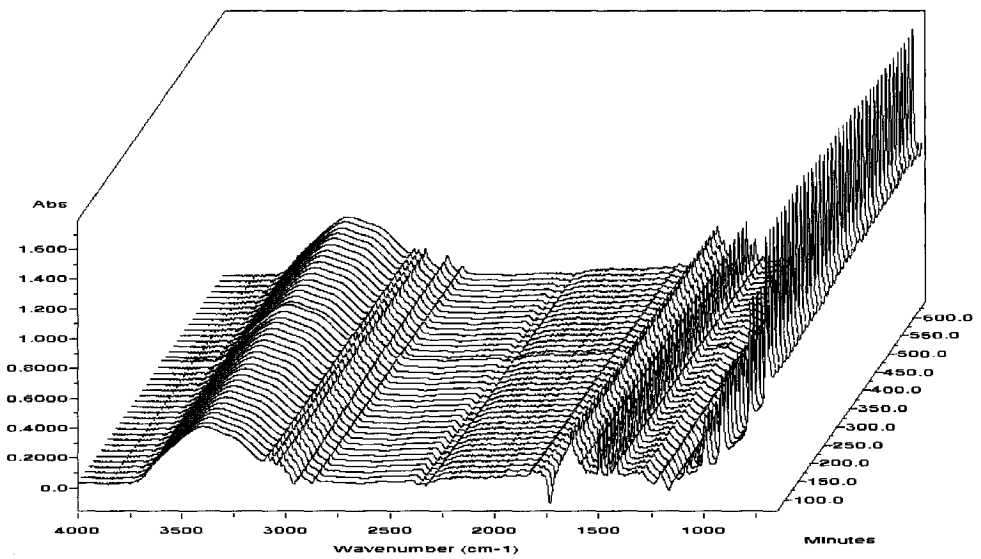

Figure 4: Typical homopolymerization spectra of styrene in mini-emulsion

With the univariate method, Equation 1 could be used to calculate the conversions of monomers, x (mole fraction), in the reaction mixture:

$$x = \frac{peak_{t=0} - peak_{t=t}}{peak_{t=0}} \qquad (1)$$

where peak at time t = 0 represents the peak height of one of the monomer peaks at the beginning of the polymerization. With Equation 1, we could calculate the conversion at the beginning of the reaction. Figure 5 shows a close-up for the monomer spectral region of the homopolymerization of styrene in mini-emulsion.

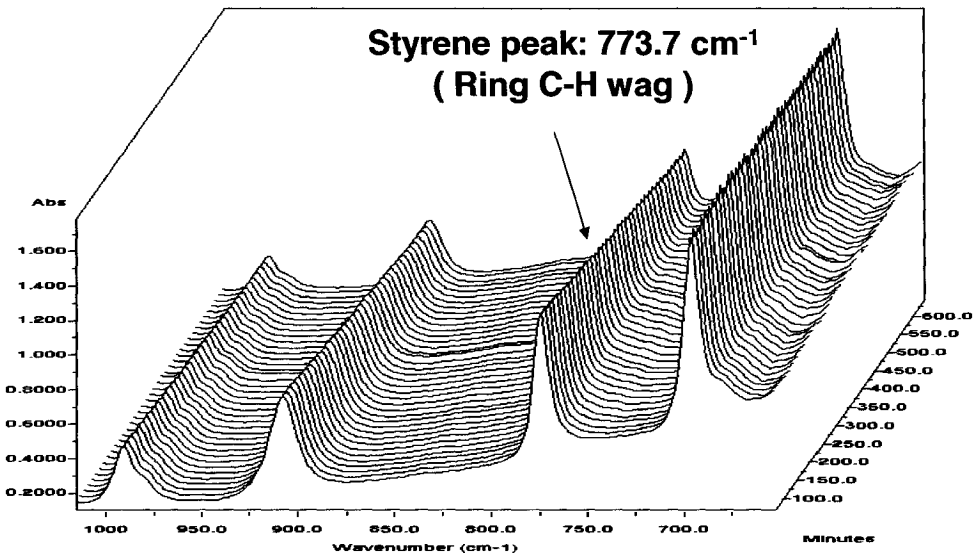

Figure 5: Monomer region for the homopolymerization of styrene in mini-emulsion

When required, Equation 2 could be used to calculate the conversions of polymers, x (mole fraction), in the reaction mixture:

$$x = \frac{peak_{t=t} - peak_{t=0}}{peak_{t=\infty} - peak_{t=0}} \tag{2}$$

where peak at time $t = \infty$ represents the peak height of one of the polymer peaks at the end of the polymerization. With Equation 2, we could not calculate the conversion at the beginning of the reaction. Figure 6 shows a close-up for the polymer spectral region of the homopolymerization of styrene in mini-emulsion.

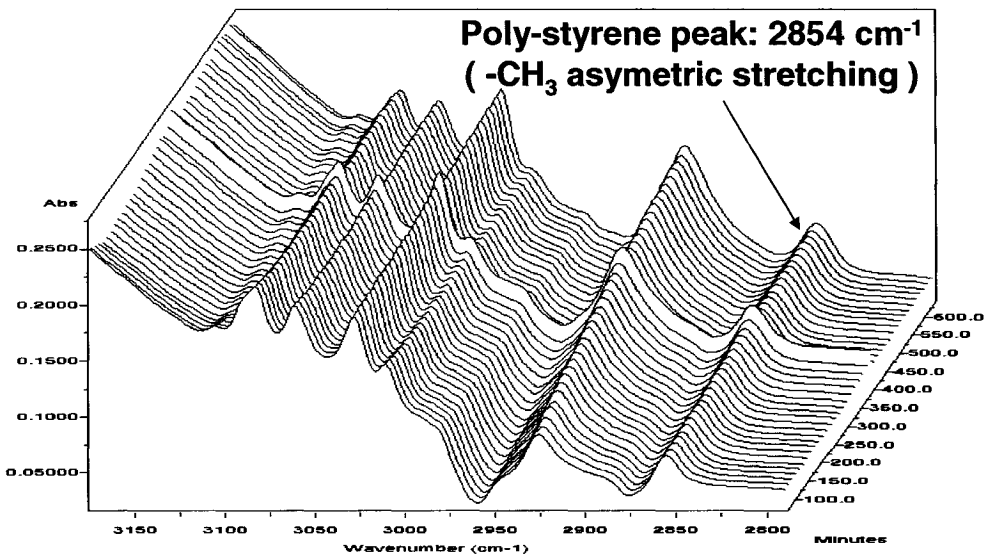

Figure 6: Polymer region for the homopolymerization of styrene in mini-emulsion

Figure 7 shows a comparison between the conversions calculated with Equation 1 and the gravimetric results. The peak chosen from the IR spectra was at 773.7 cm^{-1} since it was the most commonly used peak to follow the conversion of the homopolymerization of styrene. This figure shows the inadequacy of the chosen peak to follow the conversion of the homopolymerization of styrene in mini-emulsion. Similar results were obtained for several reactions in mini-emulsions.

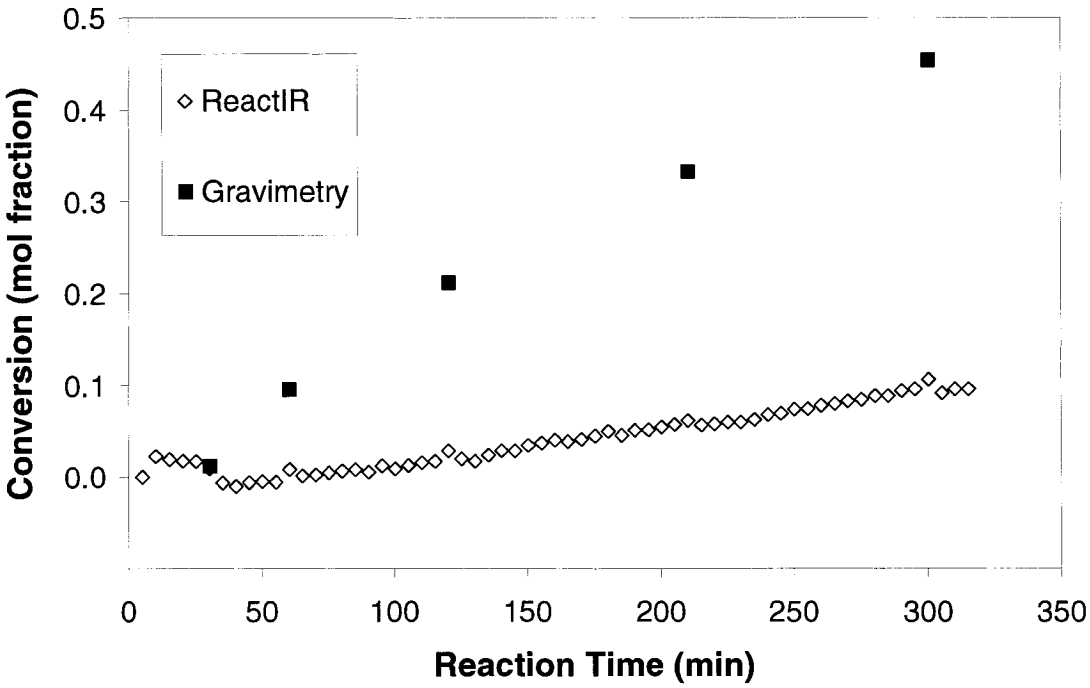

Figure 7: Homopolymerization of styrene in mini-emulsion monitored with Equation 1

Because limited success was achieved when tracking the absorbance of different monomer peaks for several reactions in mini-emulsions, it was decided to focus on the polymer peaks as a means to monitor the reaction. The original equation (Equation 2) used to transform a polymer peak height into a conversion did not allow the user to monitor the conversion from the beginning of the reaction. Equation 3 was then developed to follow polymer peaks during the reaction without the need for any additional information other than the peak height (absorbance):

$$x = \frac{peak_{t=t} - peak_{t=0}}{peak_{t=0}} \tag{3}$$

Theoretically, Equation 3 should have been difficult to apply since the peak height of a polymer at the beginning of a reaction should be equal to zero. In practice, the results

were much more promising and it might be due to the fact that the spectrum of some ingredients in the reaction mixture overlapped the chosen polymer peak and pushed this peak above zero from the beginning.

All the visually noticeable polymer peaks from the reaction spectra of the homopolymerization of styrene in mini-emulsion were evaluated with Equation 3 and the most appropriate characteristic peak was chosen. Figure 8 shows a comparison between conversions calculated with Equation 3 and the gravimetric results. The peak chosen from the IR spectra was at 2854 cm^{-1}. When compared to Figure 7, it is clear this equation was more successful at predicting the conversion.

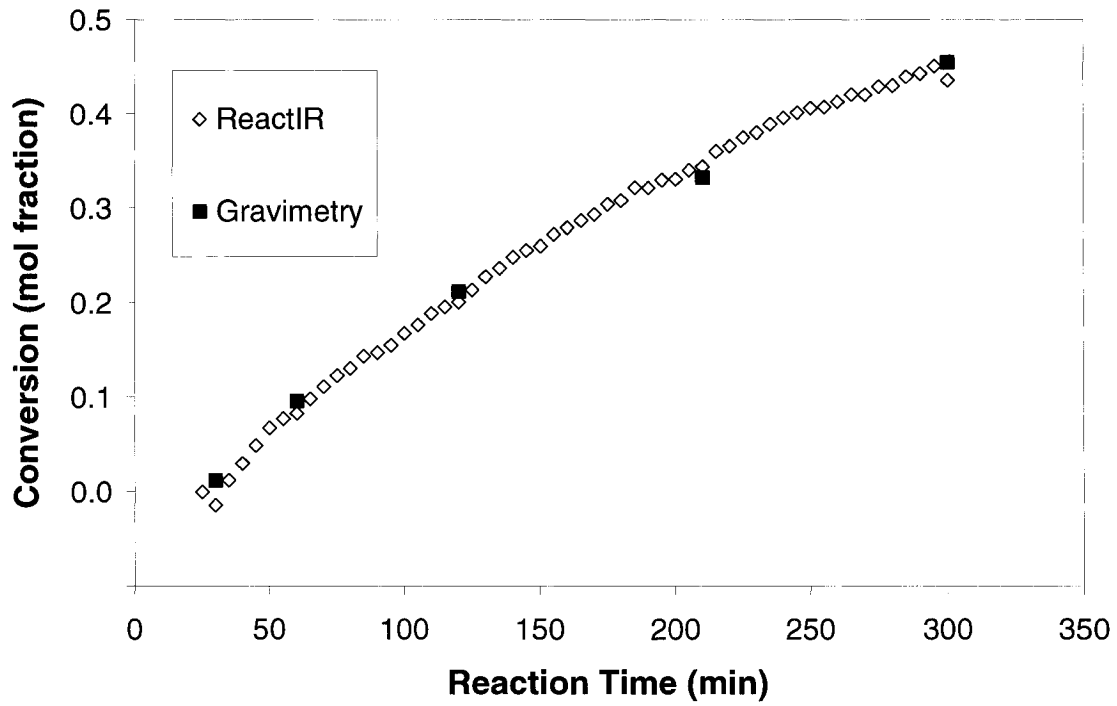

Figure 8: Homopolymerization of styrene in mini-emulsion monitored with Equation 3

Equation 3 was also tested with previous reactions and on reactions performed by colleagues in the Department of Chemical Engineering at the University of Ottawa. Figures 9 and 10 show a comparison between the conversions calculated with Equation 3 and the gravimetric results for two of those reactions.

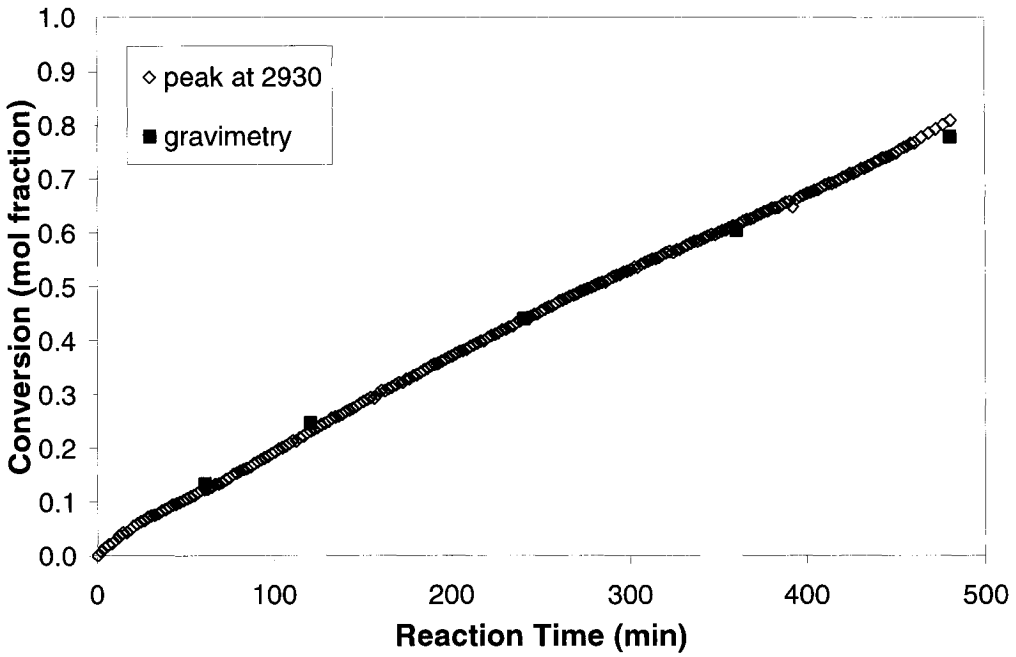

Figure 9: Copolymerization of styrene/butyl acrylate (50/50) in mini-emulsion

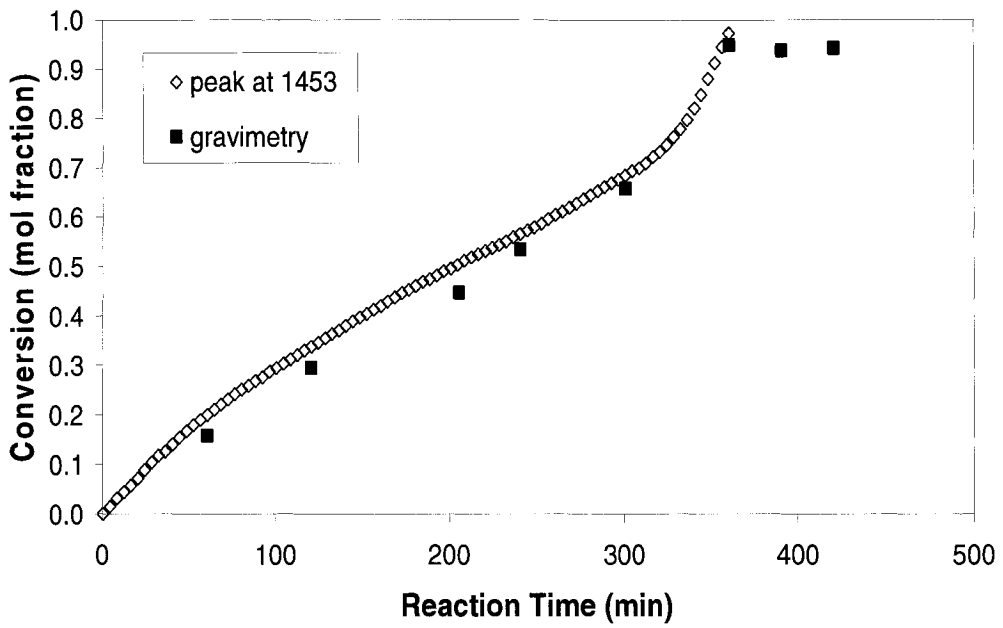

Figure 10: Copolymerization of styrene/butyl acrylate (20/80) in mini-emulsion

The conclusion form all those analyses was that the most appropriate peak to follow a mini-emulsion conversion was changing with the kind of ingredients used and their respective concentrations. Nonetheless, the procedure proved to be successful for almost all mini-emulsions tested but was always ineffective when applied to conventional emulsions or solutions polymerizations. Since this new univariate method gave inconsistent results, we decided to attempt a multivariate method (Partial Least Square (PLS)) method.

Multivariate method

Thirty-three samples from the runs shown in Table 1 were used as standards to build a calibration model for the multivariate analysis. In order to develop a good calibration equation, it was necessary to use these samples directly from the reactions instead of preparing mixtures with pure monomers. The selection of IR spectra was made from a personal database of reactions completed for PSA production; hence the range of St/BA ratios went from 5/95 to 15/85. Monomer concentrations during the polymerization were calculated using results from gravimetry and ^{1}H-NMR spectroscopy. The spectral variations recorded from these samples were related to different monomer concentrations. QuantIR version 2.1 software (ASI Applied Systems 1996, Mettler Toledo) was used to perform the chemometric analysis. In the PLS approach, the set of calibration spectra was reduced to a smaller number of key spectra (called factors) that can, when taken in linear combination, approximate the original spectral data. Each one of those factors is comprised of multiple peaks within the same spectral region. The Predicted Residual Error Sum of Squares (PRESS) analysis was used to select the optimum number of factors for each component (St and BA). As factors which represent useful information are added to the analysis, the PRESS value decreases, indicating improvement in the PLS calibration error. At some point the factors add noise or other information unrelated to concentration; the PRESS value then levels off or increases. The correct number of factors to select is associated with the minimum PRESS value. Several spectral regions were tested for the calibration but only the spectral region 650 to 1800

cm^{-1} gave acceptable results. For this chosen spectral region, typical copolymerization spectra of St/BA in mini-emulsion can be seen in Figure 11. Figure 12 shows a close-up of the most common monomer peaks usually used in the univariate analysis.

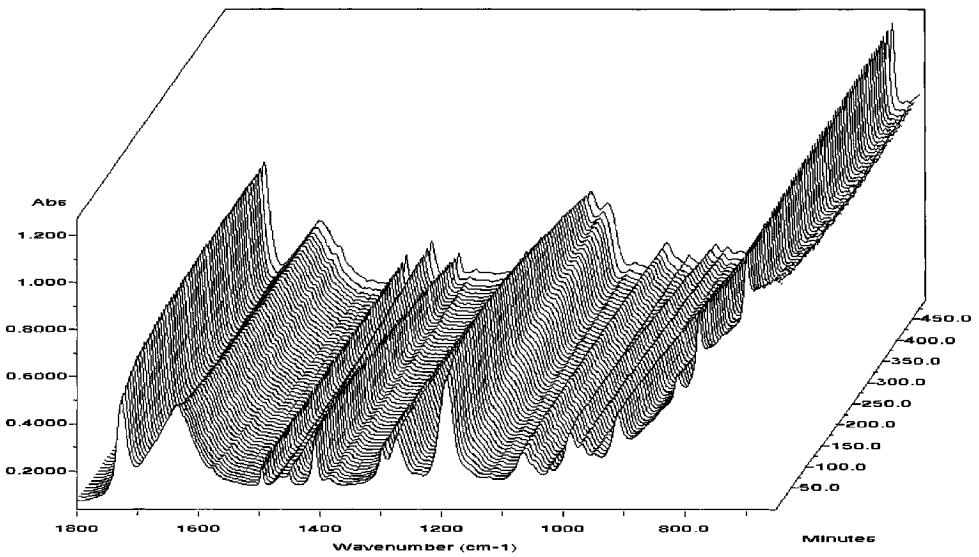

Figure 11: Typical copolymerization spectra of styrene/butyl acrylate in mini-emulsion

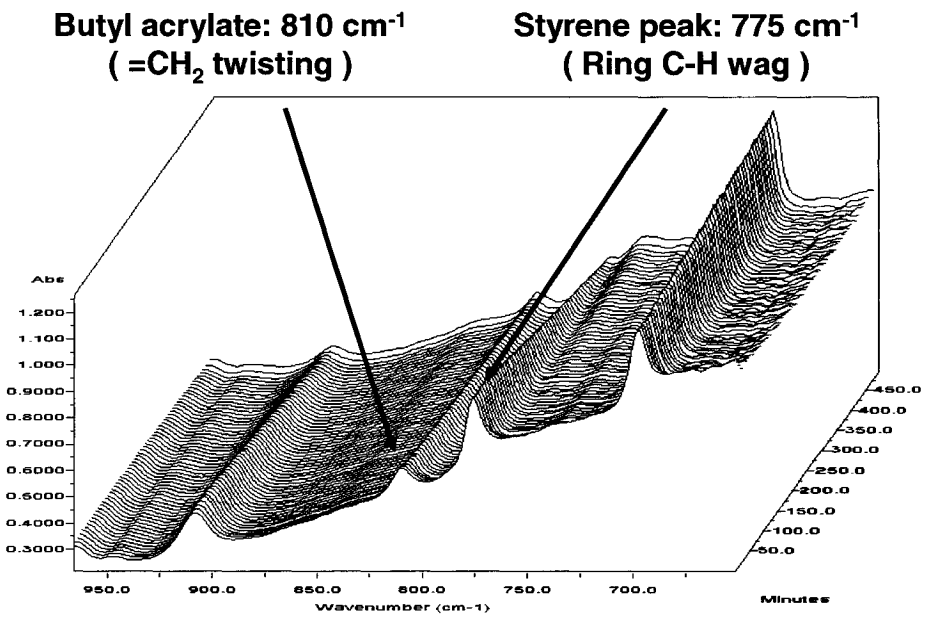

Figure 12: Common monomer peaks in the copolymerization of styrene/butyl acrylate

Initially, a maximum of 30 factors for each component was chosen to establish the model. After the PRESS analysis, 11 factors were chosen for the concentration of St and 13 factors were chosen for the concentration of BA. Different scenarios were also explored with 6 or 9 factors for each component but without success. The PRESS analysis is shown in Figure 13.

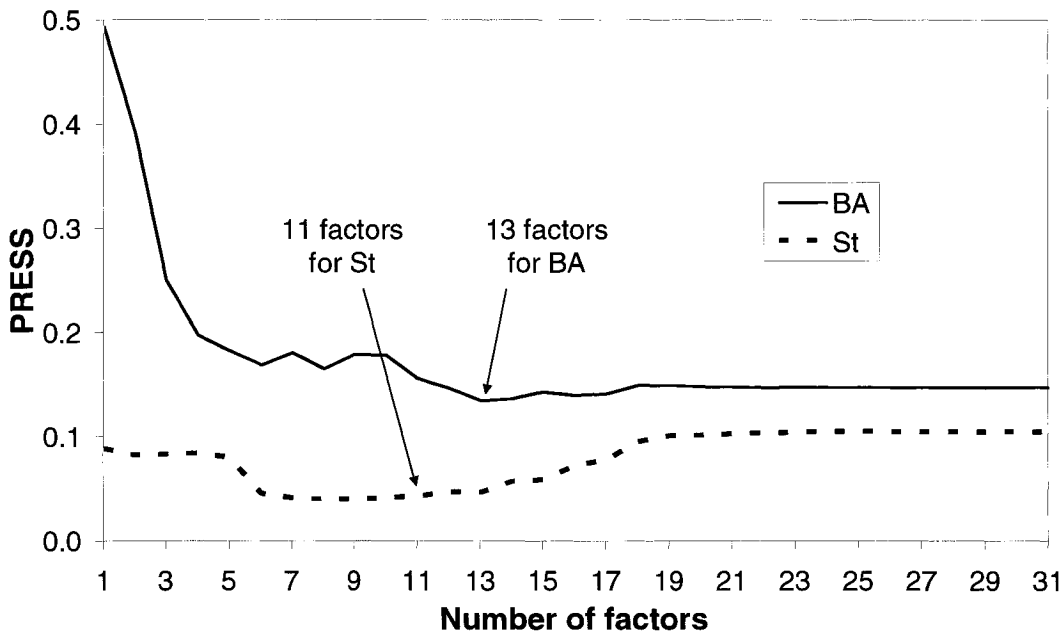

Figure 13: PRESS analysis for the PLS model

A PLS model was then built to establish a predictive relationship between the factors and the monomer concentrations. The corresponding calibration curves of the PLS predictions versus the known concentrations are shown in Figures 14 and 15. With correlation coefficients of 0.9958 for St and 0.9979 for BA, the PLS model showed signs of adequacy for predicting known concentrations. The PLS model was then used to predict the St and BA concentrations from five additional runs shown in Table 1. Model predictions were compared to actual measurements and are shown in Figures 16 and 17. The correlation coefficients were 0.9909 for St and 0.9908 for BA, suggesting a successful model.

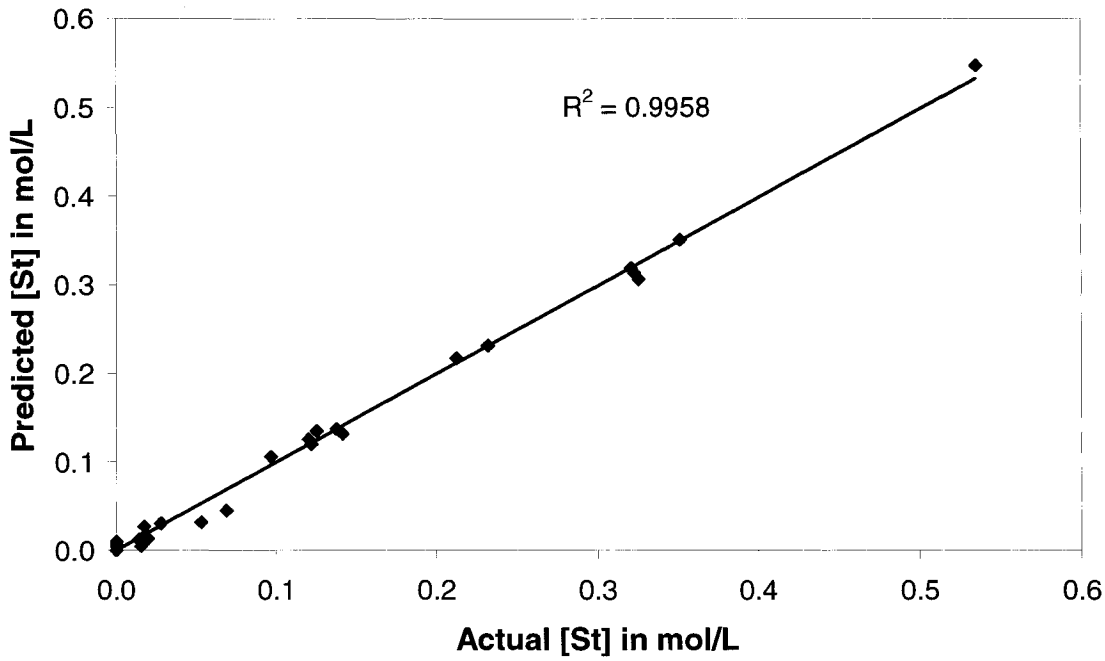

Figure 14: Styrene concentration calibration

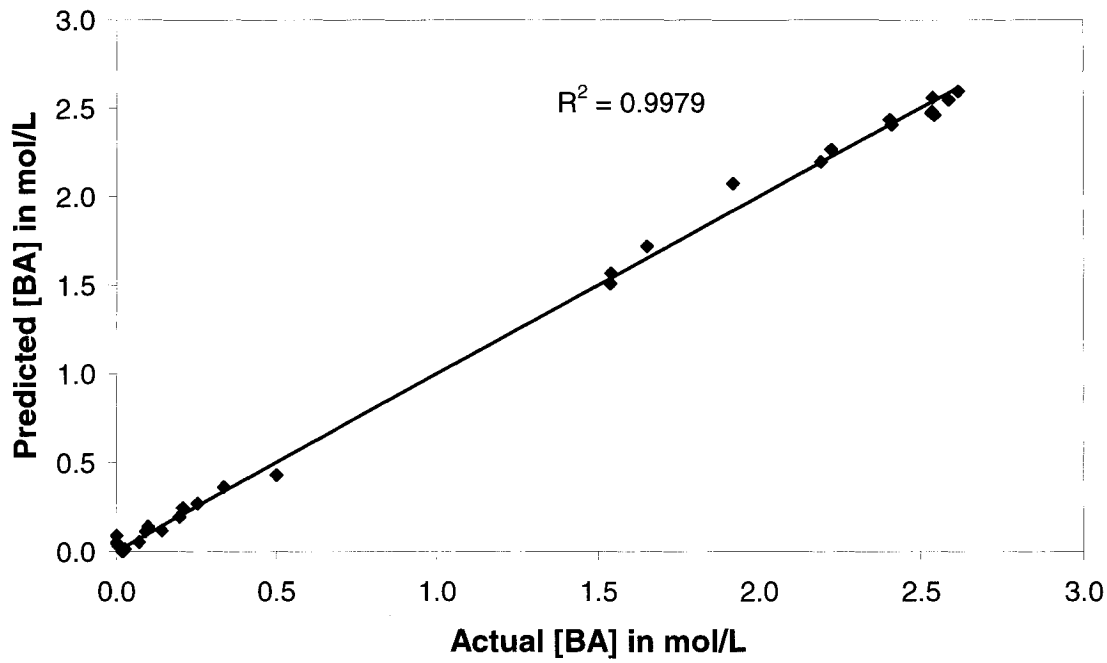

Figure 15: Butyl acrylate concentration calibration

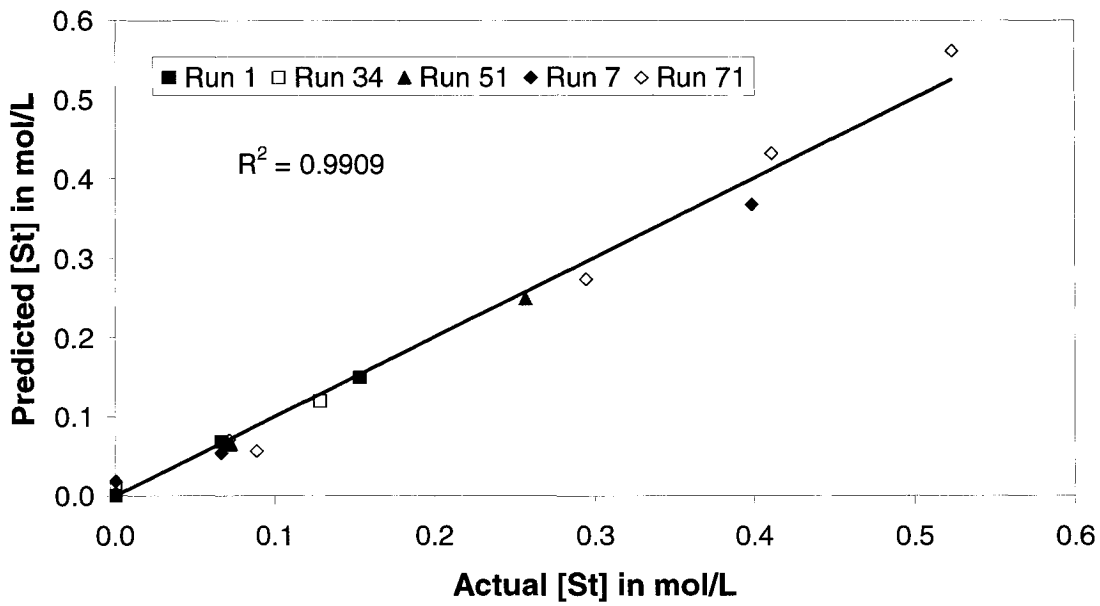

Figure 16: Styrene concentration validation

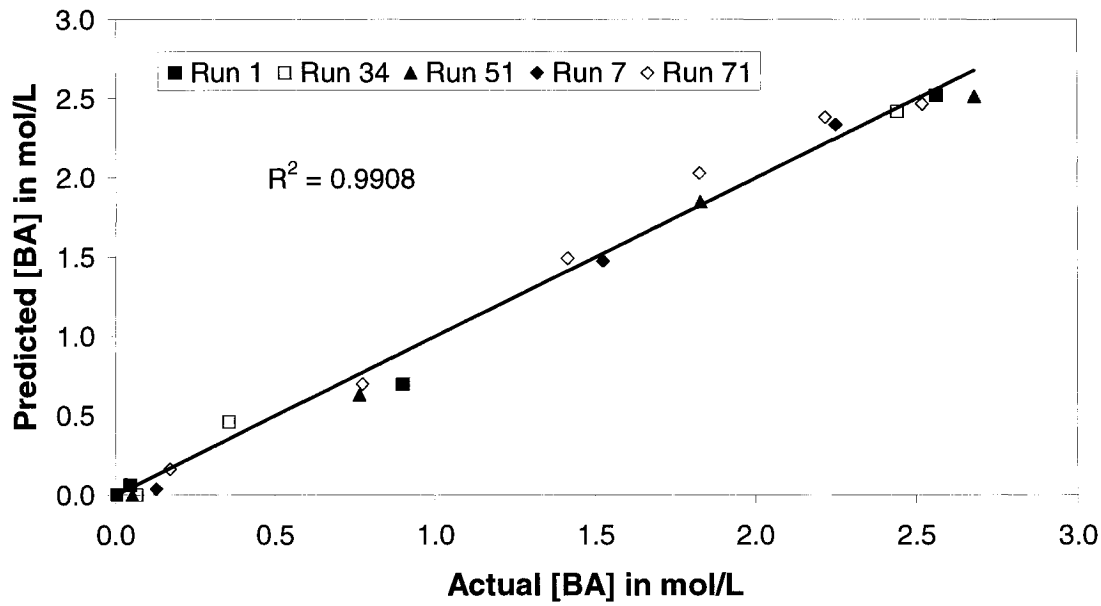

Figure 17: Butyl acrylate concentration validation

A paired comparison was also carried out between the monomer concentrations obtained by off-line measurements (gravimetry and ^{1}H-NMR spectroscopy) and the model predictions. For all the samples used in the calibration, 95% confidence intervals for the difference between the two methods were found to be [-0.0077, 0.0078] in mol/L for St and [-0.0203, 0.0203] in mol/L for BA. This showed that no significant differences existed between the two methods. For all the samples used in the validation (five additional runs), 95% confidence intervals were found to be [-0.0051, 0.0113] in mol/L for St and [-0.0545, 0.0236] in mol/L for BA, further confirming that a successful calibration model was calculated.

The predicted concentrations of St and BA from the PLS model were then used to calculate the individual and overall monomer conversions. The calculated conversions agreed well with the actual measurements. One example is shown in Figure 18 for individual conversions and in Figure 19 for overall conversions. Similar results were obtained for other runs.

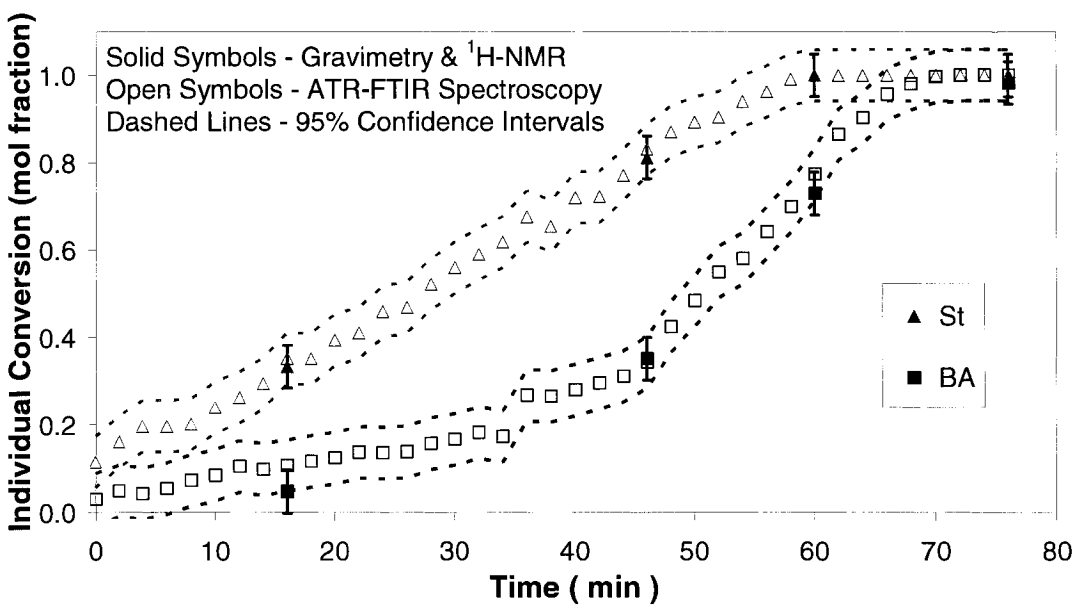

Figure 18: PLS individual conversion predictions for Run 51

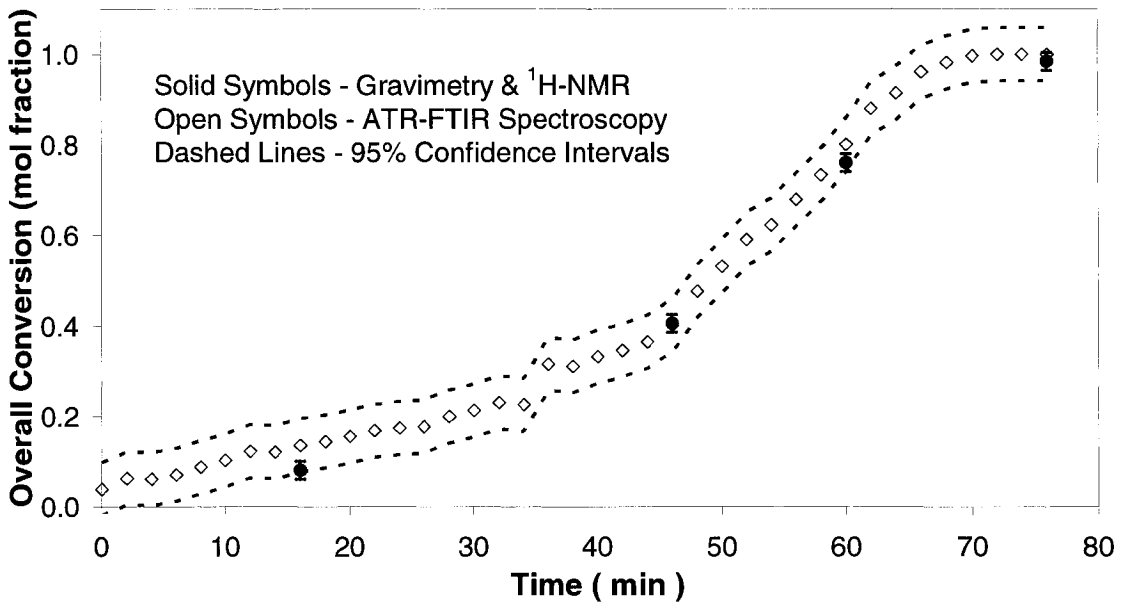

Figure 19: PLS overall conversion predictions for Run 51

Conclusions

A series of St/BA mini-emulsion copolymerizations was carried out in a 1.2L stainless steel reactor. Conversions were monitored off-line using gravimetry and in-line monitoring was performed using ATR-FTIR spectroscopy. It was found that the air background and the signal to noise ratio were both appropriate for this kind of system. No significant probe fouling was observed and the temperature effects were deemed to be negligible. In addition, Beer's law was validated and the univariate methods gave inconsistent results. A multivariate or PLS method using the full spectra of reactions gave much more promising results for the in-line mini-emulsion polymerization monitoring. No significant differences were found between the off-line (gravimetry and ^{1}H-NMR spectroscopy) results and the ATR-FTIR spectroscopy data coupled with the PLS method confirming that ATR-FTIR spectroscopy is a reliable tool for monitoring individual

monomer concentrations and conversions. Future work could consider integrating a feedback control policy to such a system.

Acknowledgements

The authors wish to gratefully acknowledge the financial support from the Natural Science and Engineering Research Council (NSERC) of Canada and the Ontario Graduate Scholarship (OGS)

References

1. Kammona, O.; Chatzi; E.G.; Kiparissides, C. Recent developments in hardware sensors for the on-line monitoring of polymerization reactions. J. Macromol. Sci. – Rev. Macromol. Chem. Phys. 1999, C39(1), 57-134.
2. Gunzler, H.; Gremlich, H.U. *IR Spectroscopy, An introduction*, Wiley-VCH; Germany, 2002, 1-361.
3. Hua, H.; Dubé, M.A. Terpolymerization Monitoring with ATR-FTIR Spectroscopy. J. Polym. Sci.: Part A: Polym. Chem. 2001, 39, 1860-1876.
4. Hua, H.; Dubé, M.A. Off-line monitoring of butyl acrylate, methyl methacrylate and vinyl acetate homo- and copolymerizations in toluene using ATR-FTIR spectroscopy. Polymer. 2001, 42, 6009-6018.
5. Hua, H.; Dubé, M.A. In-Line Monitoring of Emulsion Homo- and Copolymerizations Using ATR-FTIR Spectrometry. Polymer Reaction Engineering. 2002, 10(1-2), 21-40.
6. Smith, B.C. *Fundamentals of Fourier Transform Infrared Spectroscopy*, CRC Press, Boca Raton FL, 1996, 1-202.
7. Full, A.P.; Puing, J.E.; Gron, L.U.; Kaler, E.W.; Minter, J.R.; Mourey, T.H.; Texter, J. Polymerization of Tetrahydrofurfuryl Methacrylate in Three-Component Anionic Microemulsions. Macromolecules. 1992, 25(20), 5157-5164.

8. Storey, R.F.; Donnaley, A.B. Initiation effects in the living cationic polymerization of isobutylene. Macromolecules. 1999, 32(21), 7003-7011.
9. Storey, R.F.; Maggio, T.L. Real-time monitoring of carbocationic polymerization of isobutylene via ATR-FTIR spectroscopy. Macromolecules. 2000, 33(3), 681-688.
10. Jovanovic, R.; Dubé, M.A. Off-line monitoring of butyl acrylate and vinyl acetate homopolymerization and copolymerization in toluene. Journal of Applied Polymer Science. 2001, 82(12), 2958-2977.
11. Asua, J.M. Miniemulsion Polymerization. Prog. Polym. Sci. 2002, 27(7), 1283-1337.
12. Harkins, W.D. A General Theory of Mechanism of Emulsion Polymerization. J. Am. Chem. Soc. 1947, 69, 1428-1444.
13. Capek, I.; Chern, C.S. Radical Polymerization in Direct Mini-Emulsion Systems. Adv. Polym. Sci. 2001, 155, 105-127.
14. Lovell, P.A.; El-Aasser, M.S. *Emulsion Polymerization and Emulsion Polymers*, John Wiley and Sons, Inc.: England, 1997; 1-515.
15. Ouzineb, K. PhD thesis, Department of Chemistry, University of Claude Bernard Lyon I, Lyon, France, 2003.
16. Bechthold, N.; Landfester, K. Kinetics of miniemulsion polymerization as revealed by calorimetry. Macromolecules. 2000, 33(13), 4682-4689.
17. Colthup, N.B.; Daly, L.H.; Wiberley, S.E. *Introduction to Infrared and Raman Spectroscopy*, 3rd edition, Academic Press, Inc., San Diego, 1990, 1-547.
18. Suetaka, W. *Surface Infrared and Raman Spectroscopy, Methods and Application*, Plenum Press, New York, 1995, 1-270.
19. Odian, G.G. *Principles of Polymerization*, 3rd Ed.; John Wiley and Sons, Inc.: New York, 1991; 1-374.
20. Rudin, A. *The Elements of Polymer Science and Engineering*, 2nd Ed.; Academic Press: San Diego, 1999; 1-522. 21 Gilbert, R.G. *Emulsion Polymerization, A Mechanistic Approach*, Academic Press: San Diego, 1995; 1-362.

21. Tobing, S.D.; Klein, A. Molecular parameters and their relation to the adhesive performance of acrylic pressure-sensitive adhesives. Journal of Applied Polymer Science. 2001, 79(12), 2230-2244.

Chapter 5 – Paper on PSA Performance

Keywords: styrene, butyl acrylate, mini-emulsions, pressure-sensitive adhesives, particle size.

Introduction

Adhesives are defined as substances capable of holding at least two surfaces together. A class of adhesives called pressure-sensitive adhesives (or PSAs) is characterized by instantaneous adhesion upon application of light pressure.[1] The most common applications for PSAs are tapes, labels and protective films. In order to develop new application-specific products and improve existing processes, there is a need to identify the factors that influence the performance of PSAs. Reaction components and process conditions will affect latex properties such as copolymer composition, molecular weight distribution (MWD) and particle size distribution (PSD). Those latex properties can affect rheological properties and the film formation process. Furthermore, latex rheology and the film formation process can affect the performance of the adhesive.

Many industrial applications require materials with specific properties that can only be achieved through the use of two monomers, i.e. by copolymerization. One example is the styrene (St) and butyl acrylate (BA) system. Depending on their composition and molecular weight, among other properties, the resulting polymers from this system can be used to produce different types of adhesives, coatings and paints. Because of environmental concerns and government regulations to substitute solvent-based systems by water-borne products, there is a growing interest in producing such copolymers by mini-emulsion polymerization.[2]

The basis for the mini-emulsion polymerization process is an energetic homogenization to reduce the size of the monomer droplets and the use of both a co-emulsifier and an emulsifier to protect these droplets against degradation. An efficient mini-emulsion polymerization (efficient in terms of particle formation) is very useful as it allows us to control the number and size of particles being formed in a manner very different from particles formed by micellar or homogeneous nucleation. This improved control of the particle size distribution coupled with a control over the MWD and composition of the copolymer could offer the possibility of tailoring the desired

properties of PSAs. It was of interest in this study, to measure the effect of varying particle size and copolymer composition on adhesive properties.

Background

PSAs

A PSA must be soft and tacky hence, its glass transition temperature (T_g) should be low, ranging from -20 to -60°C. Polymers with low T_g, typically from a class of alkyl acrylates such as poly(BA) and poly(2-ethylhexyl acrylate) are inherently soft and tacky but do not possess adequate shear strength. A balanced combination of tack, peel strength and shear strength is a primary concern for a PSA. As a consequence, the copolymerization of an alkyl acrylate having a low T_g with a thermoplastic such as St or methyl methacrylate having a high T_g is useful to regulate this combination of tack, peel strength and shear strength. In addition, monomers with functional groups such as acrylic acids (AA) or methacrylic acids could be added to improve peel and shear strength although their addition often reduces tack.[3] Since tack, peel strength and shear strength are the three general adhesive properties that determine PSA performance, a brief description of each property follows.

Tack is defined as the property that enables an adhesive to form a bond of measurable strength with a surface of another material upon brief contact under light pressure [4] or no pressure.[5] Tackiness should increase when the glass transition temperature (T_g) of the copolymer decreases [6] and T_g should in turn decrease when the copolymer composition is enriched with a soft polymer like poly(BA). Because T_g depends on chain flexibility, all factors affecting chain flexibility such as sequence length distribution, MWD, and cross-linking density will affect T_g. This concept was supported by Satas [7, 8] who concluded that tackiness should increase with molecular weight. He demonstrated that an initially high value of tack associated with a low molecular weight would decrease and eventually level off when the molecular weight was increased. An increase in surfactant concentration could result in a decrease of tackiness if the water resistance is reduced or the surfactant molecules migrate to interfaces.[9] On the other hand, Brooks et al.[10] reported that the influence of a proprietary stabilizer on the tack of

a BA/VAc/MAA emulsion-based PSA was low. Peel strength represents the force required to remove a standard PSA strip from a specified test surface under a standard test angle (90 or 180°) under standard conditions. The incorporation of a high T_g component like poly(St) should improve peel strength up to the point where the adhesive becomes too stiff and does not wet the surface, thus decreasing peel strength.[1] Low molecular weight polymers will show a mediocre resistance to peel and as the molecular weight continues to increase, the resistance to peel will eventually reach a maximum before starting to deteriorate at higher molecular weights.[7, 8] When surfactant molecules migrate to the film-substrate interface, peel strength could be affected. Charmeau et al.[11] suggested that the increase in peel strength when the concentration of surfactant was also increased corresponded to the formation of a monolayer of surfactant at the PSA surface while a decrease in peel strength corresponded to the formation of a similar but much thicker layer that would behave as a weak boundary layer. Adhesive thickness is also a factor influencing peel strength. Peel strength is said to behave (increase or decrease) exponentially with respect to adhesive thickness.[1] Shear strength is the internal or cohesive strength of the adhesive mass. Usually, it represents the length of time it takes for a standard strip of PSA to fall from a test panel after application of a load. Shear resistance increases as the concentration of the high T_g component increases.[1] The resistance to shear will also be dependent on the MWD of the polymer.[7, 8] High molecular weight polymers present a good resistance to shear but this property will degrade rapidly at lower molecular weights. As well, a broad MWD will result in a lower shear resistance compared to a narrow one.[1] The presence of highly mobile small molecules like surfactant molecules are expected to decrease shear resistance.

Conventional Emulsions

The polymerization process chosen to produce PSAs can be carried out in different media such as bulk, solution or emulsion. In conventional emulsion polymerizations, the main ingredients are the monomer(s), water, surfactant and initiator. Chain transfer agents and buffers are often added to control the molecular weight and pH, respectively. When the concentration of surfactant exceeds its critical micelle

concentration (CMC), the excess surfactant molecules aggregate to form small colloidal clusters referred to as micelles. In principle, polymer particles can be formed by the entry of radicals into the micelles (heterogeneous nucleation), precipitation of growing oligomers in the aqueous phase (homogeneous nucleation), and radical entry in monomer droplets. In conventional emulsion polymerization, monomer droplets are relatively large (1-10 μm) compared to the size of monomer-swollen micelles (10-20 nm), and hence the surface area of the micelles is much greater than that of the monomer droplets. [2] Consequently, the probability for a radical to enter the monomer droplets is very low, and most particles are formed by homogeneous and heterogeneous nucleation. According to Harkins' model [12], a batch emulsion polymerization is divided into three intervals. Interval I is the particle formation, or nucleation stage. The reaction rate and the number of particles increase as a function of time in a closed reactor. The end of this interval corresponds to the disappearance of micelles (Harkins considered that micelles are the only loci of particle nucleation). During Interval II, the number of particles remains constant, and the monomer droplets, which play the role of monomer reservoir for the growing particles, maintain the concentration of monomer in the particles at the saturation point. The reaction rate is considered to be constant during this stage. The beginning of the final stage (Interval III) corresponds to the disappearance of the monomer droplets. The concentration of monomer in the particles decreases, but the number of particles remains theoretically constant. During this period, the rate can either decrease, or increase depending on the conditions. A drop in monomer concentration in the particles causes a decrease in the rate of polymerization, whereas an increase in rate can often be attributed to an accumulation of radicals inside the particles due to the well-known gel, or Tromsdorff effect, brought on by an increase in the local viscosity.

Mini-emulsions

The basis for mini-emulsion polymerization is an energetic homogenization process to reduce the size of the monomer droplets with the ingredients being basically the same as that found in a conventional emulsion with the exception of the co-surfactant. The droplet size can range from 50 to 500 nm in diameter [13] and the latex produced by

mini-emulsion is characterized by a broader PSD [2] ranging from 50 to 1000 nm in diameter.[14] If we manage to reduce the size of the droplets sufficiently, the resulting large surface area of the droplets allows them to compete effectively against the micelles to capture the oligomeric radicals and to become the main loci of polymerization. The presence of micelles in mini-emulsion is dependent on the amount of surfactant used in the formulation and on the homogenization procedure. The ideal situation, where no micelles are formed, is obtained when the surfactant concentration does not exceed the CMC and the homogenization procedure gives sufficiently small monomer droplets. An important concept in mini-emulsion polymerization is the degradation of the monomer droplets by two mechanisms. The first is the coalescence of the interactive monomer droplets due to attractive van der Waals forces. The result is the fusion of two colliding monomer droplets. This coalescence process can be minimized by adequate surfactant coverage on the monomer droplet surface to counteract the van der Waals forces. The second mechanism is the Ostwald ripening process.[2] This destabilization process refers to the diffusional degradation of droplets caused by the transport of monomer from the smaller droplets exhibiting a higher chemical potential, across the aqueous phase, and then to the large droplets. Ostwald ripening results in an increase in the average droplet size and a reduction in the total surface area of the monomer droplets. The Ostwald ripening effect can be minimized with an oil soluble co-surfactant. If they are properly stabilized, the number of particles at the end of the reaction will be the same as the number of droplets at the beginning. Ideally, droplet nucleation is the unique mechanism of particle formation in mini-emulsions if the formation of micelles can be avoided. Consequently, the stage of particle nucleation with monomer transport through the aqueous phase is avoided (Interval I and II in conventional emulsion). These critical differences mean that mini-emulsions will behave differently from a kinetic point of view than a conventional emulsion. It was proposed that there is no period of constant rate during a mini-emulsion comparable to that proposed for conventional emulsion in Harkin's theory.[15] This is due to the fact that the droplets are the site of polymerization and do not act as reservoirs. The rate of polymerization is not dependent on monomer diffusion from the droplets to the polymer particles.[15] Bechthold et al.[16] reported

similar results in their investigation of the kinetics of mini-emulsion polymerization of styrene.

Modeling Adhesive Performances

The performance of an adhesive depends heavily on its latex properties. Latex properties such as copolymer composition, MWD, PSD and gel content can be controlled by adjusting the operating conditions. Therefore, a good knowledge of the effect of operating conditions on the latex properties is required. In addition, the relationship between the latex properties and the performance of the adhesive is of equivalent importance. The relationship between the operating conditions and the latex properties can be obtained by mathematical modeling of the polymerization reactor and extensive experimentation. Considerable efforts have already been devoted to the modeling and control of at least some of the latex properties mentioned above [17, 18] and hence, this study will focus on discovering the impact of latex properties on adhesive performance. The development of these relationships in the context of mini-emulsions has been limited.[3] In that exploratory investigation, the performance of BA/methyl methacrylate PSAs produced in a conventional emulsion and a mini-emulsion was compared. Structure-property relationships between the adhesive properties and the weight-average molecular weight and average particle size were also examined. They found that adhesives made from both polymerization processes (conventional and mini-emulsion) showed similar characteristics that could be tailored to obtain the desired properties. They also concluded that mini-emulsions could provide a greater control over the latex properties because of the compartmentalized nature of the particles and finer control of the particle size.

Mini-emulsion polymerization has exploded onto the research scene in terms of the numbers of publications and the development of a wide range of useful polymeric materials.[2] However, this type of polymerization is characterized by complex kinetics and no adhesive property studies for free radical copolymerizations of styrene/butyl acrylate in mini-emulsion were found. Adhesive studies on similar systems using conventional emulsion could provide a basis for comparison. Elizalde et al. [19] presented

a model relating the adhesive properties and the complete MWD of n-butyl acrylate/styrene latexes of fixed copolymer molar composition (85/15) using partial least squares regression (PLS-R). The model was validated and combined with a control strategy to tailor the copolymer composition and MWD. Plessis et al.[20, 21] investigated a seeded semibatch emulsion polymerization of n-BA, with varying amounts of styrene as comonomer using potassium persulfate as the initiator at 75°C. They increased the amount of styrene from 0 to 10% and found that they could control the amount of gel and the level of branching by using the styrene as a control variable. They also found that the adhesive properties could be modified by adding small amounts of styrene. Furthermore, they investigated the effect of CTA (dodecane-1-thiol) on the kinetics, gel fraction, level of branching, and MWD of the sol. By increasing the CTA concentration, they noticed that the gel fraction and the sol weight-average molecular weight showed a strong dependence. On the other hand, no effects were observed on the kinetics or the level of branching. Tobing and Klein [22], compared the performance of PSAs made from a semi-continuous emulsion and a solution polymerization. The PSAs were made from two different polymers: poly(2-ethyl-hexyl acrylate-stat-acrylic acid) and poly(n-butyl acrylate-stat-acrylic acid) at 97.5/2.5 wt%. They found that the difference in film network morphology caused significantly lower shear holding power for the emulsion-based PSA compared with that of the solvent-borne film. Unlike shear holding power, the loop tack and peel of the acrylic PSAs were mainly controlled by the same sol/gel molecular parameters, regardless of originating from an emulsion or solution polymerization. The important molecular parameters were sol-to-gel ratio, entanglement molecular weight, weight average molecular weight, and to a lesser extent, glass transition temperature.

In this study, the main objective was to understand the relationships between particle size and copolymer composition on the adhesive performance of the PSA. Thus, a study of the St/BA system in mini-emulsion and the investigation of the performance of mini-emulsion-based adhesives were undertaken.

Experimental Section

Reagents

The reagents: St, BA, Acrylic Acid (AA), octadecyl acrylate (ODA), the chain transfer agent (CTA) n-dodecyl mercaptan, sodium dodecyl sulfate (SDS), Triton X-405, sodium hydrogen carbonate ($NaHCO_3$), and potassium persulfate (KPS) were used without any further purification. All components used to perform the characterizations, i.e., toluene, ethanol, methanol, chloroform-d, tetrahydrofuran (THF), sodium hydroxide (NaOH), and calcium chloride ($CaCl_2$) were used as received.

Experimental Procedure

The reactions were performed in a jacketed 1.2L stainless steel reactor with a Labmax™ setup (Mettler Toledo) and stirred at 200 rpm. The reactor was equipped with a nitrogen purging/pressurizing line, reflux condenser, sampling line and a port for the IR insertion probe. Stirring speed and temperature were automatically controlled using Camille™ software (Mettler Toledo).

St, BA and ODA were mixed for 15 minutes in a beaker while water, Triton X-405, and SDS were mixed for 15 minutes in a separate vessel. Both solutions were then combined and mixed for one hour with a magnetic stirrer. The mixture was then sonicated using a Fisher Scientific 550 sonic dismenbrator for 3 min at Level 6. The mixture was simultaneously cooled in an ice bath and well mixed while undergoing sonication.

The polymerizations were run at 80°C. The air background spectrum was recorded before the mixture was poured into the reactor. The reaction mixture was then heated and purged of oxygen by bubbling N_2 through it for at least 40 minutes. When the set point temperature was reached, a deoxygenated initiator solution made with KPS and distilled deionized water was charged into the reactor. This corresponded to time zero for the polymerization. At suitable time intervals, samples were taken through the sampling port for further analysis.

Characterization

Mass conversion based on the total polymer in the reaction mixture and percent solids were measured using gravimetry.

Proton nuclear magnetic resonance spectroscopy (^{1}H-NMR) was used to determine the average or cumulative composition of copolymers. Analyses were carried out at room temperature in deuterated chloroform (about 2% weight per volume solution) with a Bruker AMX-500 Fourier transform ^{1}H-NMR spectrometer. The acquisition time was 4.6 seconds and 16 scans were performed per sample. The relative amounts of monomer bound in the copolymer were estimated from the areas under the appropriate absorption peaks of the spectra. The spectral peaks for the $-OCH_2$ group in BA were located at ~3.4-4 ppm and the cyclic (5H) group in St was located at ~6.6-7.2 ppm.

Average molecular weights were measured using GPC. Polymer molecular weight averages and distributions were determined with a Waters Associates GPC system equipped with three Waters Styragel-HR columns (10^3, 10^4, and 10^6 Å pore size) installed in series, thermostated to 30°C, and a Waters 410 differential refractometer thermostated to 38°C. THF was used as the mobile phase and was delivered at 0.3 mL/min. Polymer samples were dissolved in THF to produce solutions with a concentration of approximately 0.005 g/10 mL and filtered through 0.45 μm filters to remove any high molecular weight gel. A quantity of 200 μL of each solution was injected into the GPC and the data were analyzed using the Millennium 32™ (version 3.05) chromatography manager software. The polymer molecular weights were calculated by using the universal calibration principle. The following Mark-Houwink parameters determined in THF were used for the calculations: for polystyrene, K and α were $16*10^3$ mL/g and 0.700, for polybutyl acrylate, K and α were $11*10^3$ mL/g and 0.708 (Hua, 2000). The values of K and α for the copolymers were obtained using weighted averages based on the cumulative copolymer composition data.

Latex particle size and particle size distribution (PSD) of the final latexes were determined using a Brookhaven disc centrifuge photosedimentometer (BI-DCP). A gradient fluid containing 0.1 mL of dodecanol, 0.2 mL methanol, and 15 mL of water was first prepared and injected into a spinning disc. A narrow polystyrene standard was used to check the accuracy of the system prior to the determination of the particle size. A

volume of 0.2 mL of each sample solution, which consisted of 3 mL of distilled de-ionized water, 1 mL of methanol, and 3 drops of the latex sample, was then injected into the spinning disc (~10,000 RPM).

Gel content was determined using the membrane partitioning method.[22] A known amount of sample was sealed between two polytetrafluoroethylene membranes (pore size of 0.2 um and diameter of 47mm). Enclosed samples were shaken for 72 hours in THF. Sealed pouches were air-dried until a constant weight was achieved. The difference between the initial and final weight of the sample was used to calculate the gel content.

Once the reaction latexes were characterized, PSAs could be created by casting a film of those latexes. Before casting the film, particle agglomerates were removed from the latexes using a size #30 mesh. Each latex were then coated onto a polyethylene terephthalate carrier using a Meyer rod #30 to give a dry film thickness of 30 μm when dried at room temperature. The films were dried for 2 days before testing. All the tests were performed according to the Test Methods for Pressure Sensitive Tapes [5] with stainless steel substrates. Three adhesive tests were performed to evaluate the tack, peel strength and shear strength of the PSAs. Two films were cast per latex and three specimens from each film were used for each adhesive test. A hierarchical design was used to test run-to-run and film-to-film differences. The analyses of the results have shown no film-to-film differences; therefore the average of the six measurements was used in the analysis of the results.

Tack was measured using the PSTC-16 (loop tack) standard. A specimen of 25.4 x 177.8 mm was cut and one inch on both sides was masked with masking tape. A loop with the adhesive facing outside was formed and placed in the upper grip of an Instron 1100 universal tester (Instron, Inc.). The loop was then brought into contact with the substrate mounted onto a loop tack fixture inserted into the bottom grip. When the loop covered and area of 25.4 x 25.4 mm, the upper grip was brought up at a crosshead speed of 300 mm/min. The maximum force required to remove the specimen was recorded as the loop tack.

Peel was measured using the PSTC-101 (180^{o} peel) standards. A specimen of 25.4 x 304.8 mm was cut and laminated onto the substrate using a 2040 g rubber coated roller.

The average force per 10 mm to peel the specimen from the substrate was recorded. The testing speed for the Instron 1100 universal tester (Instron, Inc.) was 300 mm/min.

Shear was measured using the PSTC-107 standards. A specimen of 25.4 x 152.4 mm was cut and an area of 25.4 x 25.4 mm was laminated onto the substrate using a 2040 g rubber coated roller. A 500 g weight was placed at the end of the specimen. Time to failure was recorded automatically using Labview™ software (National Instruments).

Experimental Design

A series of experiments was designed to further our understanding of the relationships between the latex properties (particle size and polymer composition) and the performance of the PSA (tack, peel and shear). Table 1 provides a list of experiments analyzed in this study. All recipes were performed as mini-emulsions with a sonication time of 3 minutes, a reaction temperature of 80°C and a solids content of 50 wt.%. The following concentrations of ingredients were also kept constant: water = 90 phm, $NaHCO_3$ = 1 phm, KPS = 0.75 phm, AA = 4 phm, CTA = 0.25 phm where phm represents parts per hundred parts of monomer.

Table 1: Batch recipes

	St (phm)[1]	BA (phm)	Triton (phm)	SDS (phm)	ODA (phm)
Run 1	5	95	0.5	0.03	0.5
Run 2	5	95	1	0.06	1
Run 3	5	95	2.5	0.15	2.5
Run 4	10	90	0.5	0.03	0.5
Run 5	10	90	1	0.06	1
Run 6	10	90	2.5	0.15	2.5
Run 7	15	85	0.5	0.03	0.5
Run 8	15	85	1	0.06	1
Run 9	15	85	2.5	0.15	2.5
Run 5-2	10	90	1	0.06	1
Run 5-3	10	90	1	0.06	1

[1]phm = parts per hundred parts monomer

In order to properly understand the relationships between particle size and copolymer composition on the adhesive performance of the PSA, a 3-level factorial design for 2 variables was planned. Because the emulsifier concentration was used to control particle size, it was decided to choose three levels of emulsifier concentration as a design variable. A system of three emulsifiers was required to prevent monomer droplet degradation and all three concentrations were changed proportionally for each level. Three polymer compositions were also chosen. Based on previous knowledge, it was assumed that certain compositions would produce PSAs with poor performance. Hence, the following constraints (in phm) were used in order to choose those three levels of compositions: 85<BA<95 and 5<St<15. As a result of this 3^2 factorial design, 11 runs (9 + 2 replicates of run 5) were performed.

A full second order polynomial model was used for each dependent variable (tack, peel strength, shear strength):

$$y = \beta_0 + \beta_1 * x_1 + \beta_2 * x_2 + \beta_{11} * x_1^2 + \beta_{22} * x_2^2 + \beta_{12} * x_1 * x_2 \qquad (1)$$

where y is the dependent variable, β's are the fitted parameters in the model, x_1 represents the St concentration in phm and x_2 represents the particle diameter in μm. The original variables were first coded in order to explain the effects of each fitted parameters because only the coded coefficients could be proportional to the observed effects. The variables were coded with the following formula:

$$\text{Coded value} = \frac{\left(\text{value} - \frac{(\max + \min)}{2}\right)}{\frac{|\max - \min|}{2}} \qquad (2)$$

The models were evaluated by looking at the residual plots, the correlation coefficient (R^2), the Significance F (in MS-Excel), and by performing a lack of fit test with $\alpha = 0.05$. The models were then reduced by looking at the precision of the parameter estimates and decoded to obtain the final form shown in this paper.

Results and Discussion

Gravimetry

Gravimetric results indicated fast reaction rates for all the reactions and they are shown in Figure 1 for Runs 1, 4, and 7. Similar results were obtained for the other runs. All the runs were completed successfully with conversions exceeding 99 wt. % in most cases.

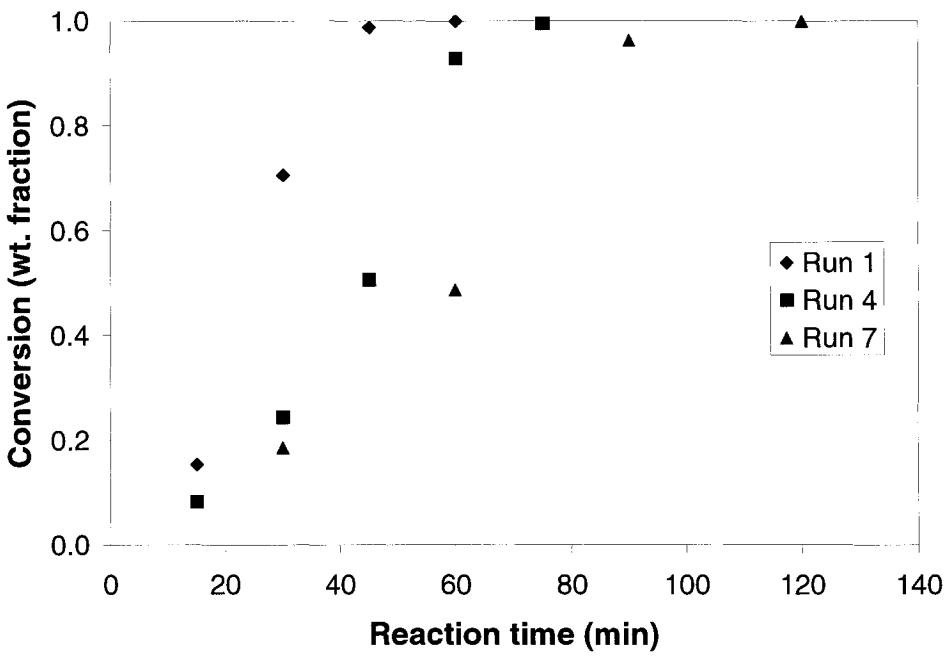

Figure 1: Conversion versus time for Runs 1, 4, 7

Monitoring of pH

As stated earlier, a small amount of acrylic acid (AA) was added to improve the peel and shear strength of the final PSA. It should be noted that the partitioning of AA in the water and oil phase will be strongly influenced by the pH of the reaction mixture.[23] In the St/BA/AA system, AA was found to be equally distributed between the water and oil phase when the pH was between 2 and 4. An increased pH of 6 and higher resulted in

the presence of AA mainly in the water phase. Furthermore, at a pH of 6 to 7, the AA propagation rate decreased. With this knowledge in mind, the pH of the reactions in this study was maintained between 4 and 5 to allow the incorporation of AA into the polymer particles.

Copolymer Compositions

The impact of monomer feed composition on cumulative copolymer composition is shown in Figure 2 for Runs 1, 4, and 7. Similar results were obtained for the other runs. As expected, the copolymer compositions were similar to the feed compositions.

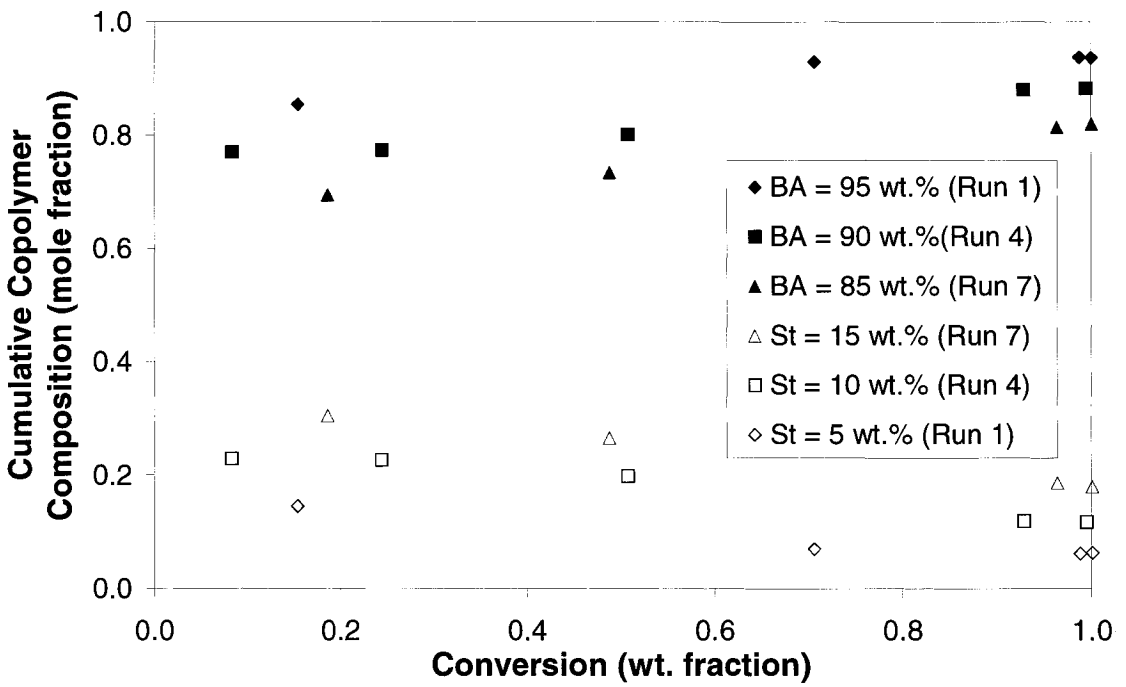

Figure 2: Cumulative copolymer compositions for different feed compositions

Glass Transition Temperatures (T_g)

An important factor affecting the performance of PSAs is T_g because it reflects the softness necessary for adhesive to flow and bond with a surface. However, Benedek et al.[1] warned that while T_g was a good predictor, it was not an absolute measure of adhesive suitability to become a PSA. When the amounts of all other components in the

recipe are kept constant, the final observed value should only be dependent on the ratio of monomers used in the recipe. Hence, the glass transition temperatures in this study were expected to range from 229 to 239 K.

Molecular Weight

Polymer molecular weight has a great influence on adhesive properties, especially in the low molecular weight range. As the molecular weight increases, its effect starts to level off. Low molecular weights exhibit good tack but their ability to peel is generally unacceptable for normal PSAs unless they can be crosslinked. Changes in PSA properties as a function of molecular weight [7] are shown in a generalized way in Figure 3. Both tack and peel strength increases with increasing molecular weight until a maximum is reached. Shear strength increases with increasing molecular weight but decreases strongly at a fairly high molecular weight. The molecular weights obtained in this study are shown in Table 2 and their polydispersity indexes ranged from 2.1 to 3.6.

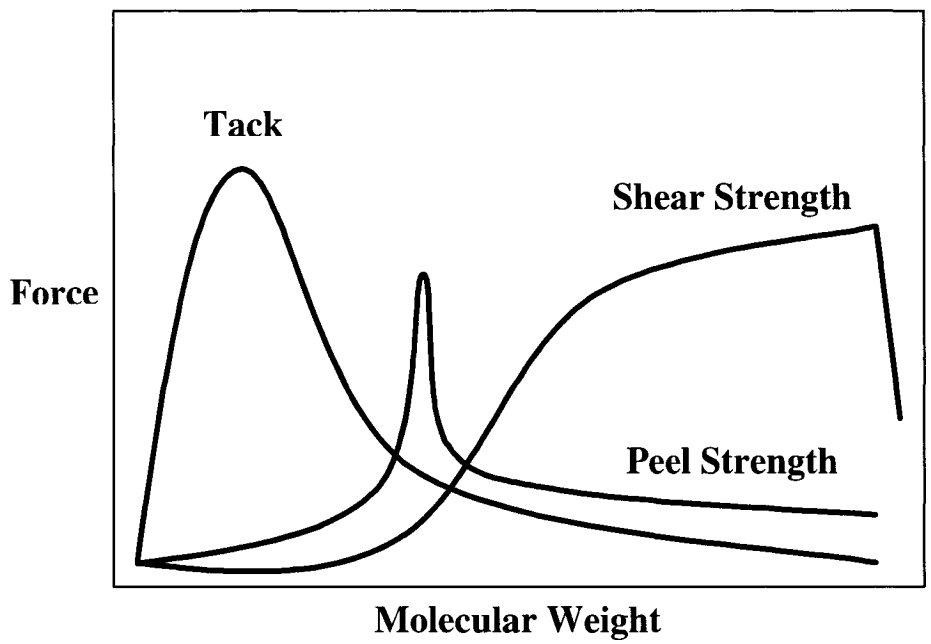

Figure 3: PSA properties as a function of molecular weight [7]

Gel Content

The gel content is another factor that could affect the performance of PSAs. An increase in gel content should increase the shear strength of PSAs while reducing tack.[24] The gel contents obtained in this study are shown in Table 2. A major contributor for the formation of gel in the latex is likely the content of BA. A high BA content can lead to "backbiting" or chain transfer to polymer, resulting in the formation of double bonds that can further polymerize and form branches or cross-links.[25] In addition, low CTA concentrations could enhance this effect because CTA is normally added to a recipe to lower the molecular weight and lower gel content. Hence with a lower concentration of CTA, the gel content could be expected to increase. Since the BA content remained fairly high for every recipe (between 85 and 95 phm), it was hard to appropriately assess the effect of gel content on PSA properties. Nonetheless, increases in tack and peel strength were observed with increases in gel content.

Modeling Adhesive Performance

All values for the dependent variables (tack, peel strength, shear strength) and the independent variables (particle diameter, polymer composition) used in the production of the models are shown in Table 2. The polydispersity indexes of the particle diameters ranged from 1.05 to 1.20.

For the determination of tack, six specimens from two films were tested. Prior to any analysis, a fully nested (hierarchical) analysis of variance (ANOVA) was performed to provide an estimate of the components of variance. This hierarchical experimental design was used to investigate run-to-run and film-to-film differences. The results shown in Table 3 were obtained with MS-Excel. Because the analysis of variance showed no statistically significant film-to-film differences, the average of six measurements were reported as a single value of tack (Table 2). As expected, the run-to-run differences were significant at the 0.05 level and were the major contributors to the total variability in the data. Similar results were obtained for peel and shear measurements.

Table 2: Experimental Results

Run	Tack (N/cm^2) ± 0.1	Peel (N/10mm) ± 0.3	Shear (h) ± 2	[St] (phm)[1] ± 0.003	d_{number} (µm) ± 0.005	$M.W._{number}$ (g/mol)	Gel Content (wt.%) ± 6
1	1.6	2.2	68	5.000	0.371	9.2E+04	13%
2	1.0	2.9	71	5.000	0.327	8.8E+04	11%
3	1.6	2.6	56	5.000	0.282	5.7E+04	19%
4	1.2	1.8	127	10.000	0.372	9.0E+04	0%
5	0.9	3.4	178	10.000	0.321	8.3E+04	28%
6	1.0	3.8	252	10.000	0.305	8.9E+04	25%
7	0.5	1.4	219	15.000	0.348	8.6E+04	0%
8	0.6	2.5	302	15.000	0.326	7.4E+04	9%
9	0.8	3.2	356	15.000	0.311	8.3E+04	19%
5-2	1.2	4.2	326	10.000	0.306	7.6E+04	22%
5-3	1.2	4.2	253	10.000	0.302	7.5E+04	34%

[1]phm = parts per hundred parts monomer
PDI = polydispersity index

Table 3: Analysis of Variance (ANOVA) for Tack

	Source	DF	SS	MS	F-calculated	F-tabulated	P
Fully Nested ANOVA	**Run**	10	7.6192	0.7619	59.160	2.1	3.48E-22
	Film	11	0.0000	0.0000	0.001	4.1	0.98
	Error	44	0.5667	0.0129			
	Total	65	8.1859				

	Source	Variance Component	% of Total	Standard Deviation
Variance Components	**Run**	0.117	93.08	0.342
	Film	0.000	0.00	0.000
	Error	0.009	6.92	0.093
	Total	0.126		

DF = Degree of Freedom, SS = Sum of Squares, MS = Mean Square
Significant difference exist if F-calculated > F-tabulated or if $P < 0.05$

All samples showed adhesive failure except for runs 1, 2 and 3 where a residue was left on the stainless steel substrate. The "softer" adhesives (runs 1, 2 and 3) showed a lack of cohesive strength with superior performance under loop tack conditions. In general, higher tack values could be associated with lower glass transition temperatures

or, to a lesser degree, higher gel contents. Despite the cohesive nature of some samples, they were included in the analysis because of their consistent behaviour with respect to the model. The coded (equation 3) and final (equation 4) forms for the tack model are:

$$\text{tack} = -0.4589 - 0.3914 * \overline{f_{St}} - 0.4079 * d_p + 1.0880 * d_p^2 - 0.4174 * \overline{f_{St}} * d_p \quad (3)$$

$$\text{tack} = 31.370 + 0.2928 * \overline{f_{St}} - 189.46 * d_p + 297.74 * d_p^2 - 1.0279 * \overline{f_{St}} * d_p \quad (4)$$

There were no trends in the residuals and no lack of fit was found. The model was significant and the correlation coefficient (R^2) was 0.9790. From the coded form of the model, the most influential parameter was the d_p^2 parameter indicating a strong curvature (with a minimum) for the relationship between particle size and tack. The model also showed the synergistic effect of particle size and polymer composition on tack. A representation of the model is shown in Figure 4. When the styrene content is decreased, the positive impact on tack is consistent with the work of Aubrey.[6] As for particle size, a possible explanation for the positive effect of smaller particles on tack could involve the film formation process. It can be speculated that smaller particles could pack more tightly together during the drying process thus increasing the area of contact between the adhesive and the substrate. The incorporation of a molecular weight variable was attempted for the tack model but its inclusion rendered the model inadequate to explain the data. This could be explained by a correlation between particle size and/or polymer composition with molecular weight. In this study, only the particle size seemed to be correlated to the molecular weight where an increase in particle size was often associated with an increase in molecular weight.

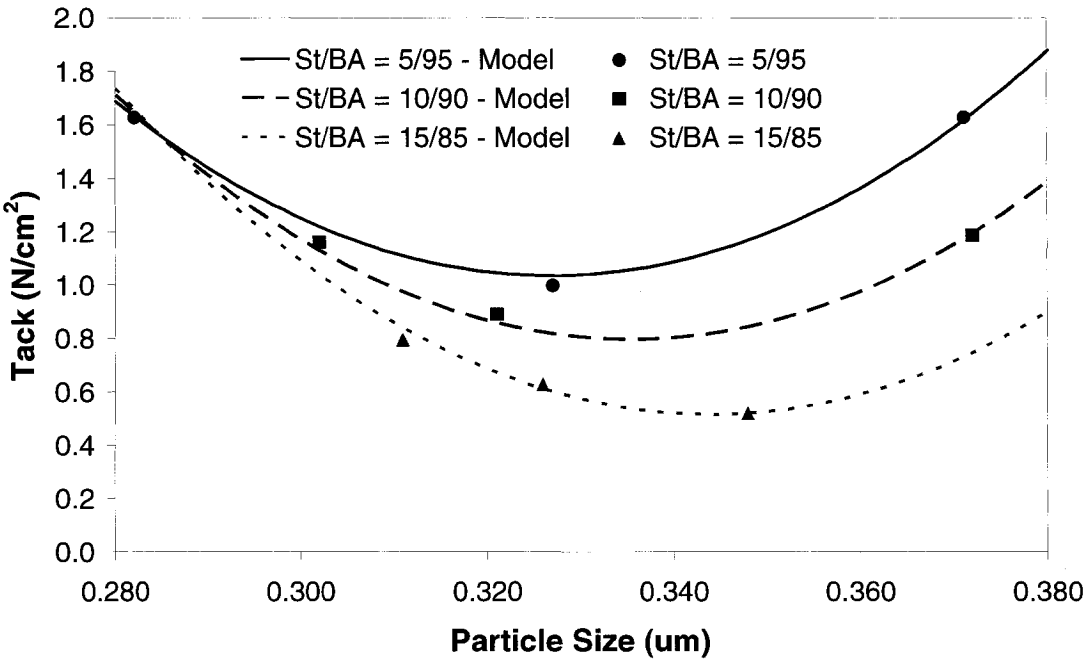

Figure 4: Tack vs. particle size and polymer composition.

As for peel strength, only the latexes associated with the higher T_g values (runs 7, 8 and 9) or with no gel content (runs 4 and 7) showed adhesive failure (no residue was left on the stainless steel substrate). The "softer" adhesives with some gel content (runs 1, 2, 3, 5 and 6) showed a lack of cohesive strength. In general, higher peel strength values could be associated with higher gel contents. Similar to tack, the consistent behaviour with respect to the model allowed the samples exhibiting cohesive strength to be included in the analysis. The coded (equation 5) and final (equation 6) forms for the peel strength model are:

$$peel = 0.3389 - 0.0322 * \overline{f_{St}} - 1.0044 * d_p - 0.5671 * \overline{f_{St}}^2 - 0.8047 * \overline{f_{St}} * d_p \quad (5)$$

$$peel = -5.7541 + 2.2125 * \overline{f_{St}} + 18.398 * d_p - 0.0310 * \overline{f_{St}}^2 - 4.8943 * \overline{f_{St}} * d_p \quad (6)$$

There were no trends in the residuals and no lack of fit was found. The model was significant and the correlation coefficient (R^2) was 0.9614. From the coded form of the

model, the most influential parameter was the d_p parameter indicating a strong linear relationship between particle size and peel strength. The coded model also showed a pronounced synergistic effect of particle size and polymer composition on peel strength. A representation of the model is shown in Figure 5. At the lowest particle sizes, the increased styrene composition produced effects consistent with the work of Benedek et al.[1] who found that it should increase the peel strength. It seems that at the highest particle sizes, the impact of increasing the styrene content reduces the peel strength. Benedek also found that increasing the styrene content should increase the peel strength up to a maximum. Beyond this maximum, the adhesive becomes too stiff and does not wet the surface appropriately hence, reducing the peel strength. During the drying process, maybe the largest particle sizes imparted some inherent weaknesses to the peel strength property and the smallest styrene content tested already exceeded the optimum value. It is likely that a possible correlation between particle size and molecular weight could have explained the failure to incorporate a molecular weight variable inside the peel strength model.

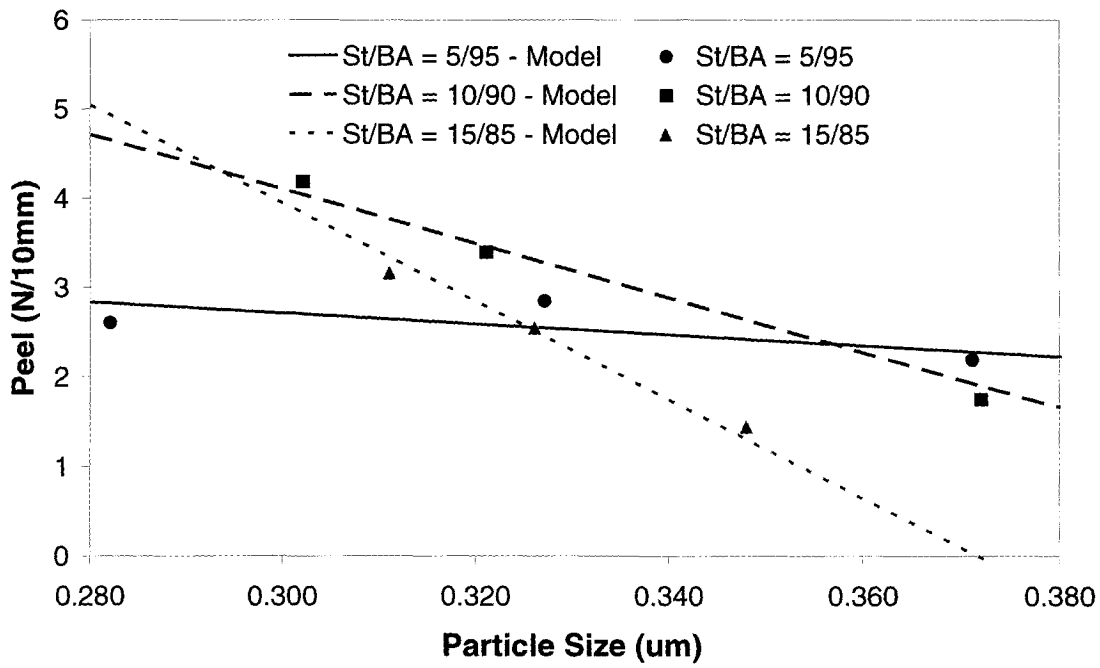

Figure 5: Peel strength vs. particle size and polymer composition

In the case of shear strength, all the samples showed cohesive failure where a residue was left on the stainless steel substrate. In general, higher shear strength values could be associated with higher glass transition temperatures. Despite the cohesive nature of those samples, they were kept in the analysis because of their consistent behaviour with respect to the model. The coded (equation 7) and final (equation 8) forms for the shear strength model are:

$$\text{shear} = 0.8011 * \overline{f_{St}} - 0.6398 * d_p - 0.1976 * \overline{f_{St}}^2 + 0.0910 * d_p^2 - 0.6545 * \overline{f_{St}} * d_p \quad (7)$$

$$\text{shear} = 191.93 * \overline{f_{St}} - 3201.1 * d_p - 1.3377 * \overline{f_{St}}^2 + 8226.7 * d_p^2 - 431.12 * \overline{f_{St}} * d_p \quad (8)$$

There were no trends in the residuals and no lack of fit was found. The model was significant and the correlation coefficient (R^2) was 0.9347. From the coded form of the model, the most influential parameter was the f_{ST} parameter indicating a strong linear relationship between polymer composition and shear strength. The coded model also showed an appreciable linear relationship with respect to particle size and a pronounced synergistic effect of particle size and polymer composition on shear strength. A representation of the model is shown in Figure 6. When the styrene content is increased, the positive impact on shear strength is consistent with the work of Benedek et al.[1] As for particle size, a possible explanation for the positive effect of smaller particles on shear strength could also involve a similar concept described for tack where smaller particles could pack more tightly together during the drying process thus increasing the area of contact between the adhesive and the substrate. Similar to the two previous models, the possible correlation between particle size and molecular weight probably rendered the shear strength model inadequate to explain the data when a molecular weight variable was introduced.

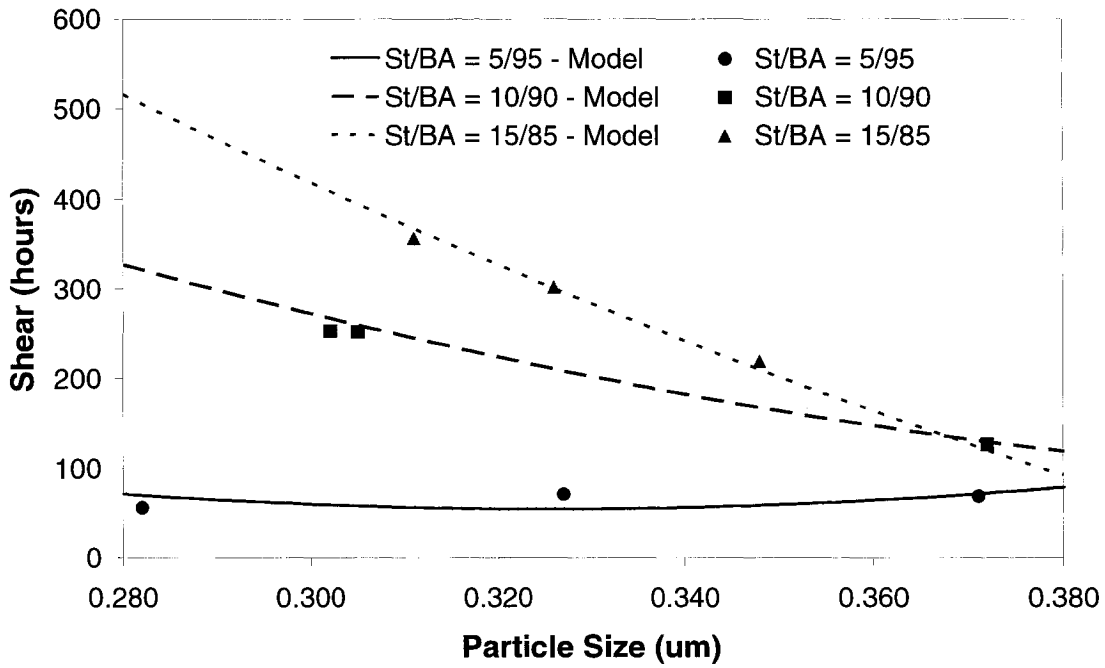

Figure 6: Shear strength vs. particle size and polymer composition

The final forms of the models allowed 3-D response surfaces to be built; these are shown in Figures 7, 8 and 9. From the tack response surface, a minimum is located in the middle of the investigated particle diameter region. Although moving away from this region in both directions would increase tack, more freedom over the polymer composition could be achieved if the particle diameter became smaller. The peel and shear strength response surfaces both indicate maximums in the smallest particle diameter region with high styrene composition. After investigating all three response surfaces, the optimal adhesive performance region should be located near the smallest particle diameter investigated with the highest styrene composition. In order to properly assess those conclusions, a more in depth study should be conducted in this optimal region.

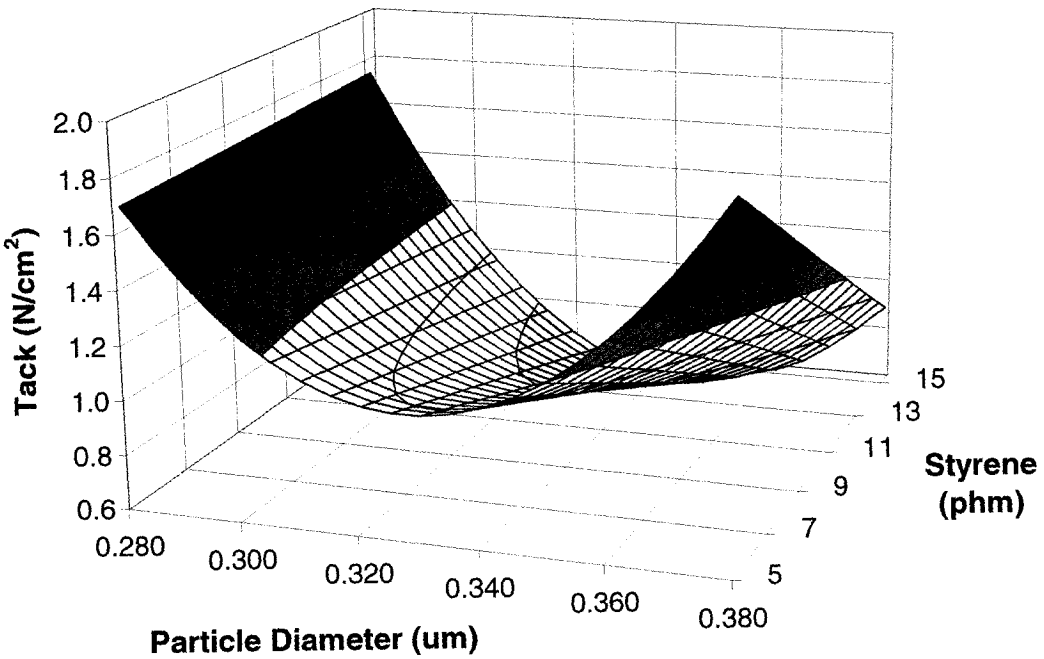

Figure 7: 3-D response surface for the tack model

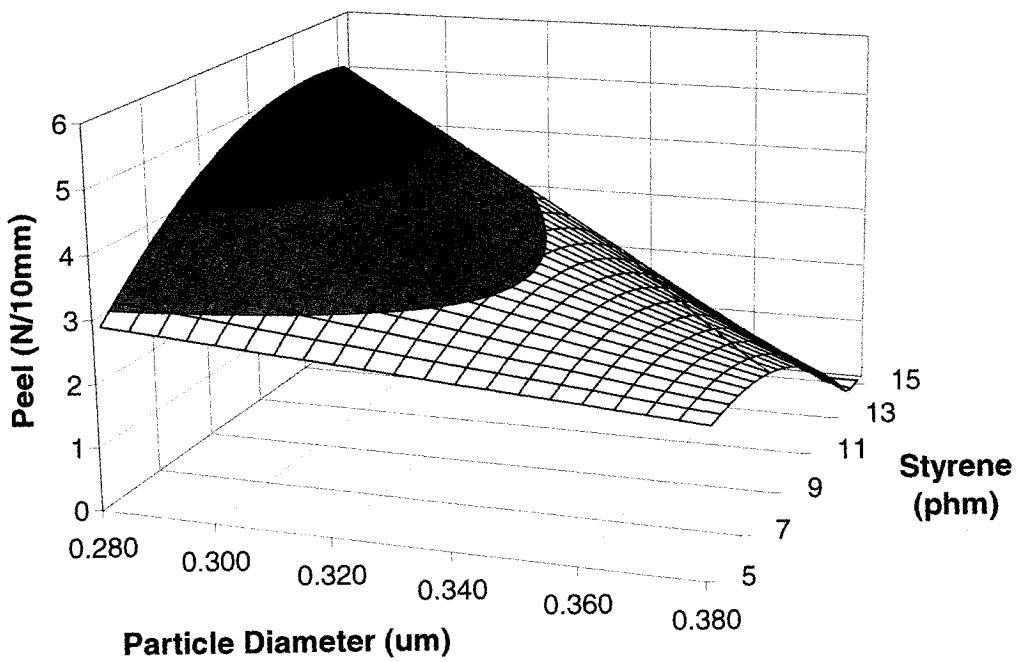

Figure 8: 3-D response surface for the peel strength model

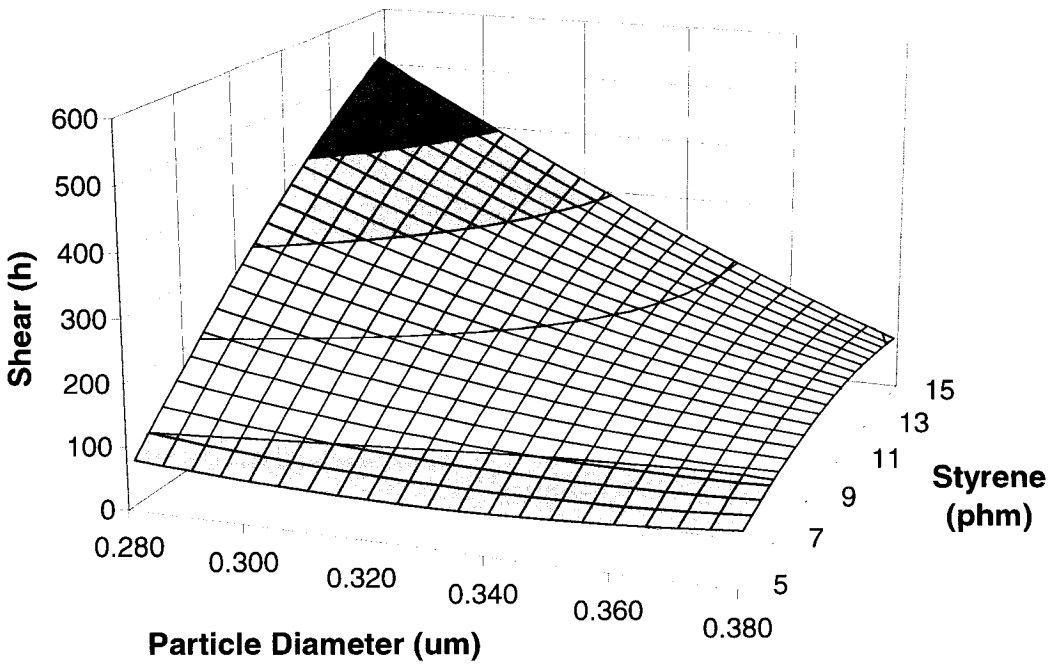

Figure 9: 3-D response surface for the shear strength model

Conclusions

A series of St/BA mini-emulsion copolymerizations was carried out in a 1.2L stainless steel reactor. All recipes were performed as mini-emulsions with a sonication time of 3 minutes, a reaction temperature of 80°C and a solids content of 50 wt.%. Conversions were monitored off-line using gravimetry and in-line monitoring was also performed using ATR-FTIR spectroscopy. All the runs were completed successfully with conversions exceeding 99 wt.% in most cases. The pH of the reactions in this study was maintained between 4 and 5 to allow the incorporation of AA into the polymer particles. The T_g's ranged from 229 to 239 K, the molecular weights ranged from $6x10^4$ to $9x10^4$ and the gel contents ranged from 0 to 33.6 wt.%.

By using a constrained mixture design, the influence of particle size and polymer composition on PSA performance was investigated. As a result of a 3^2 factorial design, 11 runs (9 runs and 2 replicates) were performed. Loop tack, peel strength and shear strength were measured and modeled empirically using a full second order polynomial.

The models were evaluated by looking at the residual plots, the correlation coefficient (R^2), the Significance F (in MS-Excel), and by performing a lack of fit test with $\alpha = 0.05$. The models were then reduced by looking at the precision of the parameter estimates. For every model, there were no trends in the residuals and no lack of fit was found. The models were also significant with high correlation coefficient (R^2). For every adhesive performance, it was necessary to conduct a fully nested ANOVA analysis to investigate the significance of film-to-film variation because the required number of samples was impossible to obtain by using only one film. In all cases, there were no statistically significant differences between films and the average of six measurements were reported as a single value.

In general, higher tack values were associated with lower glass transition temperatures and, to a lesser degree, higher gel contents. The tack model showed that the most influential parameter was the d_p^2 parameter indicating a strong curvature (with a minimum) for the relationship between particle size and tack. The tack model also agreed with the literature [6] by showing that a decrease in styrene content would be beneficial for tack. A possible explanation for the positive impact of smaller particles on tack could involve an increased area of contact created during the drying process.

In the case of peel strength, higher values were normally associated with higher gel contents. The peel model showed that the most influential parameter was the d_p parameter indicating a strong linear relationship between particle size and peel strength. At the lowest particle sizes, the peel model agreed well with the literature [1] where an increase in styrene content resulted in and improved peel strength. With the largest particle sizes, the impact of adding more styrene to the recipe was always detrimental to peel strength. As stated by Benedek et al.[1], if the maximum peel strength is achieved with a certain styrene composition, the addition of more styrene to the polymer chain could only result in a reduced performance. Hence with the largest particle sizes, maybe the optimum styrene content was already exceeded.

In the case of shear strength, higher values could normally be associated with higher glass transition temperatures. From the shear model, the most influential parameters were the styrene composition and d_p parameters indicating strong linear relationships between polymer composition and particle size on shear strength. The shear

model also showed some consistency with the literature [1] by exhibiting positive effects on shear strength when the styrene content was increased. A possible explanation for the positive effect of smaller particles on shear strength could also involve a similar concept described for tack where smaller particles could pack more tightly together during the drying process thus increasing the area of contact between the adhesive and the substrate

The final forms of the models also allowed 3-D response surfaces to be built and the optimal adhesive performance region was located near the smallest particle diameter investigated with the highest St composition. Ultimately, this study has shown that the control over particle sizes afforded by mini-emulsions could enable us to affect the properties of PSA in a controlled manner. This could be coupled with an in-depth exploration of the experimental space around the optimal adhesive performance region in future studies.

Acknowledgements

The authors wish to gratefully acknowledge the financial support from the Natural Science and Engineering Research Council (NSERC) of Canada and the Ontario Graduate Scholarship (OGS)

References

1. Benedek, I.; Heymans, L.J. *Pressure-Sensitive Adhesives Technology*, Marcel Dekker Inc.: New York, 1997.
2. Asua, J.M. Miniemulsion Polymerization. Prog. Polym. Sci. 2002, 27(7), 1283-1337.
3. Jovanovic, R.; Ouzineb, K.; McKenna, T.F.; Dubé, M.A. Butyl acrylate/methyl methacrylate latexes: Adhesive properties. Macromolecular Symposia. 2004, 206, 43-56.

4. ASTM D2979-88. Standard Test Method for Pressure-Sensitive Tack of Adhesives Using an Inverted Probe Machine, Annual Book of ASTM Standards, American Society for Testing and Materials: Philadelphia, 1995; Vol. 15.06.
5. PSTC-5. Quick Stick of Pressure Sensitive Tapes, Test Methods for Pressure Sensitive Adhesive Tapes (13th ed), Pressure Sensitive Tape Council: Northbrook, 2000.
6. Aubrey, D.W. *Pressure Sensitive Adhesives - Principles of Formulation. Developments in Adhesives*, Wake, W.C., Ed.; Applied Sci., Publishers: Barking, England, 1977.
7. Satas, D. Tailoring pressure sensitive adhesive polymers. Adhes. Age. 1972, 15(10), 19-23.
8. Satas, D. *Handbook of Pressure Sensitive Adhesive Technology*; Van Nostrand Reinhold: New York, 1989.
9. Taylor, M.A. *Polymer Dispersions and Their Industrial Applications*, Wiley-VCH: Weinheim, 2002.
10. Brooks, T.W.; Kell, R.M.; Boss, L.G.; Nordhaus, D.E. Analysis of Factors Important in Emulsion Acrylic Pressure Sensitive, Adhesive Design. TAPPI Proceedings. TAPPI Polymers, Laminations and Coating Conference, Boston, September, 1984, 469-476.
11. Charmeau, J.Y.; Gerin, P.A.; Vovelle, L.; Schirer, R.; Holl, Y. Adhesion of Latex Films. III. Surfactant Effects at Various Peel Rates. J. Adhes. Sci. Technol. 1999, 13(2), 203-215.
12. Harkins, W.D. A General Theory of Mechanism of Emulsion Polymerization. J. Am. Chem. Soc. 1947, 69, 1428-1444.
13. Capek, I.; Chern, C.S. Radical Polymerization in Direct Mini-Emulsion Systems. Adv. Polym. Sci. 2001, 155, 105-127.
14. Lovell, P.A.; El-Aasser, M.S. *Emulsion Polymerization and Emulsion Polymers*, John Wiley and Sons, Inc.: England, 1997; 1-515.
15. Ouzineb, K. PhD thesis, Department of Chemistry, University of Claude Bernard Lyon I, Lyon, France, 2003.

16. Bechthold, N.; Landfester, K. Kinetics of miniemulsion polymerization as revealed by calorimetry. Macromolecules. 2000, 33(13), 4682-4689.
17. Dubé, M.A.; Soares, J.B.P.; Pendilis, A. Mathematical Modeling of Multicomponent Chain-Growth Polymerizations in Batch, Semibatch, and Continuous Reactors: A Review. Ind. Eng. Chem. Res. 1997, 36(4), 966-1015.
18. Gao, J.; Penlidis, A. Mathematical modeling and computer simulator/database for emulsion polymerizations. Progress in Polymer Science. 2002, 27(3), 403-535
19. Elizalde, O.; Vicente, M.; Leiza, J.R.; Asua, J.M. Control of the adhesive properties of n-butyl acrylate/styrene latexes. Polym. React. Eng. 2002, 10(4), 265-283.
20. Plessis, C.; Arzamendi, G.; Leiza, J.R.; Schoonbrood, H.A.S.; Charmot, D.; Asua, J.M. Kinetics and polymer microstructure of the seeded semibatch emulsion copolymerization of n-butyl acrylate and styrene. Macromolecules. 2001, 34(15), 5147-5157.
21. Plessis, C.; Arzamendi, G.; Leiza, J.R.; Alberdi, J.M.; Schoonbrood, H.A.S.; Charmot, D.; Asua, J.M. Seeded semibatch emulsion polymerization of butyl acrylate: Effect of the chain-transfer agent on the kinetics and structural properties. J. Polym. Sci.: Part A: Polym. Chem. 2001, 39(7), 1106-1119.
22. Tobing, S.D.; Klein, A. Molecular parameters and their relation to the adhesive performance of acrylic pressure-sensitive adhesives. Journal of Applied Polymer Science. 2001, 79(12), 2230-2244.
23. Dos Santos, A.M.; McKenna, T.F.; Guillot, J. Emulsion copolymerization of styrene and n-butyl acrylate in presence of acrylic and methacrylic acids: Effect of pH on kinetics and carboxyl group distribution. Journal of Applied Polymer Science. 1997, 65(12), 2343-2355.
24. Zosel, A.; Ley, G. Influence of crosslinking on structure, mechanical properties, and strength of latex films. Macromolecules. 1993, 26(9), 2222-2227.
25. Lovell, P.A.; Shah, T.H.; Heatley, F. Polymer Communications. 1991, 32(4), 98-103.
26. Rudin, A. *The Elements of Polymer Science and Engineering*, 2nd Ed.; Academic Press: San Diego, 1999; 1-522.

Chapter 6 – Conclusions and Recommendations

Traditional polymerization monitoring is often carried out using off-line characterization of samples from a process flow line. A disadvantage of off-line techniques for conversion and composition monitoring, such as gravimetry and ^{1}H-NMR spectroscopy is the time lag between sampling and results. IR spectroscopy techniques are especially suited for real-time reaction monitoring as they allow spectral measurements to be obtained directly in the process stream without the need of sampling devices for on-line analysis. Because in-line monitoring using ATR-FTIR spectroscopy was successful on different emulsion systems, it was of interest in this thesis to validate the method for mini-emulsions.

In Chapter 4, the in-line monitoring of mini-emulsions using ATR-FTIR spectroscopy was investigated. A series of styrene/butyl acrylate mini-emulsion copolymerizations were carried out in a 1.2L stainless steel reactor. Conversions and copolymer compositions were monitored off-line using gravimetry ^{1}H-NMR spectroscopy, respectively. Real time, in-line monitoring was also performed using ATR-FTIR spectroscopy. It was found that the air background and the signal to noise ratio were both appropriate for this kind of system. No significant probe fouling was observed and the temperature effects were deemed to be negligible. In addition, Beer's law was validated and the univariate methods gave inconsistent results. A multivariate or PLS method using the full spectra of reactions gave much more promising results for the in-line mini-emulsion polymerization monitoring. No significant differences were found between the off-line (gravimetry and ^{1}H-NMR spectroscopy) results and the ATR-FTIR spectroscopy data coupled with the PLS method confirming that ATR-FTIR spectroscopy is a reliable tool for monitoring individual monomer concentrations and conversions.

Mini-emulsion polymerizations are also very useful as they allow one to control the number and size of the particles being formed. This improved control of the particle size distribution coupled with a control over the molecular weight distribution and composition of the copolymer could offer the possibility of tailoring the desired

properties of PSAs. The main interest in this thesis was to measure the effect of varying particle size and copolymer composition on adhesive properties.

In Chapter 5, the effects of varying particle size and copolymer composition on adhesive properties were investigated. A series of styrene/butyl acrylate mini-emulsion copolymerizations were carried out in a 1.2L stainless steel reactor. Conversions were monitored off-line using gravimetry and in-line monitoring was also performed using ATR-FTIR spectroscopy. By using a constrained mixture design, the influences of particle size and polymer composition were investigated. As a result of a 3^2 factorial design, 11 runs (9 runs and 2 replicates) were performed. Loop tack, peel strength and shear strength were measured and modeled empirically using a full second order polynomial. For every model, there were no trends in the residuals and no lack of fit was found. The models were also significant with high correlation coefficient (R^2). In general, higher tack values were associated with lower glass transition temperatures and, to a lesser degree, higher gel contents. The tack model showed that the most influential parameter was the d_p^2 parameter indicating a strong curvature (with a minimum) for the relationship between particle size and tack. The tack model also agreed with the work of Aubrey 1977 by showing that a decrease in styrene content would be beneficial for tack. A possible explanation for the positive impact of smaller particles on tack could involve an increased area of contact created during the drying process. In the case of peel strength, higher values were normally associated with higher gel contents. The peel model showed that the most influential parameter was the d_p parameter indicating a strong linear relationship between particle size and peel strength. At the lowest particle sizes, the peel model agreed well with the work of Benedek et al. 1997 where an increase in styrene content resulted in and improved peel strength. With the largest particle sizes, the impact of adding more styrene to the recipe was always detrimental to peel strength. As stated by Benedek et al. 1997, if the maximum peel strength is achieved with a certain styrene composition, the addition of more styrene to the polymer chain could only result in a reduced performance. Hence with the largest particle sizes, maybe the optimum styrene content was already exceeded. In the case of shear strength, higher values could normally be associated with higher glass transition temperatures. From the shear model, the most influential parameters were the styrene composition and d_p parameters

indicating strong linear relationships between polymer composition and particle size on shear strength. The shear model also showed some consistency with the work of Benedek et al. 1997 by exhibiting positive effects on shear strength when the styrene content was increased. A possible explanation for the positive effect of smaller particles on shear strength could also involve a similar concept described for tack where smaller particles could pack more tightly together during the drying process thus increasing the area of contact between the adhesive and the substrate. The final forms of the models also allowed 3-D response surfaces to be built and the optimal adhesive performance region was located near the smallest particle diameter investigated with the highest styrene composition. Ultimately, this study has shown that the control over particle sizes afforded by mini-emulsions could enable us to affect the properties of PSA in a controlled manner.

Future work regarding St/BA mini-emulsion-based PSA should include the following:

1. In order to gain an improved control over the latex properties of mini-emulsions, a feedback control policy could be integrated to an ATR-FTIR spectroscopy system coupled with a PLS method for full spectra. This would allow the tailoring of desired latex properties.

2. In future studies, it would be interesting to explore in more depth the experimental spaces around the optimal adhesive performance region found in the paper on PSA performance. Ultimately, a model covering a greater number of particle sizes and styrene compositions in the optimum region could be used to improve our understanding of the latex properties required to achieve the desired PSA performances.

References

1. Aubrey, D.W. *Pressure Sensitive Adhesives - Principles of Formulation. Developments in Adhesives*, Wake, W.C., Ed.; Applied Sci., Publishers: Barking, England, 1977.

2. Benedek, I.; Heymans, L.J. *Pressure-Sensitive Adhesives Technology*, Marcel Dekker Inc.: New York, 1997.

Appendix A – Sample Calculations

St/BA (20/80 wt%) mini-emulsion copolymerization at 60°C is selected to illustrate the calculation procedures throughout Appendix A. This represents a previous copolymerization executed during my B.A.Sc. thesis (Roberge, S. B.A.Sc. thesis, Department of Chemical Engineering, University of Ottawa, 2002).

Polymerization recipe

Table A.1: Polymerization Recipe

	Ingredient	Weight (g)	phm	Wt. Fraction
monomer	St	200.31	19.98	0.0695
monomer	BA	802.47	80.02	0.2786
medium	Water	1801.46	179.65	0.6253
emulsifier	Triton X-405	25.06	2.50	0.0087
emulsifier	SDS	1.50	0.15	0.0005
co-emulsifier	ODA	25.00	2.49	0.0087
initiator	KPS	15.07	1.50	0.0052
buffer	$NaHCO_3$	0.00	0.00	0.0000
CTA	n-dodecyl mercaptan	9.99	1.00	0.0035
Total		2880.86		1.00

*phm = parts per hundred monomers

Parts per hundred monomers for a given ingredient

$$\text{phm(i)} = \frac{\text{weight of ingredient}}{\text{total weight of monomers}} \qquad \text{phm(St)} = \frac{200.31}{200.31 + 802.47} = 19.98$$

Weight fraction for a given ingredient

$$\text{w(i)} = \frac{\text{weight of ingredient}}{\text{total weight}} \qquad \text{w(St)} = \frac{200.31}{2880.86} = 0.0695$$

Experimental calculations for gravimetric data

Table A.2: Experimental values for gravimetric data

Time (min)	Empty dish (g)	Latex + dish (g)	Dry latex + dish (g)	Solids	Conversion
60	1.263	2.096	1.331	0.082	0.158
120	1.275	2.182	1.392	0.129	0.294
205	1.277	2.155	1.437	0.182	0.447
240	1.265	2.060	1.434	0.213	0.534
300	1.269	1.994	1.454	0.255	0.657
360	1.272	2.108	1.570	0.356	0.948
390	1.268	2.107	1.564	0.353	0.937
420	1.265	2.286	1.627	0.355	0.942

Solids for a given time

$$\text{Solids} = \frac{(\text{wt. of dry latex and dish - wt. of empty dish})}{(\text{wt. of latex and dish - wt. of empty dish})}$$

$$\text{Solids} = \frac{(1.331 - 1.263)}{(2.096 - 1.263)} = 0.082$$

Conversion for a given time

$$\text{Conversion} = \frac{\text{Solids - wt. fr. Triton - wt. fr. SDS - wt. fr. ODA - wt. fr KPS - wt. fr CTA}}{\text{initial wt. fr. monomers}}$$

$$\text{Conversion} = \frac{0.082 - 0.0087 - 0.0005 - 0.0087 - 0.0052 - 0.0035}{0.2786 + 0.0695} = 0.158$$

Experimental calculations for ATR-FTIR data (univariate method)

Table A.3 Experimental values for ATR-FTIR data

Time (min)	Peak (775)	x1(St)	Peak (810)	x2(BA)	X
0	0.87864	0.00000	0.60569	0.00000	0.00000
2	0.87404	0.00523	0.60403	0.00275	0.00399
4	0.87692	0.00196	0.60356	0.00351	0.00274
6	0.87190	0.00767	0.60253	0.00522	0.00645
8	0.87402	0.00526	0.60236	0.00549	0.00538
10	0.87551	0.00356	0.60141	0.00707	0.00531
12	0.87400	0.00528	0.60037	0.00878	0.00703
14	0.87465	0.00455	0.59947	0.01028	0.00741
16	0.87291	0.00652	0.59810	0.01253	0.00953
18	0.87526	0.00384	0.59828	0.01223	0.00804
20	0.87595	0.00306	0.59692	0.01448	0.00877

Individual monomer conversion x(i)

$$x\ (\text{mol fraction}) = 1 - \frac{\text{peak height at time t}}{\text{peak height at time t} = 0}$$

$$x_1\ (\text{mol fraction}) = 1 - \frac{0.87404}{0.87864} = 0.00523$$ peak for St at 775 cm^{-1}

$$x_2\ (\text{mol fraction}) = 1 - \frac{0.60403}{0.60569} = 0.00275$$ peak for BA at 810 cm^{-1}

Overall conversion X(mass fraction)

$$X\ (\text{mass fraction}) = \frac{m_1}{m_1 + m_2} x_1\ (\text{mol fraction}) + \frac{m_2}{m_1 + m_2} x_2\ (\text{mol fraction})$$

where $\frac{m_i}{m_i + m_j}$ represents the mass fraction of monomer i in the reaction mixture

$$X\ (\text{mass fraction}) = 0.5 * 0.00523 + 0.5 * 0.00275 = 0.00399$$

Appendix B – Extra Figures and Tables

Figures B.1, B.2: Monomer peak assignment

Figure B.3: ^{1}H-NMR spectrum

Figure B.4: Particle size determination

Figures B.5 to B.10: PLS results for conversion predictions

Figure B.11: Temperature profiles

Figure B.12: pH profiles

Figures B.13 to B.15: Overall conversions by gravimetry

Figures B.16 to B.31: Copolymer compositions

Styrene Monomer		Poly(styrene)	
Spectral Region (cm-1)	Absorbance Assignment	Spectral Region (cm-1)	Absorbance Assignment
3081	=CH2 stretching		
3060	Ring C-H stetching vibration	3028	Ring-CH stretching
3027	Ring C-H stetching vibration		
3010	-CH=stretching	2927	-CH2 asymetric stretching
1630	C=C stretching	2858	-CH3 asymetric stretching
1602	Ring quadrant stretching	1599	Ring quadrant stretching
1576	Ring quadrant stretching		
1495	Ring semi-circle stretching	1491	Ring semi-circle stretching
1449	Ring semi-circle stretching	1452	Ring semi-circle stretching
1412	=CH2 deformation	1367	-CH-CH2 wag
1202	C-CH=stretching	1166	-CH-CH2 wag
1082	Ring semi-circle stretching	1066	Ring semi-circle stretching
1021	Ring semi-circle stretching	1027	Ring semi-circle stretching
991.8	-CH=wag		
906.9	-CH2 wag		
773.7	Ring C-H wag	758	Ring C-H wag
696.6	Ring bending	695.1	Ring bending

Figure B.1: Styrene peak assignment (Rivard, T. M.A.Sc. thesis, Department of Chemical Engineering, University of Ottawa, 2002).

Butyl Acrylate Monomer		Poly(butyl acrylate)	
Spectral Region (cm-1)	Absorbance Assignment	Spectral Region (cm-1)	Absorbance Assignment
2950-2850	Aliphatic C-H stretching	3000-2800	Methyl, methylene and methane C-H stretching
1725	C=O stretching	1740	C=O stretching
1638-1621	Acrylate C=C doublet		
1466	Acrylate C=C	1470	C-H deformation in methyl and methylene bands
1409	C-H deformation in =CH2	1400-1300	C-H deformation in C-CH3 band
1273	=CH rocking		
1187	=C-(C=O)-O-CH2- stretching of aliphatic ester	1270-1150	=C-(C=O)-O-CH3 stretching of aliphatic ester
1063	=CH2 rocking		
984	Trans =CHR wagging		
967	=CH2 wagging		
810	=CH2 twisting		
668	C=O wagging	486	C=O wagging

Figure B.2: Butyl acrylate peak assignment (Rivard, T. M.A.Sc. thesis, Department of Chemical Engineering, University of Ottawa, 2002).

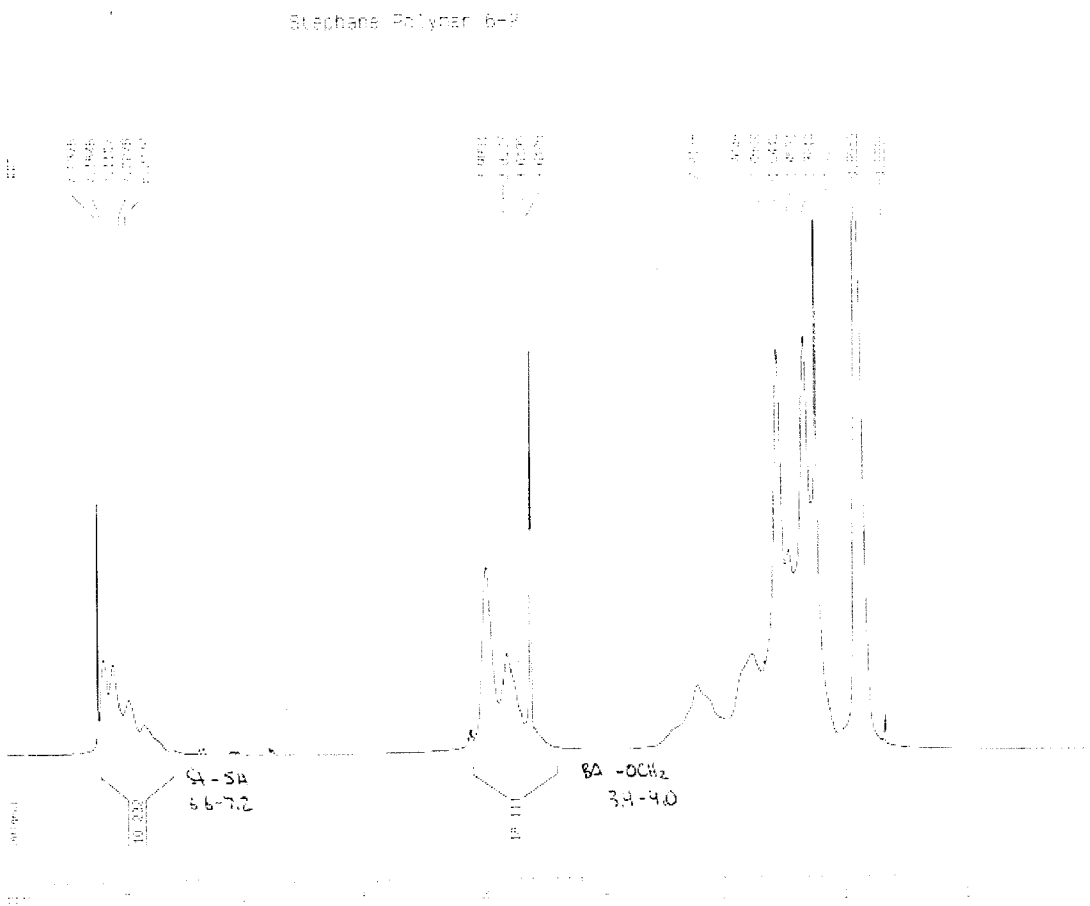

Figure B.3: ^{1}H-NMR spectrum for styrene/butyl acrylate/acrylic acid

Brookhaven Instruments Corporation.
Disc Centrifuge Particle Size Analyzer [Line Start] Ver. 3.44

Date: Aug 4, 2004
Time: 13:13:10
Batch: 1

Sample I.D. **run 2 18/06/04 (Run 1)**
Operator I.D. **Steph**
Notes **04/08/04**

Measurement Parameters:

Scan Mode	= F	Spin Fluid	= Aqueous
Disc Speed	= 10001.70 rpm	Spin Fluid Volume	= 15.7 ml
Particle Density	= 1.04 g/cc	Spin Fluid Density	= 0.997 g/cc
Run Time	= 10 min	Spin Fluid Viscosity	= 0.861 cP
Temperature	= 26.5 C	Scattering Correction	= ps-led.prm

Start Concentration = 0.207 volts Clear Spin Liquid = 0.207 volts

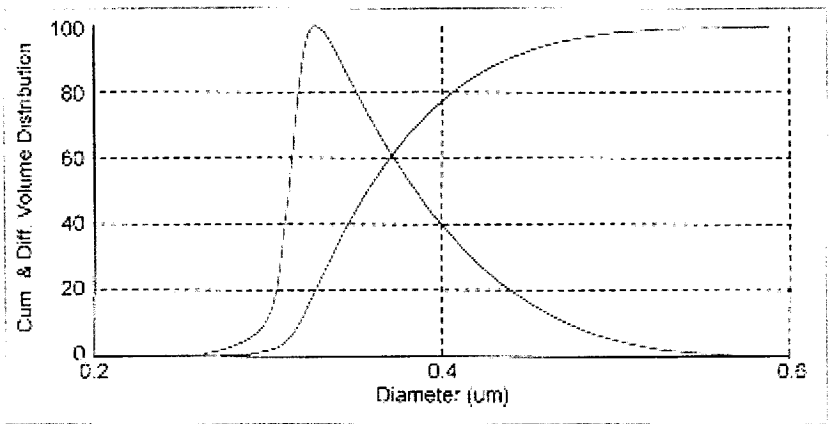

Cum Distribution

% less	Size (µm)
1	0.291
10	0.318
20	0.327
30	0.336
40	0.346
50	0.357
60	0.370
70	0.386
80	0.406
90	0.438
99	0.524

Analysis Results : Volume/Mass

d10	= 0.318 µm	Mean	= 0.368 µm
d16	= 0.323 µm	Std Deviation	= 0.062 µm
d50	= 0.357 µm	Mode	= 0.327 µm
d84	= 0.417 µm	FWHM	= 0.073 µm
d90	= 0.438 µm	FWHM/Mode	= 0.224
Span=(d90-d10)/d50	= 0.337		
d84/d50	= 1.168	Geometric Mean	= 0.365 µm
d50/d16	= 1.103	Geometric Std Dev	= 1.135 µm
Specific Surface (Sw)	= 15.924 sq m/g		

Figure B.4: Example of particle size determination with BI-DCP

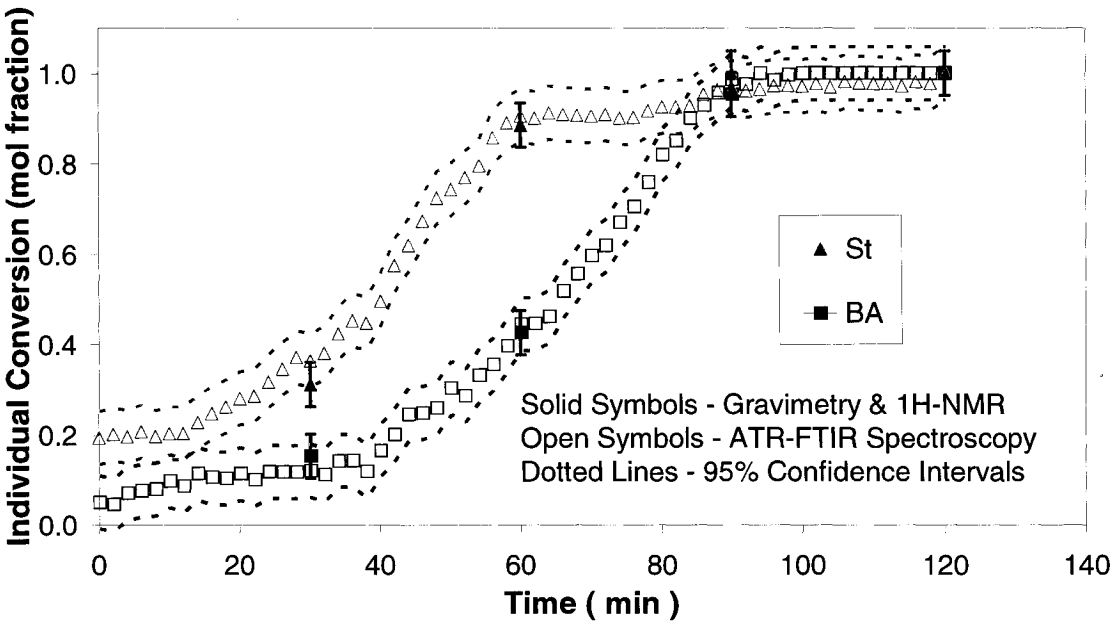

Figure B.5: PLS individual conversion predictions for Run 7

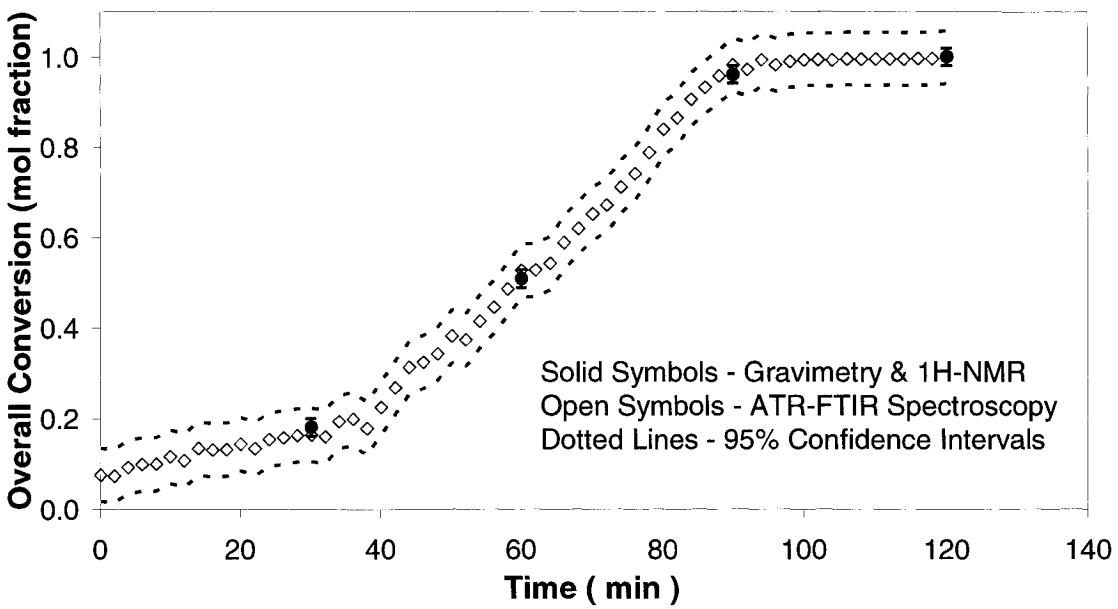

Figure B.6: PLS overall conversion predictions for Run 7

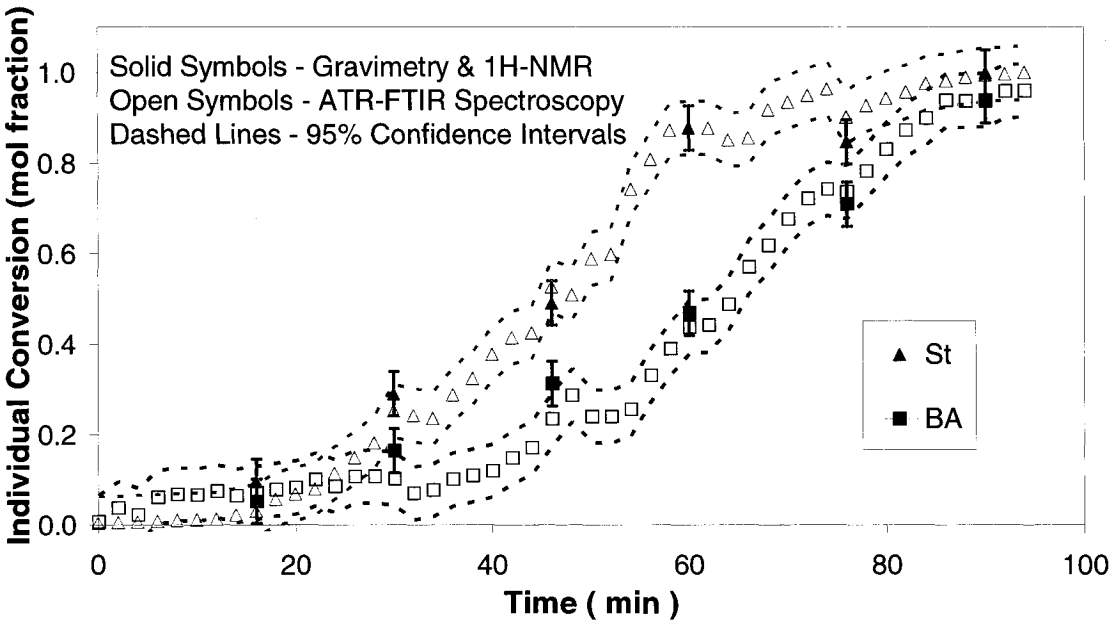

Figure B.7: PLS individual conversion predictions for Run 71

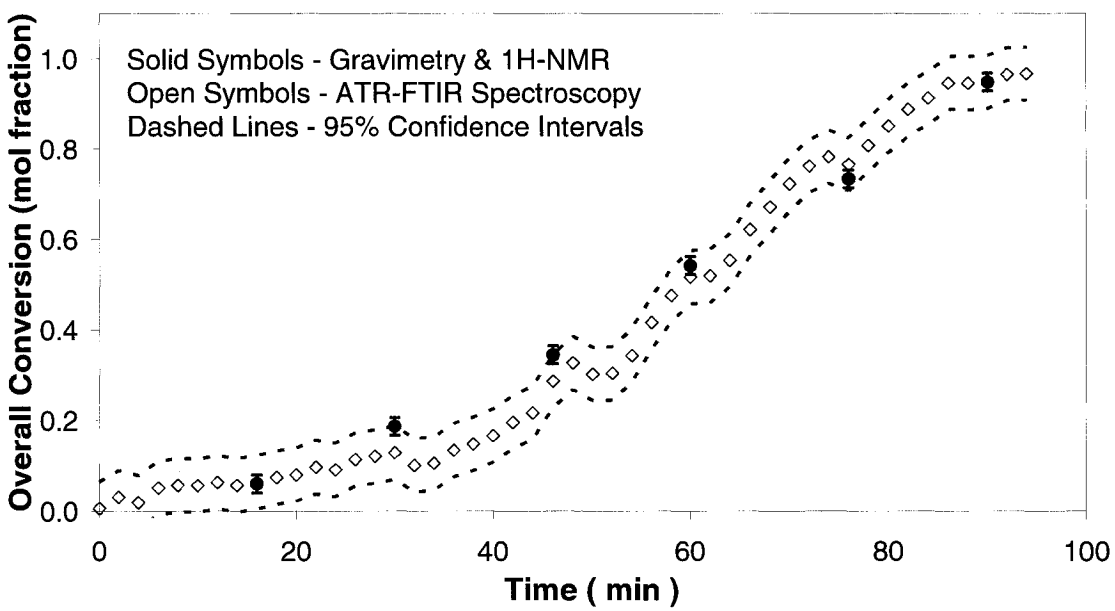

Figure B.8: PLS overall conversion predictions for Run 71

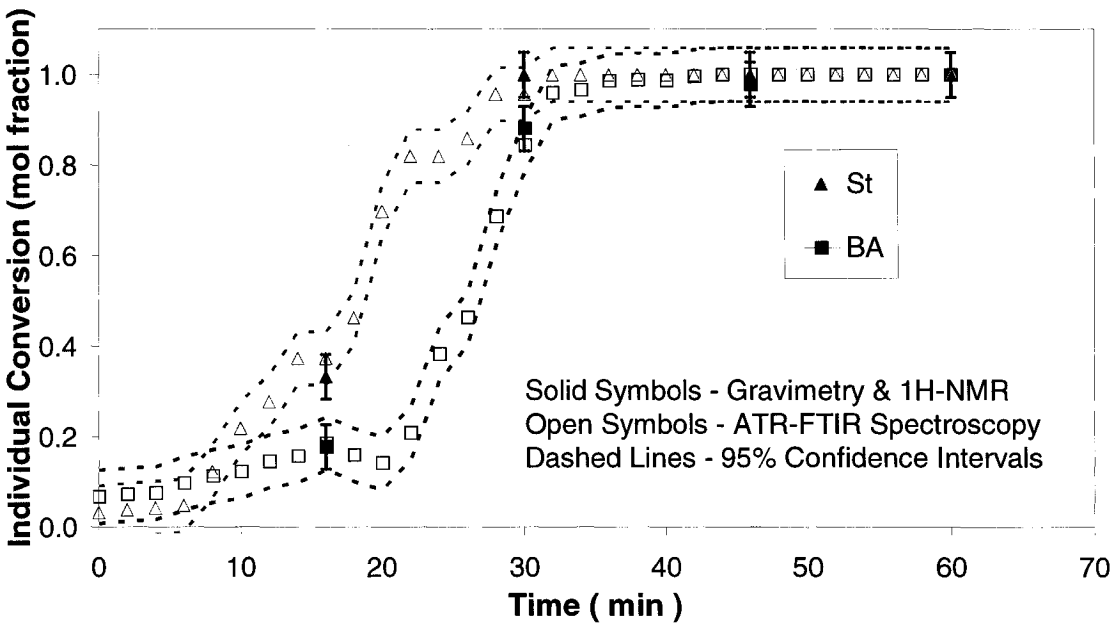

Figure B.9: PLS individual conversion predictions for Run 34

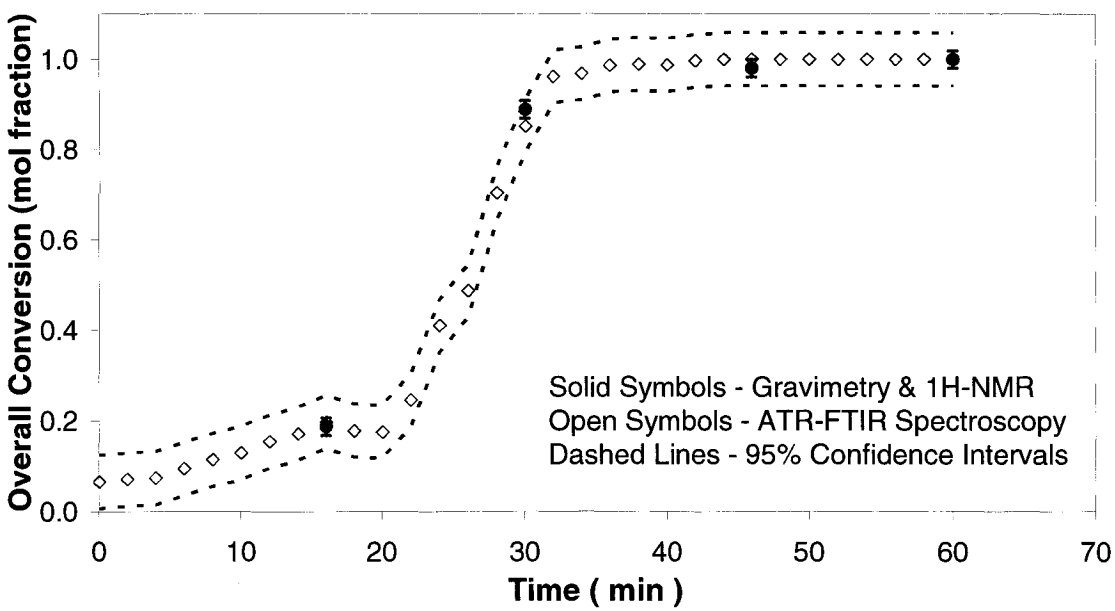

Figure B.10: PLS overall conversion predictions for Run 34

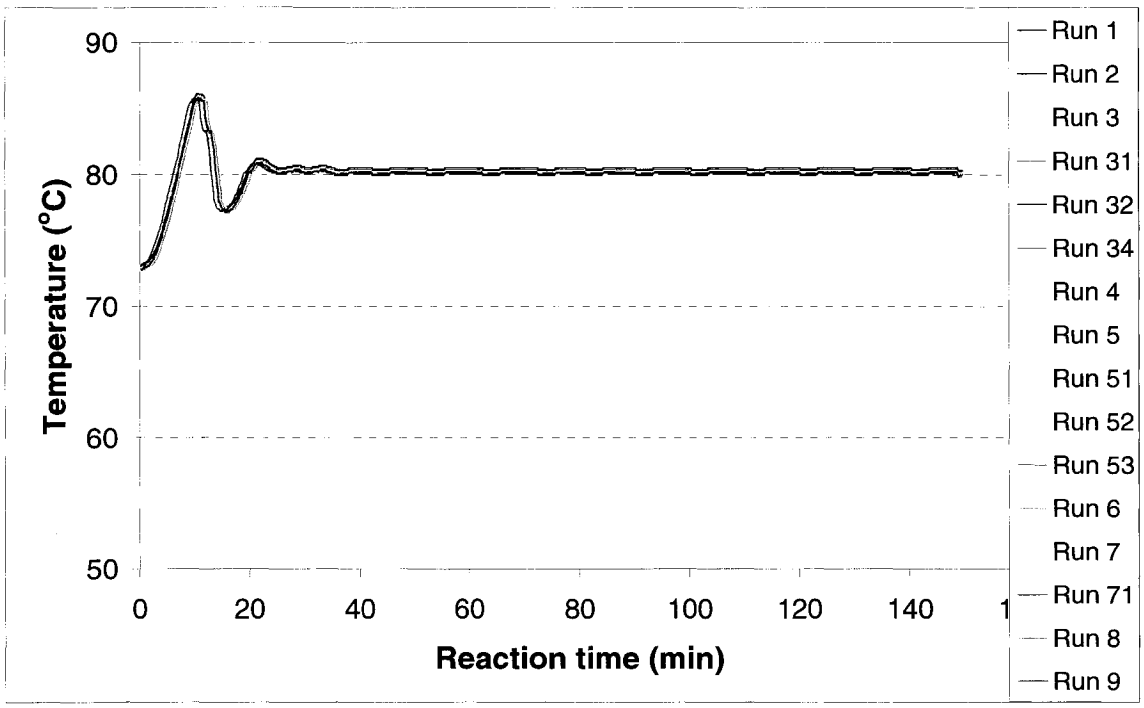

Figure B.11: Temperature profiles for all the runs

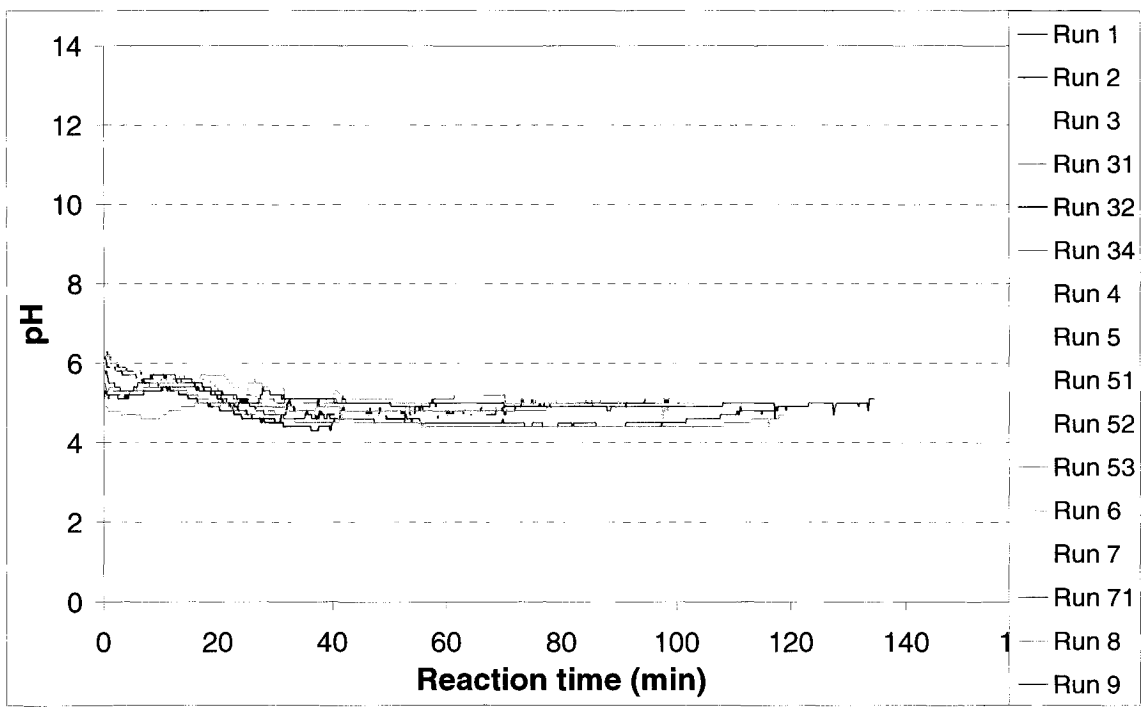

Figure B.12: pH profiles for all the runs

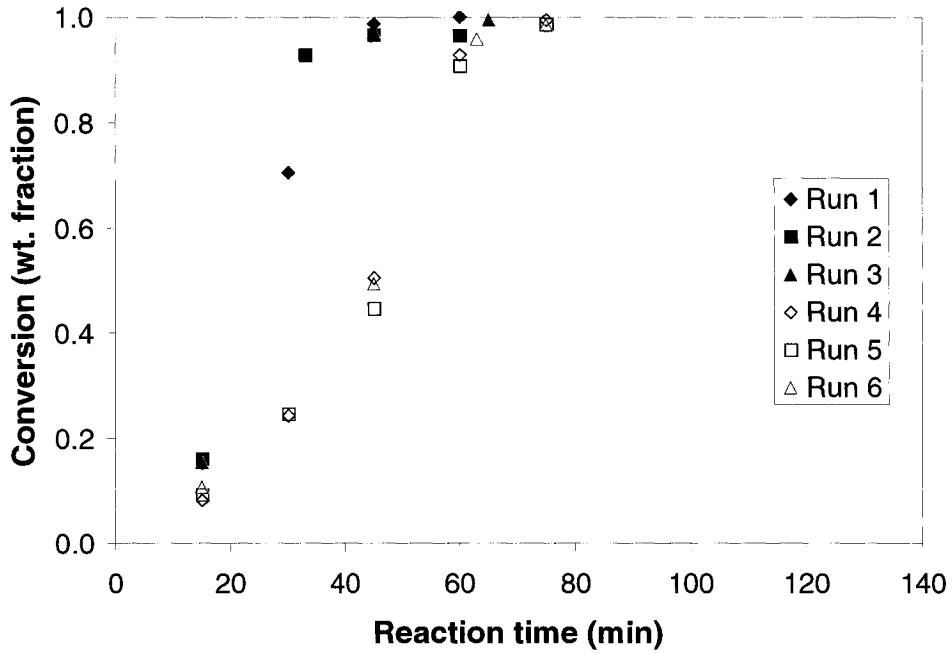

Figure B.13: Conversion versus time for Runs 1, 2, 3, 4, 5, 6

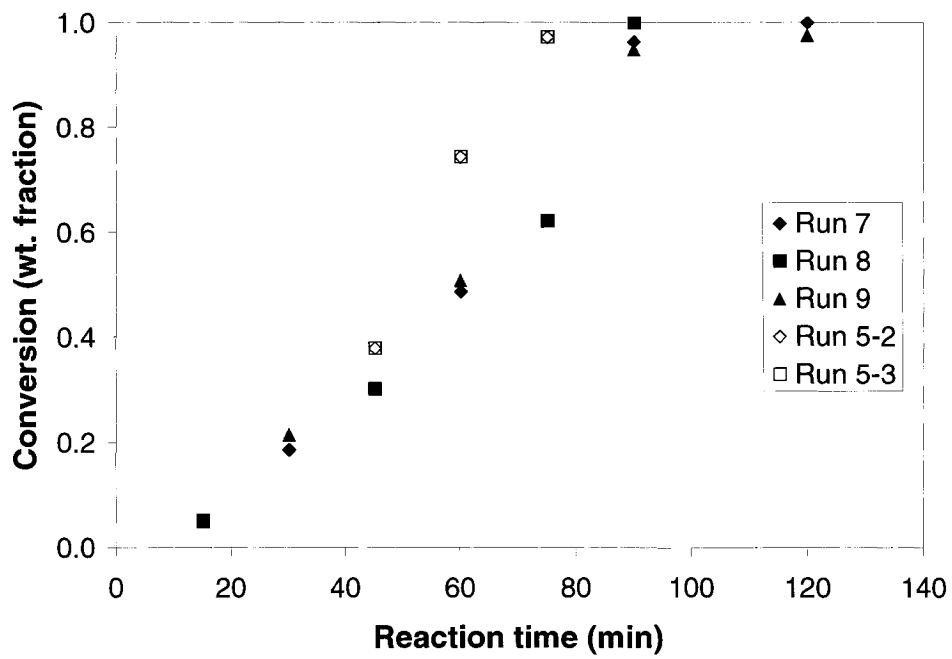

Figure B.14: Conversion versus time for Runs 7, 8, 9, 5-2, 5-3

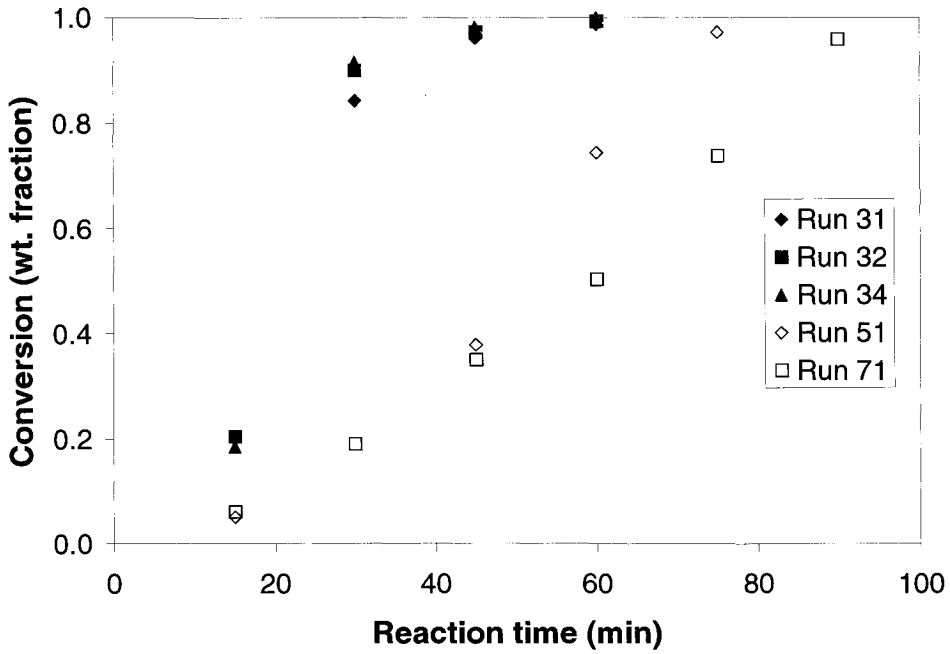

Figure B.15: Conversion versus time for Runs 3-1, 3-2, 3-4, 5-1, 7-1

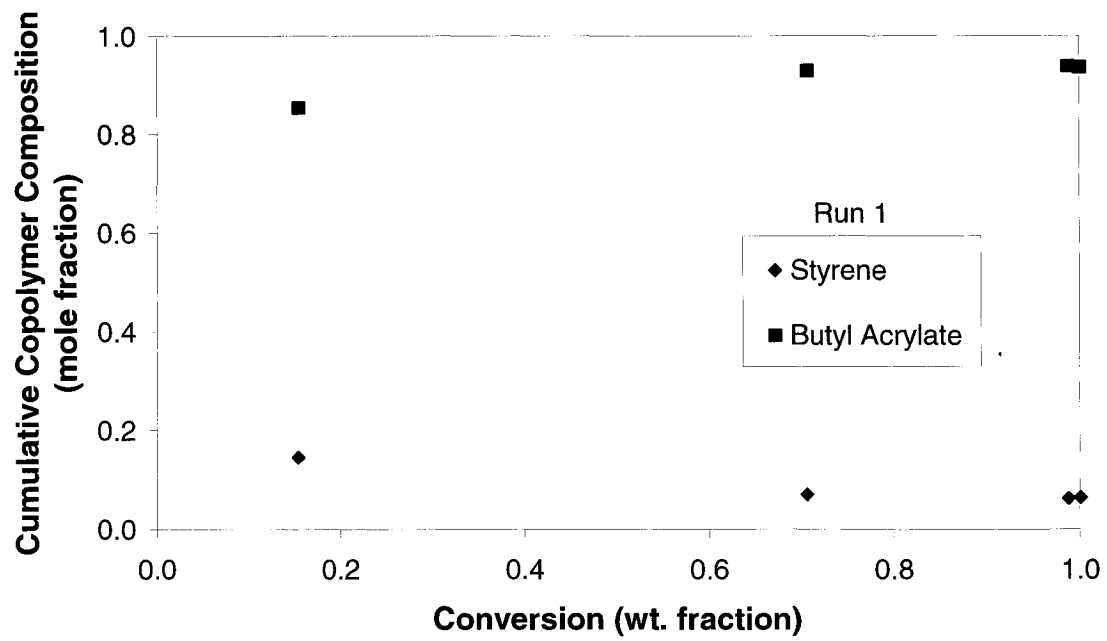

Figure B.16: Cumulative copolymer composition for Run 1

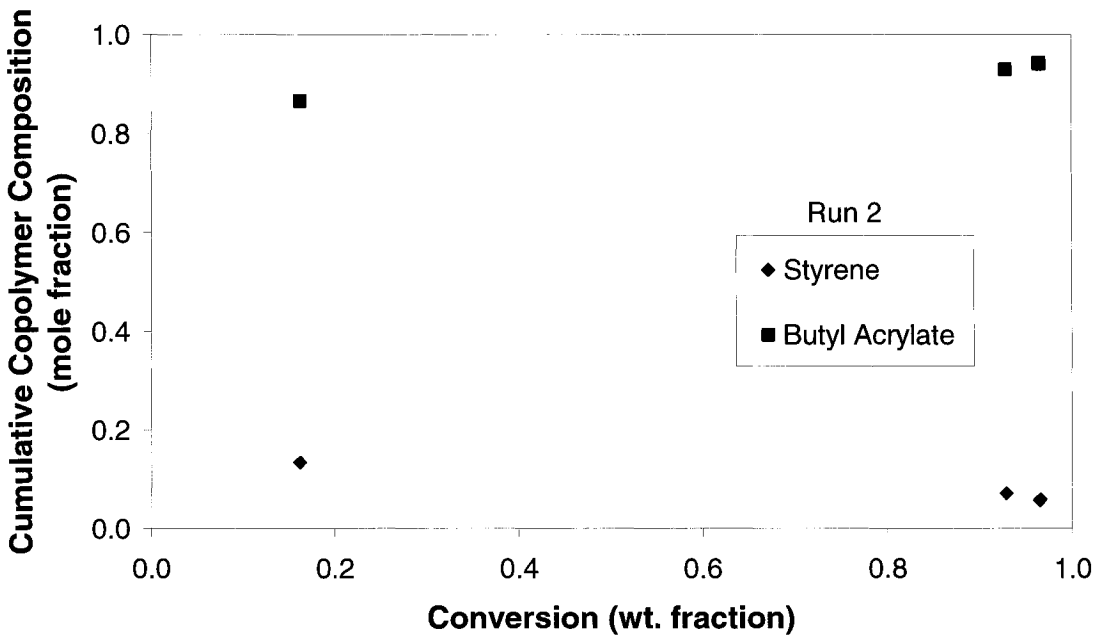

Figure B.17: Cumulative copolymer composition for Run 2

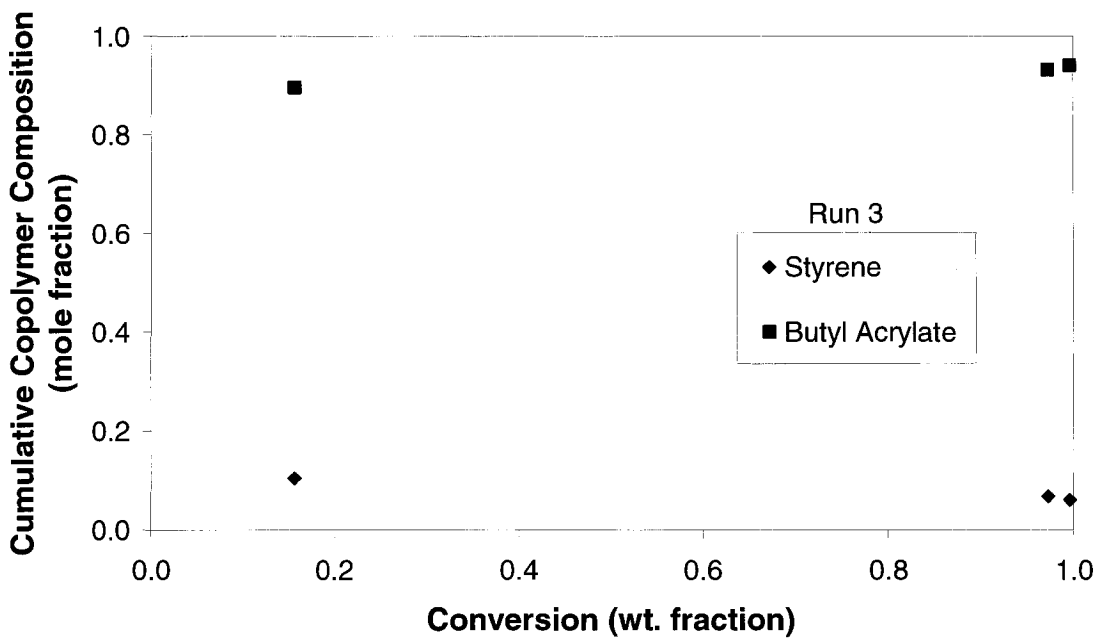

Figure B.18: Cumulative copolymer composition for Run 3

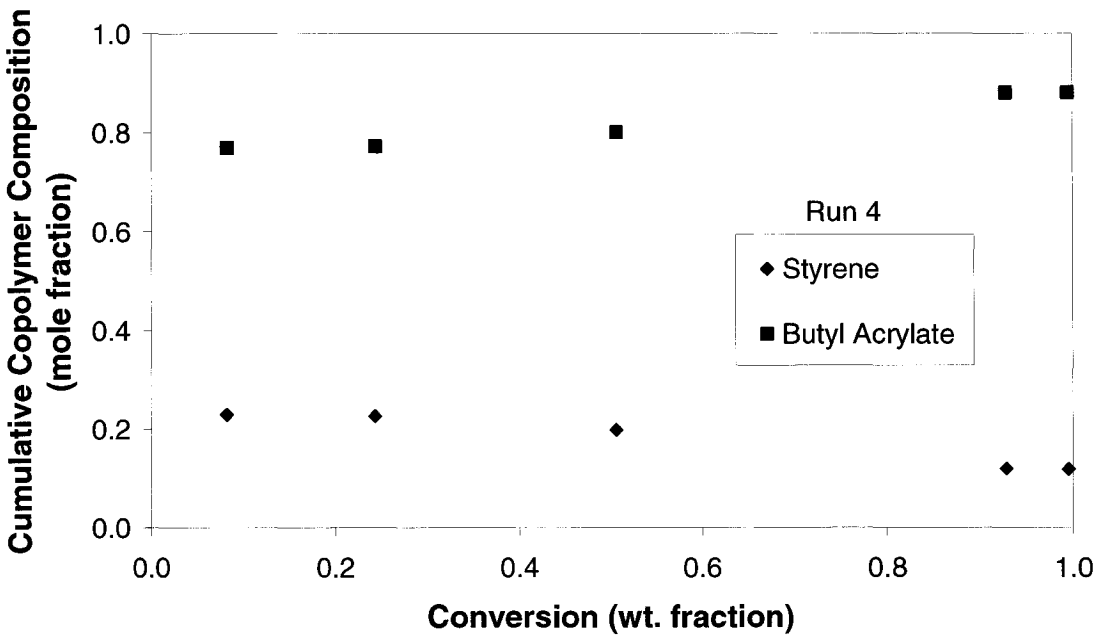

Figure B.19: Cumulative copolymer composition for Run 4

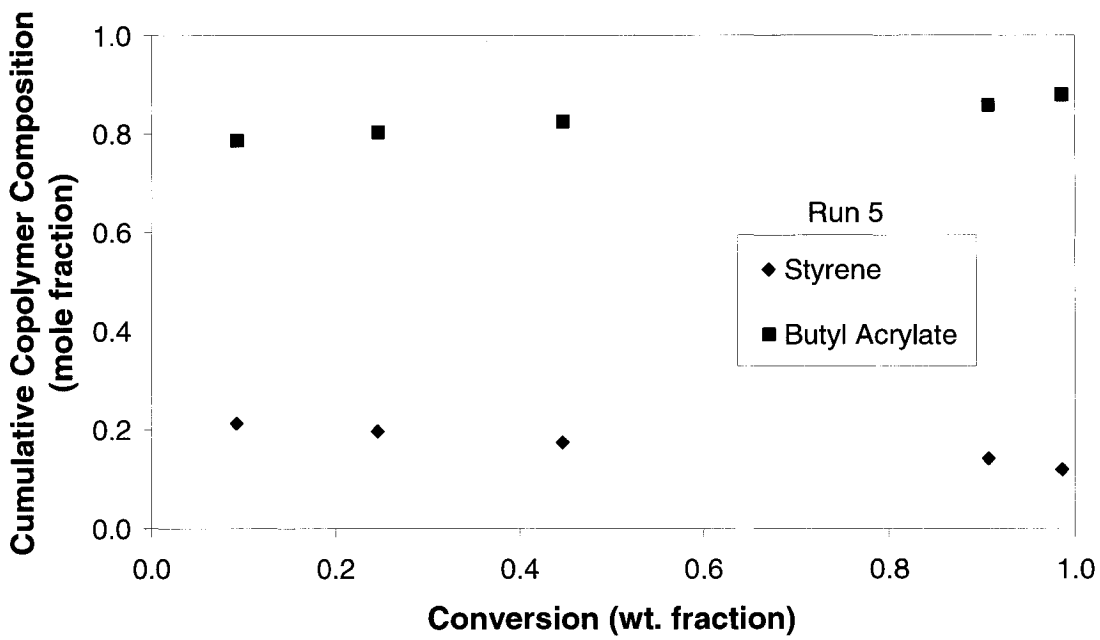

Figure B.20: Cumulative copolymer composition for Run 5

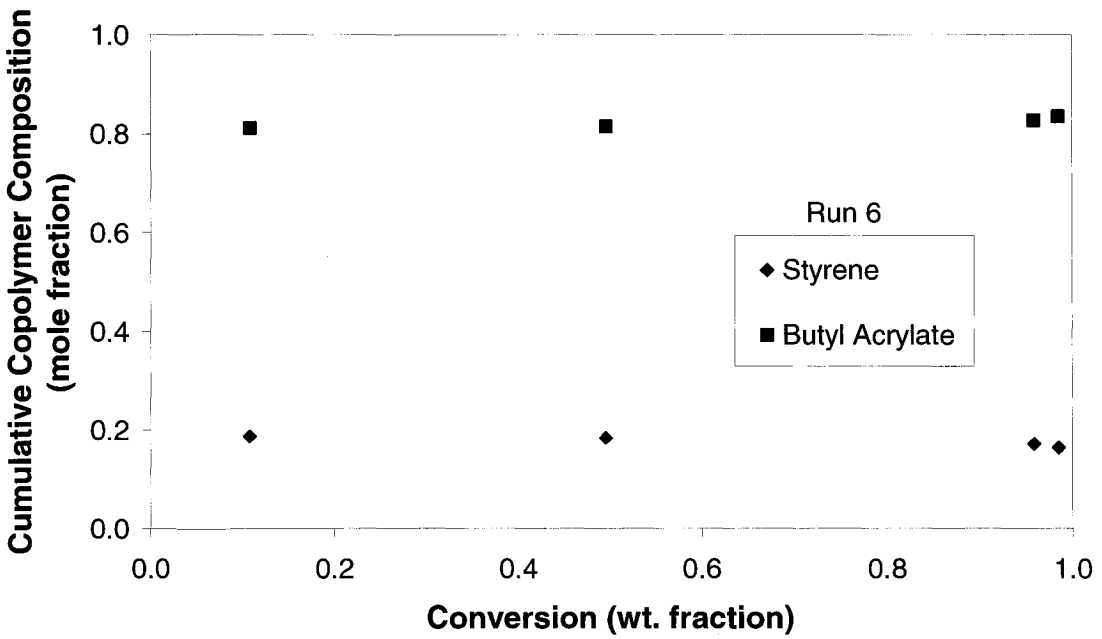

Figure B.21: Cumulative copolymer composition for Run 6

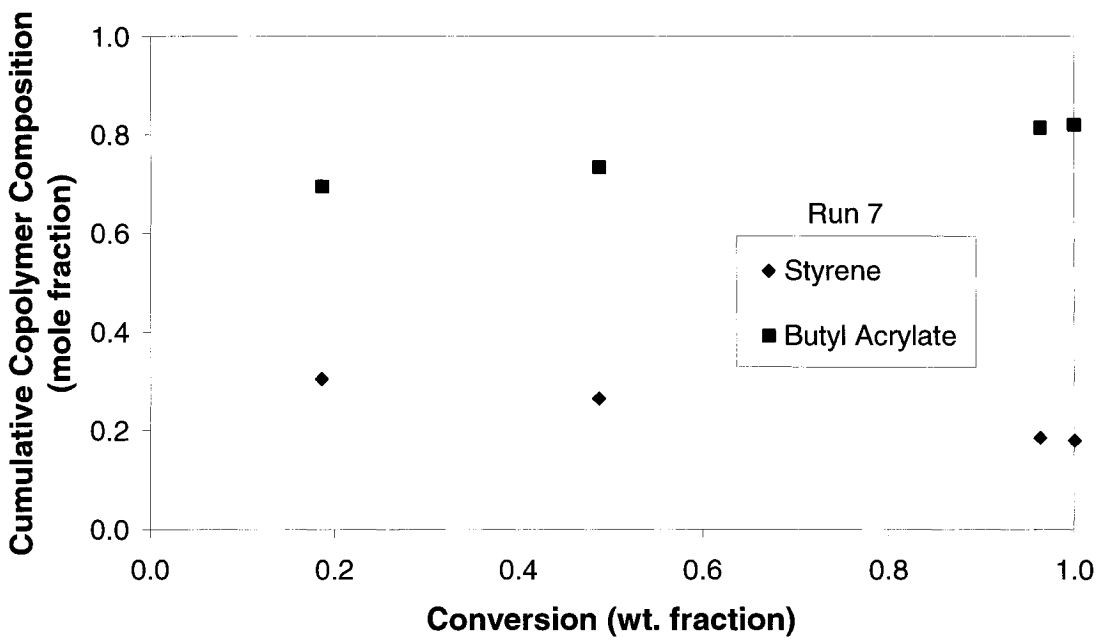

Figure B.22: Cumulative copolymer composition for Run 7

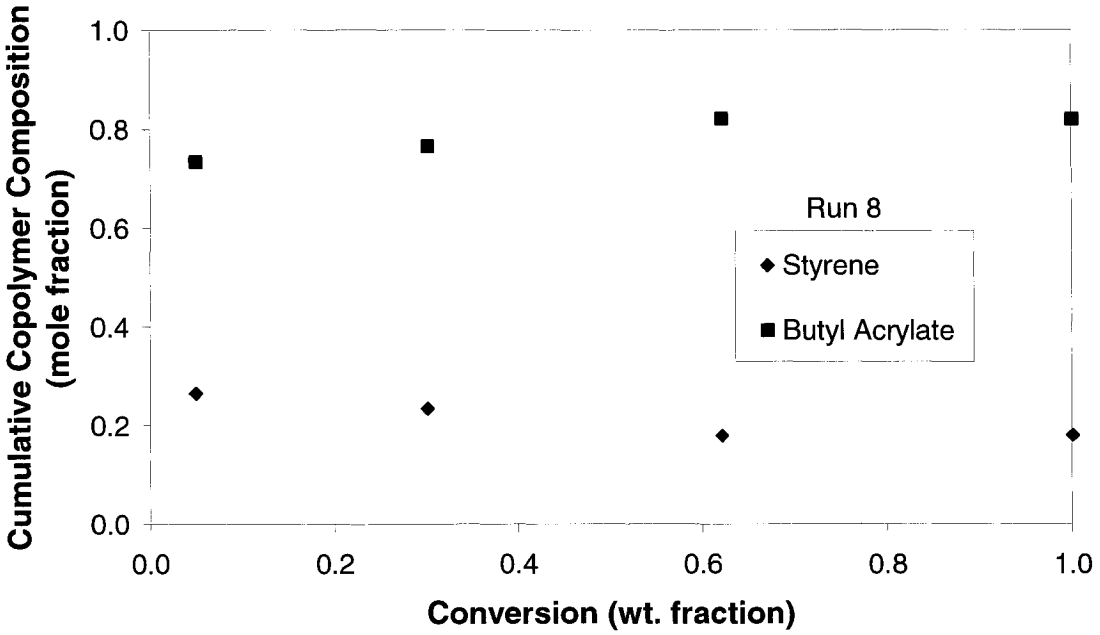

Figure B.23: Cumulative copolymer composition for Run 8

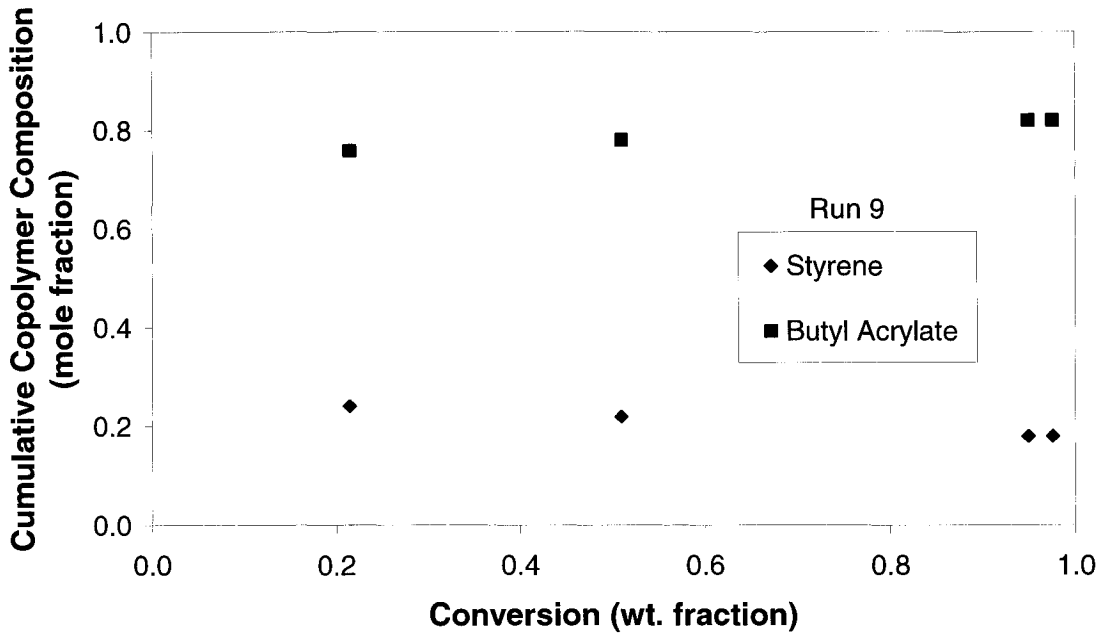

Figure B.24: Cumulative copolymer composition for Run 9

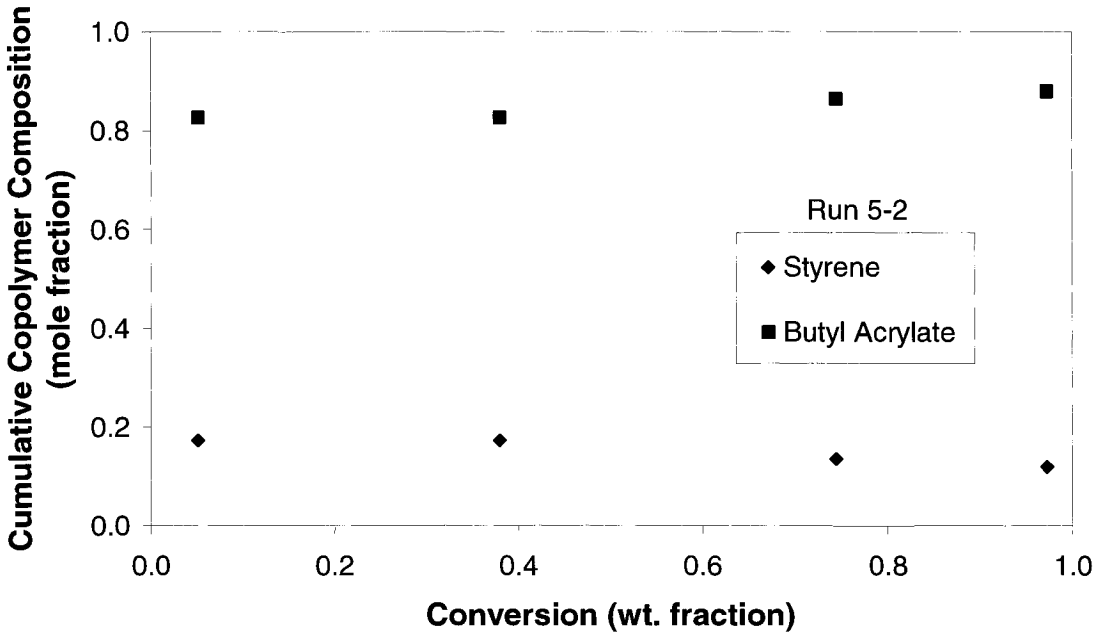

Figure B.25: Cumulative copolymer composition for Run 5-2

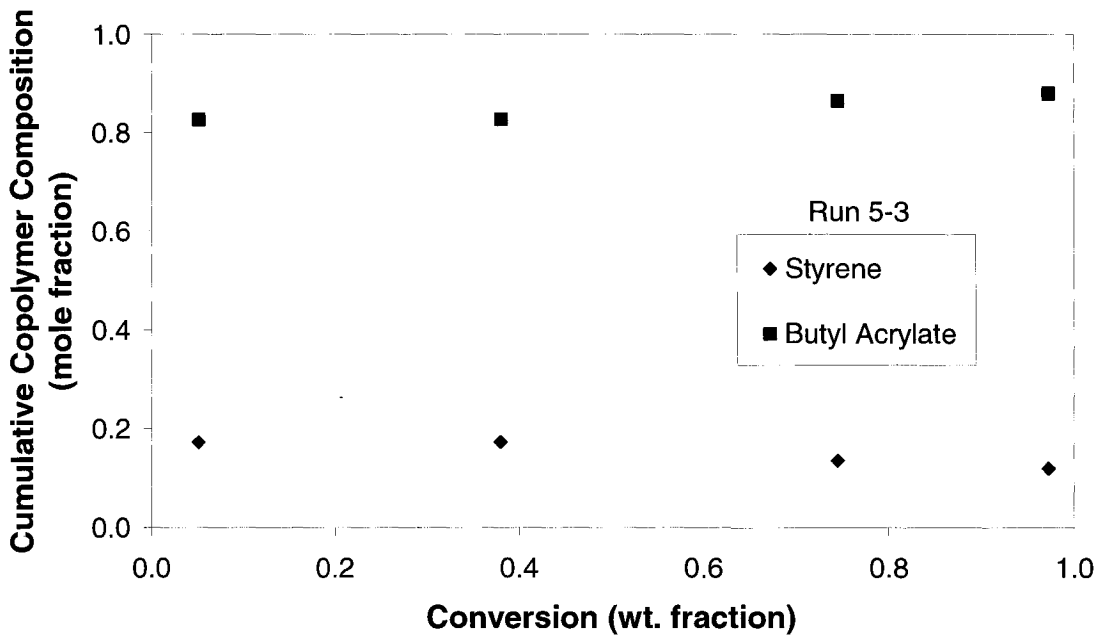

Figure B.26: Cumulative copolymer composition for Run 5-3

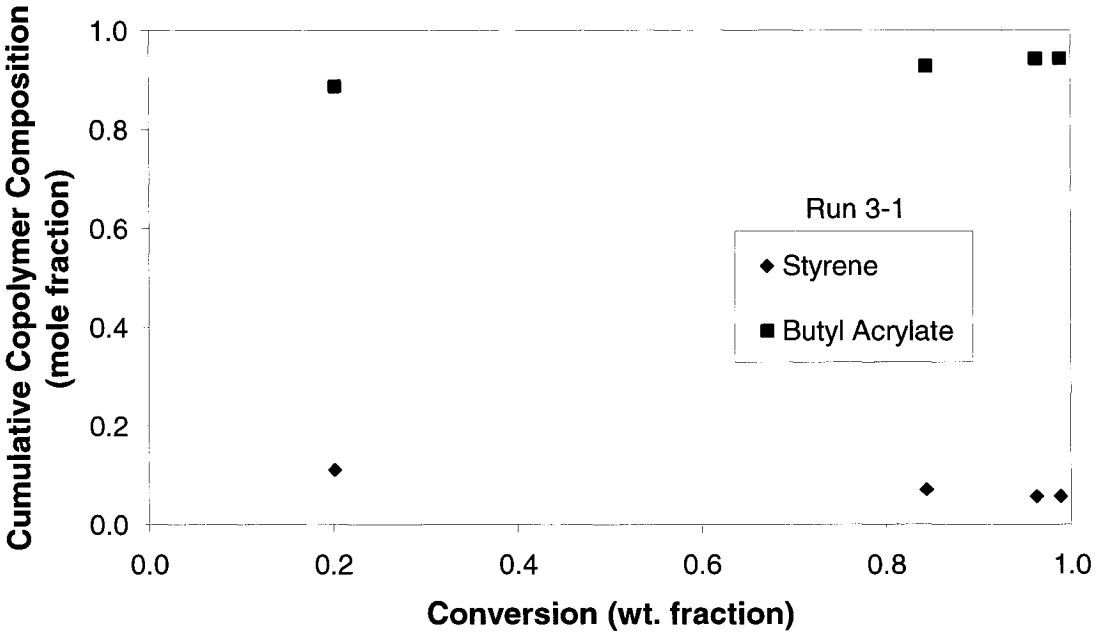

Figure B.27: Cumulative copolymer composition for Run 3-1

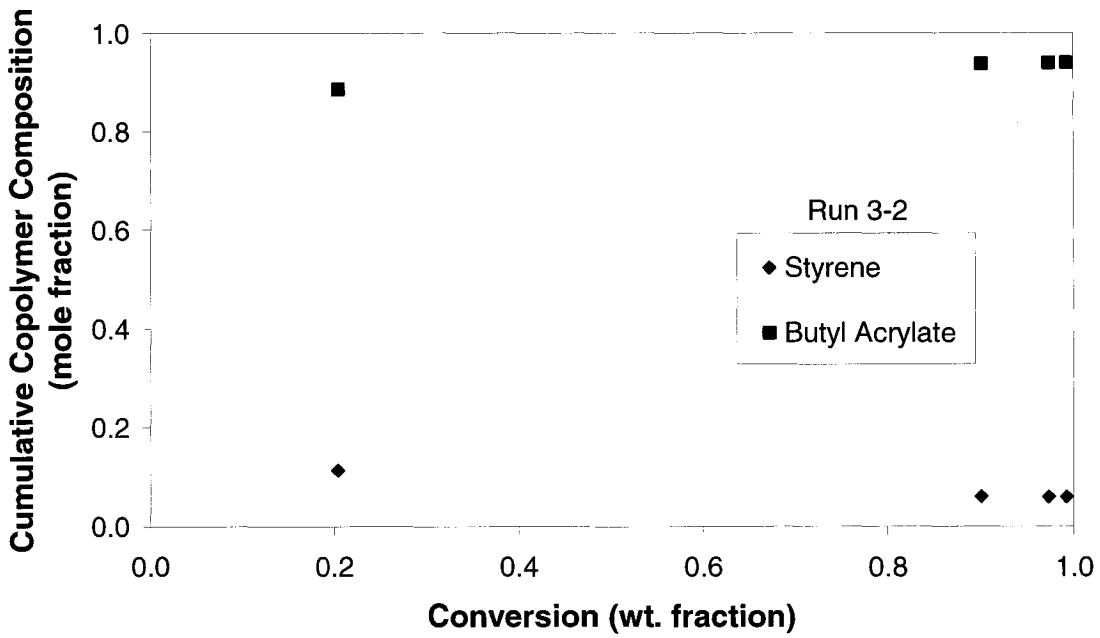

Figure B.28: Cumulative copolymer composition for Run 3-2

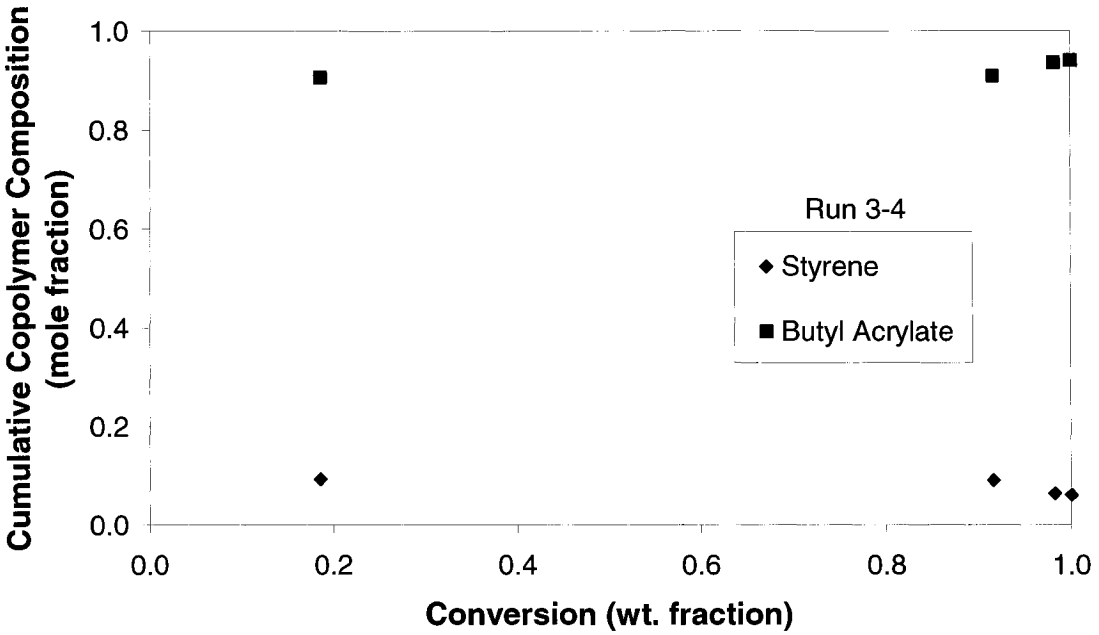

Figure B.29: Cumulative copolymer composition for Run 3-4

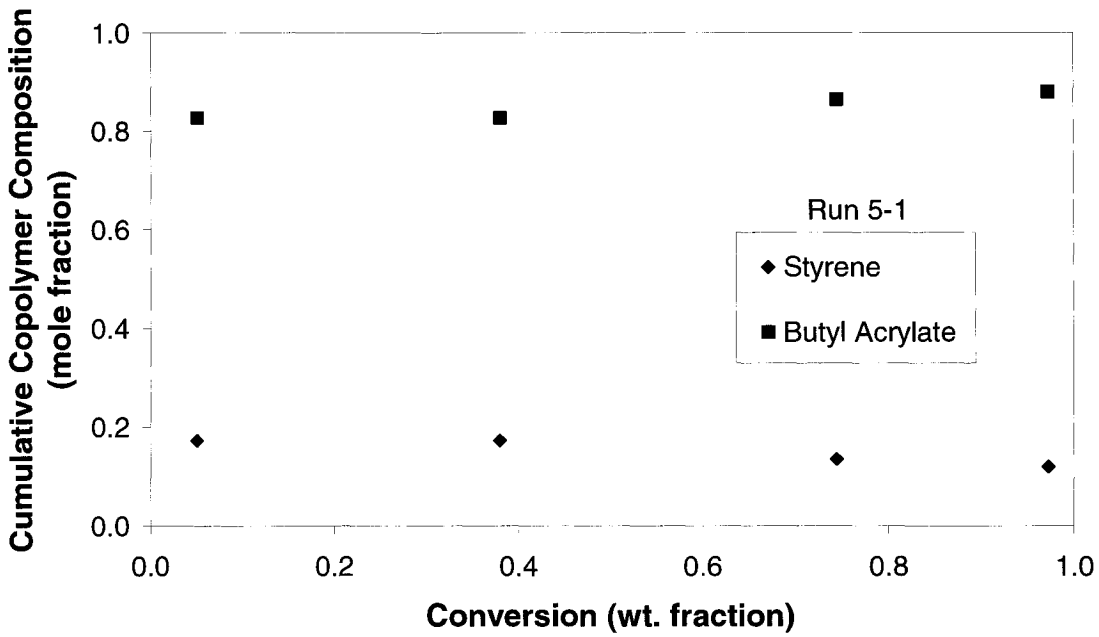

Figure B.30: Cumulative copolymer composition for Run 5-1

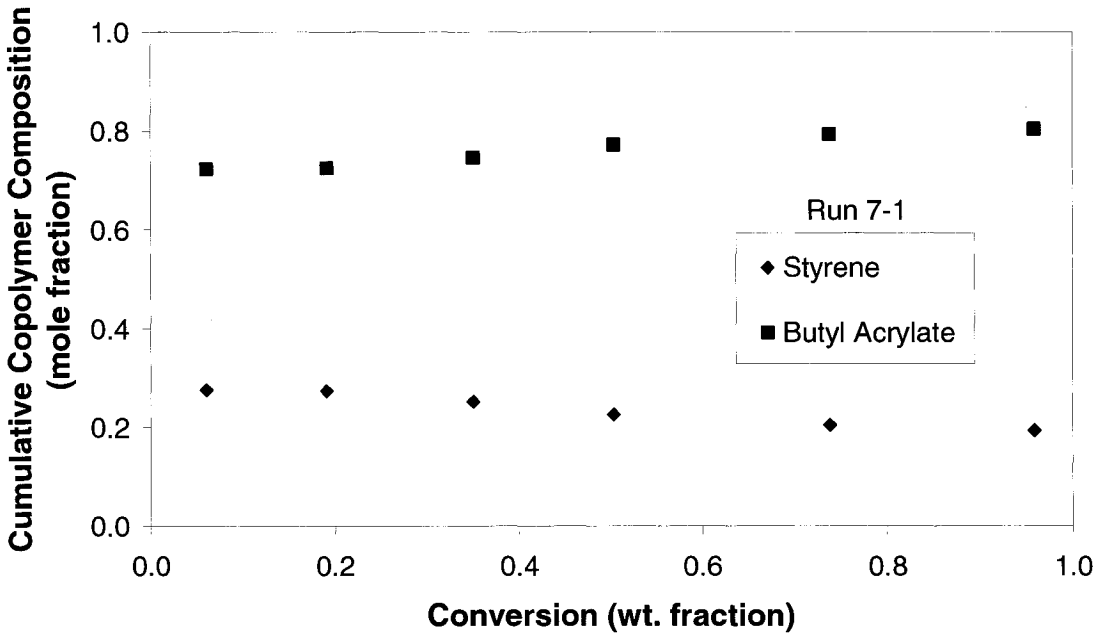

Figure B.31: Cumulative copolymer composition for Run 7-1